OZONE-INDUCED ALTERATIONS IN MACROPHAGE FUNCTION AND THE PROTECTIVE ROLE OF SR-BI

By: Myles Xavier Hodge

May 2020

Director of Dissertation: Dr. Kymberly Gowdy

Department of Pharmacology and Toxicology, Brody School of Medicine, East Carolina University

ABSTRACT

Ozone (O_3), a criteria air pollutant, is the primary component of photochemical smog. Currently, over 140 million people in the United States are exposed to levels of O_3 deemed unhealthy by the Environmental Protection Agency. Short and long-term exposure to O_3 has been associated with increased susceptibility and/or exacerbations of chronic pulmonary diseases through lung injury and inflammation. O_3 induces pulmonary inflammation in part through generating damage associated molecular patterns (DAMPs), which are recognized by pattern recognition receptors (PRRs), such as toll like receptors (TLRs) and scavenger receptors (SRs). This inflammatory response is mediated by alveolar macrophages (AMs) which highly express PRRs, including Scavenger Receptor B-I (SR-BI). SR-BI is a PRR known to recognize DAMPs, apoptotic cells, and facilitate the phagocytosis of apoptotic cells termed ‘efferocytosis’. The central hypothesis of this study was that SR-BI resolves O_3-induced inflammation and injury by facilitating clearance of DAMPs and maintaining alveolar macrophage efferocytosis. The first aim of this study was to determine whether acute O_3 exposure impairs AM efferocytosis whereas the second aim of this study was to determine if SR-BI mediates

AM efferocytosis following O_3 exposure leading to resolution of lung inflammation and/or injury. Our findings demonstrated that acute O_3 exposure impairs AM efferocytosis. Additionally, we proved that SR-BI is protective against O_3-induced lung inflammation by decreasing airspace neutrophilia and maintaining AM efferocytosis. Collectively, these results identified novel mechanisms of how O_3 induces pulmonary inflammation and increase the susceptibility and/or exacerbations of chronic lung diseases.

OZONE-INDUCED ALTERATIONS IN MACROPHAGE FUNCTION AND THE PROTECTIVE ROLE OF SR-BI

A Dissertation

Presented to

the Faculty of the Department of Pharmacology and Toxicology

Brody School of Medicine at East Carolina University

In Partial Fulfillment of the Requirements for the Degree

Doctor of Philosophy in Pharmacology and Toxicology

by

Myles Xavier Hodge

May 2020

OZONE-INDUCED ALTERATIONS IN MACROPHAGE FUNCTION AND THE PROTECTIVE ROLE OF SR-BI

by

Myles X. Hodge

Approved By:

DIRECTOR OF DISSERTATION _____
Kymberly M. Gowdy, Ph.D.

COMMITTEE MEMBER _____
Rukiyah T. Van Dross-Anderson

COMMITTEE MEMBER _____
Jacques Robidoux, Ph.D.

COMMITTEE MEMBER _____
Johanna L. Hannan, Ph.D.

COMMITTEE MEMBER _____
Joseph M. McClung, Ph.D.

CHAIR OF THE DEPARTMENT OF PHARMACOLOGY AND TOXICOLOGY _____
David A. Taylor, Ph.D.

DEAN OF THE GRADUATE SCHOOL _____
Paul J. Gemperline, Ph.D.

To my wife, Lisa, and child Angelia.

Thank you for your strength and support that

has been a blessing every day.

ACKNOWLEDGEMENTS

Since I learned about the scientific method in grade school, I have always had a passion towards solving scientific problems. Then, when I went to high school, I joined the North Carolina Project SEED program, where I was exposed to basic science research. Then, after I graduated from East Carolina University as an undergraduate, I decided to attend the Summer Biomedical Research Program where I learned about opportunities at the medical school and graduate programs at the Brody School of Medicine. From then on, I decided to pursue my doctorate in Pharmacology and Toxicology. However, this reality would not have been possible without several important individuals.

First, my wife Lisa, for supporting me since before and after starting this program. I could not have survived my classes without your consistent reliability and gourmet cooking. I will never be able to thank you enough for always being an ear to vent to or a wise woman I can always come to for help. I do not think I would have been able to make it this far without you giving me a shoulder to lean on. I am truly blessed to have you as my wife and mother of my first child that can see me accomplish this feat. Also, thank you Angelia for showing me how much I can accomplish in my career with no sleep!

Next, I would like to thank my parents for pushing me to be the best man I can be and to always go the extra mile. Without their support and parenting, I would not have even considered pursuing my doctorate. Additionally, I would like to thank my other set of parents, through marriage, that have been a big help in supporting me while I am in school as well, along with babysitting my child to give me time to work. I will never be able to thank you all enough for all the prayers, talks, and hearing me vent my frustrations.

Third, I would like to thank all the lab members (current and former) of Dr. Gowdy's lab. Thank you, Dr. Sky Reece, Ms. Bin Luo, and Dr. Brita Kilburg-Basynat for having the patience with me in teaching me techniques in the lab that gave me the data I have collected over the past 4 years. Without you all putting me through Gowdy lab bootcamp, I would not have understood how to troubleshoot my experiments and optimize them correctly to get the best data possible.

I would like to thank my committee members: Dr. Rukiyah Van Dross-Anderson, Dr. Jacques Robidoux, Dr. Johanna Hannan, and Dr. Joseph McClung for all their suggestions, guidance, as well as constructive criticism that made me a better scientist. A special thanks to my fellow graduate students and the faculty and staff in the department of Pharmacology and Toxicology for always being willing to help with my numerous questions and advice seeking. Your support is part of what motivated me to keep going through graduate school. A special thanks to Dr. Korin Leffler, for being my sole colleague when we came into this program together in 2015. I will never forget our many study sessions and visits to each other's lab to talk about how 'successful' our experiments were. The past four years have been about achieving my doctoral degree, but they have also been about my growth as an individual and each of you have become so memorable in my life.

Lastly, a huge thanks to Dr. Kymberly Gowdy for being with me from the start of my graduate school career. Since joining her lab, I have gained a monumental amount of knowledge from her. I cannot thank her enough for always pushing me and giving me higher expectations to get to where I am at now. Being that we were each other's first student and mentor respectively, I feel that her guidance throughout my graduate school

career has helped me learn more about her and myself as well. She has helped me blossom into an incredible scientist with a bright future. From the bottom of my heart, thank you for giving me a chance.

TABLE OF CONTENTS

LIST OF TABLES

LIST OF FIGURES

LIST OF SYMBOLS/ABBREVIATIONS

AM	Alveolar Macrophage
BAL Fluid	Bronchoalveolar lavage Fluid
BLT-2	Block lipid transport-2
C18Kodia-PC	1-O-octadecyl-2-acetyl-sn-glycero-3-phosphocholine
CCL2	C-C Motif Chemokine Ligand 2
CCL3	C-C Motif Chemokine Ligand 3
CD163	Cluster of Differentiation 163
CD36	Cluster of Differentiation 36
CXCL1	C-X-C Motif Chemokine Ligand 1
CXCL2	C-X-C Motif Chemokine Ligand 2
Eos	Eosinophil
EI	Efferocytic Index
Epi	Epithelial Cell
FA	Filtered Air
HDL	High Density Lipoprotein
HMGB1	High Mobility Group Box 1 Protein
IL-1β	Interleukin-1β
IL-6	Interleukin-6
IL-10	Interleukin-10
IM	Interstitial Macrophage
LDL	Low Density Lipoprotein
Lymph	Lymphocyte

МΦ	Macrophage
MARCO	Macrophage receptor with collagenous structure
MerTK	MER Proto-Oncogene, Tyrosine Kinase
O_3	Ozone
OxPAPC	Oxidized 1-palmitoyl-2-arachidonyl-sn-glycero-3-phosphorylcholine
OxPL	Oxidized Phospholipid
PAzPC	1-Palmitoyl-2-azelaoyl-sn-glycero-3-phosphocholine
PBS	Phosphate Buffered Saline
PGPC	1-palmitoyl-2-glutaryl-sn-glycero-3-phosphocholine
PMN	Neutrophil
PONPC	1-Hexadecanoyl-2-(9-oxo-nonanoyl)-sn-glycero-3-phosphocholine
POVPC	1-palmitoyl-2-(5'-oxo-valeroyl)-sn-glycero-3-phosphocholine
PRR	Pattern Recognition Receptor
SAzPC	1-stearoyl-sn-glycero-3-phosphocholine
SR-AI/II	Scavenger Receptor class A type 1/type II
SR-BI	Scavenger receptor class B type 1
SGPC	1-stearoyl-2-glutaroyl-sn-glycero-3-phosphocholine
SONPC	1-stearoyl-2-(9-oxo-nonanoyl)-sn-glycero-3-phosphocholine
SOVPC	1-stearoyl-2-(5-oxovaleroyl)-sn-glycero-3-phosphocholine
SR-BI	Scavenger Receptor B-I
Tim4	T-cell immunoglobulin mucin protein 4
TGF-β	Transforming growth factor-β
TNF-α	Tumor-necrosis factor-α

CHAPTER 1: GENERAL INTRODUCTION

1.1 Scientific Premise

Ambient air pollution is a significant cause of morbidity and mortality, contributing to approximately 9 million premature deaths annually (Landrigan et al., 2018). Additionally, the World Health Organization estimates that approximately 7 million people die prematurely due to ambient air pollutant exposure (World Health Organization et al., 2014). Most air pollution related deaths occur in individuals with underlying pulmonary and/or cardiovascular complications, including chronic lung disease (Miller et al., 2016 & Carlsen et al., 2013). In addition, increases in ambient criteria air pollutants increases the prevalence of chronic lung diseases (Bai et al., 2018 & Orru et al., 2017).

The Environmental Protection Agency (EPA) currently monitors several criteria air pollutants known to cause negative health effects. These criteria air pollutants include particulate matter (PM), sulfur dioxide, nitrogen dioxide, lead, carbon monoxide, and ground-level ozone (O_3) (Bai et al., 2018 & Suh et al., 2000). Despite stricter air quality standards to reduce levels of these criteria air pollutants, ground-level O_3 levels continue to rise (Orru et al., 2017, Zhang et al., 2016, Tibbetts 2015). The National Ambient Air Quality Standard (NAAQS) for O_3 is 0.070 ppm for 8 hours; however, this level of exposure is still known to induce upper respiratory issues, including shortness of breath, coughing, and throat irritation (U.S EPA). Therefore, there is an urgent need to identify mechanisms by which O_3 induces pulmonary dysfunction and exacerbates chronic respiratory diseases to design effective therapeutics.

1.2 O_3 and the Innate Immune Response

O_3 exposure induces both pulmonary and cardiovascular inflammation and injury (Bourdrel et al., 2017, Ierodiakonou et al., 2016, Carlsen et al., 2013, Tager et al., 2005, Al-Hegalan et al., 2011 & Bouthillier et al., 1998). It is thought that O_3 does this through oxidizing components of lung lining fluid, such as phospholipids, cholesterol, and surfactant proteins (Bromberg 2016 & Michaudel et al., 2016). These secondary oxidation products are known as damage associated molecular patterns (DAMPs) that are recognized by pattern recognition receptors including toll like receptors (TLRs) and scavenger receptors (SRs) present on the surface of epithelial cells and alveolar macrophages (AMs) (Michaudel et al., 2016, Bauer et al., 2012, Al-Hegelan et al., 2011). This activation of the pattern recognition receptors increases pro-inflammatory cytokine secretion from Mϕs, leading to lung inflammation and injury (Hodge et al., 2019, Jakab et al., 1995, Gilmour et al., 1991). The secretion of pro-inflammatory cytokines and chemokines recruit neutrophils (PMNs) to the lung where these innate immune cells generate reactive oxygen species and perpetuate the inflammatory response. Although, O_3 generates an inflammatory response, the underlying molecular mechanisms that trigger this response are currently unknown (Kilburg-Basnyat et al., 2018 & Backus et al., 2010). If the O_3-induced inflammatory response is not resolved, then necrosis, tissue injury, and development of chronic lung disease can ensue (Morimoto et al., 2012).

1.3 Scavenger Receptors and the Lung

Scavenger receptors are pattern recognition receptors known to recognize and clear DAMPs, such as oxidized lipids and oxidized proteins, but also to facilitate clearance of apoptotic cells (Canton et al., 2013). Currently, there are 10 classes of scavenger

receptors, classes A-H, that have been identified; however, few have been examined in the context of O_3-induced lung inflammation/injury. (Canton et al., 2013 & PrabhuDas et al., 2017). Two class A scavenger receptors, macrophage receptor with collagenous structure (MARCO) and SR-AI/II, have been found to scavenge oxidized phospholipids and cholesterols that are generated by O_3 (Dahl et al., 2007 & Arredouani et al., 2007). The class B scavenger receptor, CD36, has been shown to potentiate the inflammatory response and mediate vascular dysfunction in mice exposed to O_3 (Robertson et al., 2013). However, more studies are needed to understand the importance of these receptors in the context of O_3-induced lung inflammation.

1.4 Scavenger Receptor Class B Type 1

SR-BI is a class B scavenger receptor that plays a vital role in cholesterol homeostasis, lipoprotein metabolism, and innate immunity (Linton et al., 2017, Rigotti et al., 2003, Krieger et al., 1999). SR-BI was discovered as an extracellular high-density lipoprotein (HDL) receptor, that is responsible for reverse cholesterol transport between HDL and extrahepatic tissues (Linton et al., 2017, Shen et al., 2018, Van Eck et al., 2003). However, SR-BI is also responsible for the uptake of cholesterol esters from HDL in the liver for biliary excretion (Acton et al., 1996 & Hoekstra et al., 2017). By mediating HDL uptake, SR-BI preserves HDL function and decreases serum levels of low-density lipoproteins (LDL). Humans with loss-of-function mutations in this receptor are adrenally insufficient, have high levels of HDL, and a 1.8-fold increased risk for developing coronary artery disease. These characteristics are also noted in the SR-BI deficient murine model (Vergeer et al., 2011 & Khovidhunkit et al., 2011). Although this receptor is ubiquitously expressed in all tissues, it is predominantly expressed on steroidogenic tissues,

endothelial cells, and Mϕs (Shen et al., 2018 & Hu et al., 2013). The role of SR-BI has been mainly studied in the aspect of cardiovascular disease, but its roles in pulmonary immune response have not been fully understood.

Prior studies by Gowdy et al., have highlighted the protective role of SR-BI in the lung following bacterial infection of *Klebsiella pneumoniae*, where SR-BI deficient (SR-BI$^{-/-}$) mice display increased morbidity, mortality, and decreased clearance of bacteria in both the lung and blood compared to their wildtype (SR-BI$^{+/+}$) counterparts. Additionally, SR-BI has been shown to mediate the glucocorticoid response following endotoxin-induced sepsis, but also in attenuating the pro-inflammatory signaling response *in vivo* and *in vitro* through interaction with TLR4 surface expression and signaling (Gowdy et al., 2015, Cai et al., 2012 & Cai et al., 2008). However, it is unknown whether SR-BI mediates pulmonary inflammation/injury induced by criteria air pollutants such as O_3.

1.5 Efferocytosis in the Lung

Typically, after an inflammatory response in the lung, resolution of tissue inflammation must occur to prevent further injury and restore homeostasis. The processes known to promote the resolution of inflammation include apoptosis of recruited immune cells (PMNs, Eosinophils, Lymphocytes), production of anti-inflammatory mediators (IL-10 and TGF-β), and the process of Mϕ uptake and clearance of apoptotic cells termed ‘efferocytosis’(Gheibi Hayat et al., 2019 & Angsana et al., 2016, Donnelly et al., 2012). Mϕ efferocytosis is a tightly regulated process that attenuates the innate immune response by engulfing apoptotic cells and secreting anti-inflammatory mediators including IL-10, TGF-β, and PGE2 (Garabuczi et al., 2015, Fadok et al., 1998, Becker et al., 1991). Mϕs use phagocytic receptors such as MERTK, MFG-E8, RhoA, TIM4, BAI1, TG2, and

scavenger receptors, CD36, SR-A1, SR-F1, and SR-BI, to recognize apoptotic cells through directly binding with extracellular phosphatidylserine or direct cell-cell communication (Das et al., 2016, Frasch et al., 2011, Marik et al., 2011, Zahuczky et al., 2011). Previous studies have also emphasized SR-BI activates the MAPK/GULP/Rac1 pathway to mediate efferocytosis in sertoli cells (Osada et al., 2009). Likewise, recent studies have shown that SR-BI$^{-/-}$ peritoneal Mϕs have an impaired efferocytic response in atherosclerotic lesions through suppressed activation of the Src/PI3K/Rac1 pathway and increased secretion of pro-inflammatory cytokines (Tao et al., 2015). Taken together, these data indicate that SR-BI is critical in processes known to resolve tissue inflammation and injury.

Impaired efferocytosis contributes to the pathogenesis of chronic lung diseases like asthma and interstitial pulmonary fibrosis (Grabiec et al., 2017 & Frasch et al., 2011). Uncleared apoptotic cells in the lung lead to secondary necrosis and autoimmunity, which promote and increase the severity of chronic lung diseases (Gregoire et al., 2018 & Vandivier et al., 2009). The functions of the previously listed phagocytic receptors have been characterized extensively; yet, further study of how scavenger receptors, including SR-BI, can mediate efferocytosis in the context of lung inflammation/injury is needed.

1.6 Innovation

These studies would be the first to uncover the effects of O_3 inhalation on the resolution of pulmonary inflammation and injury. Additionally, it will define the role of SR-BI in mediating efferocytosis in the context of O_3-induced pulmonary injury. A well-planned research strategy will generate first-hand data on how O_3 will impair the resolution of the pulmonary inflammatory response and how that can increase one's

susceptibility to developing chronic respiratory diseases. Lastly, this project will uncover the role of SR-BI following a non-infectious pulmonary inflammatory response. Data collected from this project will help us understand how patients who have single nucleotide polymorphisms in SR-BI are not only susceptible to cardiovascular disease, but also to environmental lung diseases.

1.7 Aims of the Study

Specific Aim 1: Determine whether acute O_3 exposure impairs alveolar macrophage efferocytosis.

Rationale: O_3 induces inflammation and injury through generation of DAMPs, oxidative stress, and impairing AM phagocytosis of bacteria (Bromberg et al., 2016, Park et al., 2013, Cai et al., 2008). Moreover, O_3 exacerbates chronic pulmonary diseases and increases one's susceptibility to developing respiratory infections (Madrigano et al., 2015). However, the underlying mechanisms of how O_3 can exacerbate respiratory diseases is unknown. One factor is the impairment of efferocytosis. Efficient efferocytosis in the lung is imperative in resolving inflammation and restoring tissue homeostasis. However, impaired efferocytosis is a known indicator of chronic pulmonary diseases including asthma, chronic obstructive pulmonary disease, and acute lung injury (Morimoto et al., 2012, Hou et al., 2007, Jakab et al., 1995, Gilmour et al., 1993, Gilmour et al., 1991). In Aim 1, we will determine whether acute O_3 exposure impairs efferocytosis and potentiates pulmonary inflammation and injury. These integrative studies will address unresolved questions about this environmental issue. These experiments will address the question:

1. Does O_3 exposure impair the resolution of pulmonary injury through decreasing the efferocytic response?

Specific Aim 2: Determine if SR-BI mediates alveolar macrophage efferocytosis in the lung following O_3 exposure to resolve pulmonary inflammation and injury.

Rationale: SR-BI has mainly been studied in the context of vascular physiology and atherosclerosis as an HDL receptor, but few studies have uncovered its function in innate immunity. It is known that SR-BI mediates peritoneal Mϕ efferocytosis in atherosclerotic lesions through activation of the Src/PI3K/Rac1 pathway (Tao et al., 2015). However, it is unknown whether O_3-induced impairment of alveolar macrophage efferocytosis is dependent on SR-BI. Efferocytosis of apoptotic PMNs is a critical process in resolving inflammation after an innate immune response in the lung. Preliminary data shows that exposing wild-type (WT) mice to O_3 decreases SR-BI mRNA but increases protein expression in whole lung tissue. Also, through cell sorting pulmonary Mϕ populations in WT mice exposed to O_3, we uncovered that O_3 increases SR-BI mRNA in interstitial macrophages 24 hours following exposure. Additionally, SR-BI$^{-/-}$ mice have increased pulmonary airspace neutrophilia and secretion of pro-inflammatory cytokines compared to WT mice 24 hours post O_3 exposure. SR-BI$^{-/-}$ mice were observed to have increased total apoptotic cells 24 hours post O_3 exposure. In Aim 2, we will determine whether SR-BI mediates efferocytosis following O_3-induced pulmonary inflammation. These integrative studies will address these unresolved questions about this environmental issue**:**

1. Is SR-BI protective during O_3-induced pulmonary inflammation and injury by mediating alveolar macrophage efferocytosis?

2. Does SR-BI scavenge oxidized phospholipids generated by O_3 to mitigate the pulmonary inflammatory response?

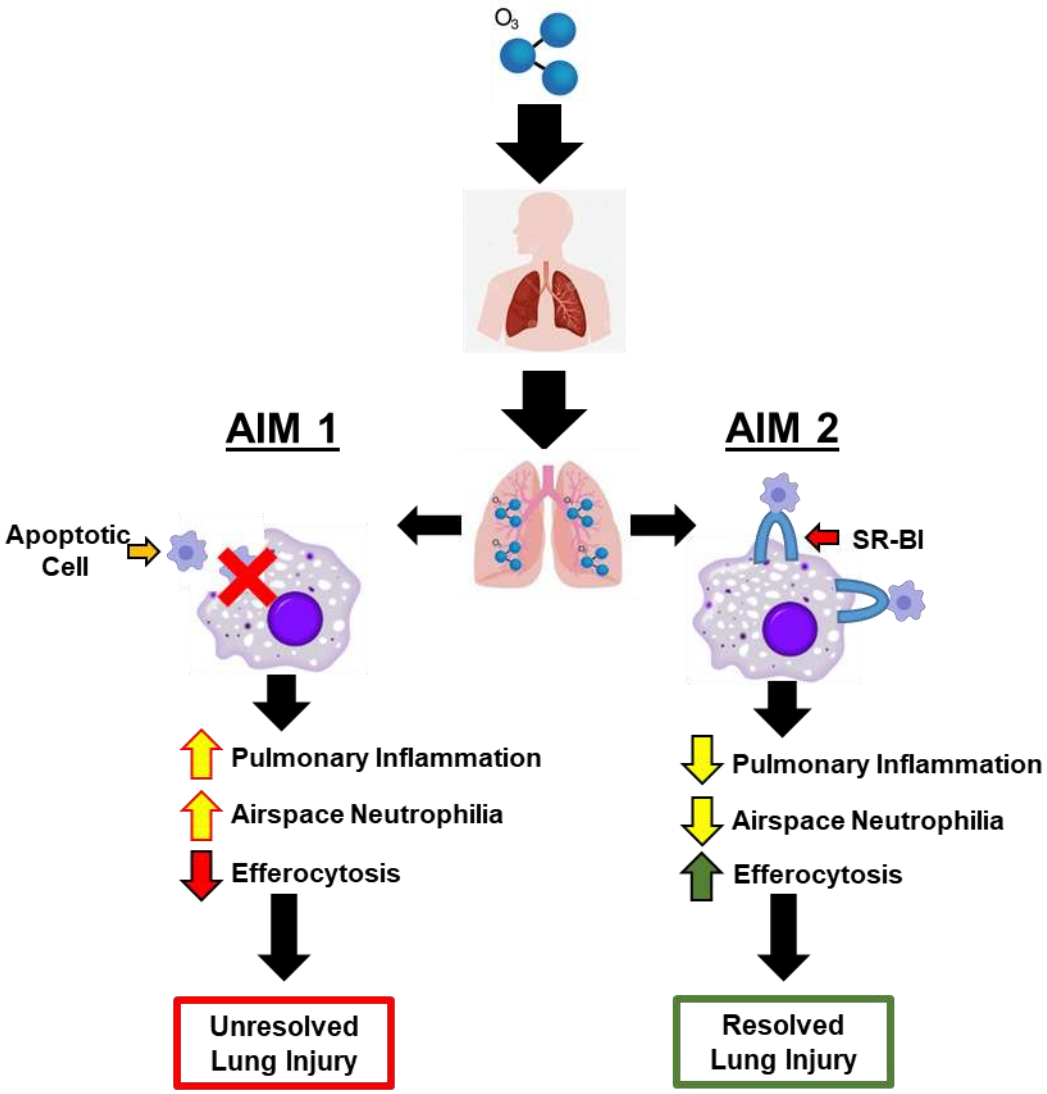
O3
AIM 1
AIM 2
Apoptotic Cell
SR-BI
Pulmonary Inflammation
Airspace Neutrophilia
Efferocytosis
Unresolved Lung Injury
Pulmonary Inflammation
Airspace Neutrophilia
Efferocytosis
Resolved Lung Injury

Figure 1

Figure 1: Specific aims of study. Aim 1 is determining whether acute O_3 exposure impairs alveolar macrophage efferocytosis to cause unresolved pulmonary inflammation/injury. Aim 2 is determining whether SR-BI mediates efferocytosis in the lung after O_3 exposure leading to resolution of pulmonary inflammation.

CHAPTER TWO: OZONE EXPOSURE IMPAIRS ALVEOLAR MACROPHAGE EFFEROCYTOSIS *IN VIVO*

2.1 ABSTRACT:

Ozone (O_3) is a criteria air pollutant that exacerbates and increases the incidence of chronic pulmonary diseases. O_3 exposure is known to induce pulmonary inflammation but little is known how exposure alters processes important in the resolution of inflammation. Efferocytosis is a resolution process whereby macrophages phagocytize apoptotic cells. The purpose of this protocol was to measure alveolar macrophage efferocytosis following O_3-induced lung injury and inflammation. Several methods have been described in the literature for measuring efferocytosis however most require *ex vivo* manipulations. Herein, we described in detail a protocol to measure alveolar macrophage efferocytosis *in vivo* 24 h after O_3 exposure, which avoids *ex vivo* manipulations of macrophages and gives an accurate representation of perturbations in this resolution process. Our protocol is a technically non-intensive and relatively inexpensive method that involves whole body O_3 inhalation followed by an oropharyngeal aspiration (i.e., inhalation) of apoptotic cells (i.e. Jurkat T cells) while under general anesthesia. Alveolar macrophage efferocytosis is then measured by light microscopy evaluation of macrophages collected from bronchoalveolar (BAL) lavage. Efferocytosis is measured by calculating an efferocytic index (i.e. the ratio of alveolar macrophages that have phagocytosed apoptotic Jurkat T cells compared to alveolar macrophages without apoptotic cell uptake). Collectively, the methods outlined in this protocol serve as the basis for a simple experimental technique that can be used to accurately quantify

efferocytic activity in the lung *in vivo*, while serving to analyze the negative health effects of O_3 or other inhaled insults.

2.2 INTRODUCTION:

The lung is constantly exposed to environmental insults, including air particulates, viruses, bacteria, and oxidant gases that trigger pulmonary inflammation (Puttur et al., 2019, Gregoire et al., 2018, Fan et al., 2018). These insults can compromise gas exchange and induce irreversible tissue injury (Bhattacharya et al., 2016 & Michlewska et al., 2007). Alveolar macrophages, which constitutes approximately 95% of the immune cells found in murine and human lungs at homeostasis, are critical regulators of pulmonary inflammation after environmental insults (Puttur et al., 2019, Gregoire et al., 2018, Fan et al., 2018, Bhattacharya et al., 2016, Michlewska et al., 2007). Alveolar macrophages are essential during host defense by phagocytizing and eliminating pathogens. Recently, alveolar macrophages have been shown to promote tissue homeostasis and the resolution of inflammation through efferocytosis (Donnelly et al., 2012 & Morimoto et al., 2012). Efferocytosis is a phagocytic program where macrophages engulf and eliminate apoptotic cells (Grabiec et al., 2017, Vandivier et al., 2009, Chen et al., 2001). The process of efferocytosis also results in the production of mediators, such as IL-10, TGF-β, PGE_2, and nitric oxide, that further augment the process, resulting in the resolution of inflammation (Grabiec et al., 2017, Angsana et al., 2016, Brouckaert et al., 2004, O'Brien et al., 2002, Chen et al., 2001, Gao et al., 1998). This process is necessary in preventing secondary necrosis and promoting tissue homeostasis (Allard et al., 2018, Shen et al., 2017, O'Brien et al., 2002). Several research studies have linked impaired efferocytosis with various chronic lung diseases, including asthma, chronic obstructive

pulmonary disease, and idiopathic pulmonary fibrosis (Hamon et al., 2018, Grabiec et al., 2017, Karaji et al., 2017, Angsana et al., 2016, Vandivier et al., 2009).

Ozone (O_3) is a criteria air pollutant that exacerbates and increases the incidence of chronic pulmonary diseases (Kilburg-Basnyat et al., 2018, Gonzalez-Guevara et al., 2014, Robertson et al., 2013). O_3 induces pulmonary inflammation and injury and is known to impair alveolar macrophage phagocytosis of bacterial pathogens (Jakab et al., 1995 & Gilmour et al., 1991). However, it is unknown if O_3 impairs alveolar macrophage efferocytosis. Investigating O_3-induced alterations in alveolar macrophage efferocytosis will provide potential mechanisms of how exposure can lead to chronic pulmonary disease incidence and exacerbation. Below we describe a simple method to evaluate alveolar macrophage efferocytosis in the lungs of female mice after acute O_3 exposure.

The method outlined in this protocol has several advantages over other efferocytosis protocols commonly used in the field by eliminating the use of costly fluorescent dyes, extensive flow cytometry measurements, and *ex vivo* manipulation of alveolar macrophages (Nayak et al., 2018 & Tao et al., 2015). Additionally, this protocol measures alveolar macrophage efferocytosis in the context of the lung microenvironment which can influence macrophage function.

2.3 MATERIALS AND METHODS:

All methods described here have been approved by the Institutional Animal Care and Use Committee (IACUC) of East Carolina University.

1. Day 1: Ozone (O_3) and Filtered Air Exposures

1.1 Place a maximum of 12 8-12-week-old C57BL/6J female mice in a steel cage (has 12 separate compartments) with wire mesh lids into O_3 exposure chamber.

1.2 Place thermometer in exposure chamber with cage to accurately record temperature and humidity.

1.3 Turn on oxygen and ultraviolet (UV) light that is attached to the apparatus. To note, the O_3 apparatus delivers a regulated airflow (>30 air changes/h) with controlled temperature (22-23 °C) and relative humidity (45-50%). The system generates O_3 in the exposure chamber by directing 100% oxygen through an UV light generator and then mixing with a filtered air supply.

1.4 Adjust the O_3 concentration to 1 ppm and regularly record O_3 levels every 10 min for 3 h. Temperature and humidity of chamber air are monitored continuously, as is the O_3 concentration with a T400 ultraviolet light photometer. Filtered air exposures are done in a similar apparatus with just a filtered air supply flowing through the exposure chamber.

1.5 Return the animals to their respective cages with bedding, food, and water ad libitum after 3 h of O_3/filtered air exposure.

2. Day 2: Preparation of Jurkat T Cell Line (ATCC CRL-2899) (All procedures are conducted in a Class II Biological Safety Cabinet)

2.1 Culture Jurkat T cells in 24 mL of basal cell culture medium + 10% FBS + 5% Penicillin Streptomycin at 37 °C + 5% CO_2 (Table of Materials). Jurkat T cells are a suspension cell line that can be maintained through passaging 1:6-1:8 into pre-warmed culturing media every 3 days. Do not shake.

2.2 To prepare apoptotic cells, grow them to 90% confluency in each flask (which takes 3-4 days to achieve after passaging them). For this study, 5 T75 flasks of cells are

sufficient for the number of cells used in this protocol. NOTE: A confluent flask contains about 20-24 million cells.

2.3 Pipet up cells (which is the entire flask) from each flask (approximately 24 mL) and transfer cells to a sterile 50 mL conical tube using a serological pipet. Use multiple conical tubes for multiple flasks.

2.4 Count cells by removing an 11 µL aliquot of cells from 50 mL conical tube and mix with 11 µL of trypan blue stain and pipette 11 µL onto hemocytometer slides.

2.5 Insert slide into an automated cell counter and record the number of live cells to calculate the total cell count in each flask by multiplying the number of live cells by 24 as each flask contains 24 mL of media.

2.6 Centrifuge cell suspension at 271 x g for 5 min at room temperature to pellet cells.

2.7 Discard supernatant by aspiration and resuspend cell pellet in the amount of media used to obtain $3.0*10^6$ cells per mL.

2.8 Aliquot 5 mL of cells in 100 x 20 mm tissue culture dishes (approximately 9 dishes will be used and the total amount of cells in each dish should be approximately $15*10^6$).

2.9 Use 1 dish for control/unexposed, and the remaining dishes will be exposed to UV.

2.10 Set UV crosslinker to correct energy level, press the energy button and enter in 600 using the number pad, which the machine will read as 600 µJ/cm^2*100. NOTE: UV crosslinker energy units is in µJ/cm^2 *100, therefore, to achieve 60 millijoules/cm2, you must convert units to the UV crosslinker.

2.11 Irradiate all dishes with cells, not including the control, at 60 millijoules (mJ)/cm^2 using a UV Crosslinker, NOTE: Remove the top cover of the tissue culture dishes during UV exposure. UV light will not penetrate plastic cover.

2.12 Incubate all the dishes in a cell culture incubator, including unexposed control, at 37 °C at 5% CO_2 for 4 h.

2.13 Confirm apoptosis by flow cytometry using an apoptosis assay detection kit containing Annexin V and Propidium Iodide (PI), which are markers for apoptosis and necrosis respectively, after 4 h of incubation, per manufacturer's instructions [26-27]. When irradiating Jurkat T cells in the UV Crosslinker at an energy level of 600 µJ/cm^2, following a 4 h incubation lead to ≥75% of apoptotic (both early and late) cells having more early apoptotic cells than late apoptotic cells makes it easier for alveolar macrophages to recognize them and engulf as their membranes are uncompromised unlike late apoptotic cells, leading to a higher efferocytic index and more accurate imaging of alveolar macrophage efferocytosis in this study.

2.13.1 Pool 333 µL ($1*10^6$ cells) of Jurkat T cells from several dishes (both No UV and UV exposed) together to use for compensation analysis tubes.

2.13.2 Aliquot 333 µL of Jurkat T cells in an unstained, annexin V single stain, PI single stain, no UV control, and 600 µJ/cm^2 UV exposed labelled flow cytometry tubes.

2.13.3 Centrifugation tubes at 188 x g for 5 minutes at room temperature and decant supernatant.

2.13.4 Wash cells by resuspending in 500 µL of cold 1X Phosphate buffered saline (PBS).

2.13.5 Centrifuge and pellet cells at 188 x g for 5 minutes at room temperature. Discard supernatant after centrifugation.

2.13.6 Prepare 400 µL of 1X binding buffer per flow tube by diluting 10X binding buffer with distilled water while cells are centrifuging.

2.13.7 Prepare Annexin V and PI incubation reagent (100 µL per sample/tube) per manufacturer's instructions.

2.13.8 Decant supernatant after centrifugation and gently resuspend all tubes in 400 µL of 1X binding buffer, then add 100 µL of Annexin V incubation reagent to each sample tube. Lastly, add 100 µL of Annexin V single stain and PI single stain to their respective tubes, but do not add anything beyond the 1X binding buffer to the unstained tube.

2.13.9 Incubate tubes in the dark for 15 minutes at room temperature.

2.13.10 Centrifuge all cells at 188 x g for 5 minutes at room temperature and decant supernatant.

2.13.11 Resuspend cells in 400 µL of 1X binding buffer and then analyze samples for apoptosis by flow cytometry. Collect at least 10,000 events per tube to allow accurate representation of staining.

2.14 Combine all the irradiated cells from dishes into a 50 mL conical tube and pellet cells by centrifugation at 271 x g for 5 min at room temperature.

2.15 Discard supernatant from tube by aspiration and resuspend cells in 24 mls of sterile phosphate buffered saline (PBS) and pellet cells by centrifugation at 271 x g for 5 min at room temperature.

2.16 Discard supernatant from tube by aspiration and resuspend cells in the amount of PBS used for dosing mice approved by IACUC. The dose used is between 5-10 x 10^6 cells/50 µL per mouse; therefore, for 10 mice resuspend in 500 µL (number of cells in each dose will vary on how many cells are cultured for irradiation). Recommended: make up at least 2 additional doses to account for any liquid that might stick to the sides of the pipette tip resulting in the loss of cells.

Day 2: Murine Oropharyngeal (o.p.) Instillation of Apoptotic Cells

3.1 Prepare dosing inoculum of apoptotic cells using a P200 pipette prior to anesthetizing mice to expedite procedure. As per institutional guidelines, a volume of 50 µL containing approximately 5-10 x 10^6 cells is utilized for oropharyngeal (o.p.) instillation to ensure best results.

3.2 Anesthetize mice in a clear chamber with isoflurane gas (e.g., 2% isoflurane at flow rate of 1 L/min) or as per institutional guidelines. The number of mice to anesthetized together is determined by comfort level of the experimenter, usually 1-2 are done at a time. Observe breathing and confirm level of anesthesia once deep breaths are visible and 2-3 sec can be counted between breaths.

3.3 Once a mouse is anesthetized, position it in a semi recumbent supine position, suspended by the maxillary incisors from a surgical string tied between pegs on a slanted acrylic sheet board.

3.4 Lightly grab and pull the mouse tongue with a pair of blunt non-ridged forceps and deposit dose of apoptotic cells into the oral cavity with a P200 pipette. Exercise great care to avoid inducing trauma to either the tongue or the oropharynx before instillation. Dosing is successful when the mice make a crackling noise 1-2 sec after giving dose.

3.5 Gently occlude the nose with a gloved finger until the mouse inhales while the tongue is retracted and cover the nose until the mouse has taken two or more inhalations, and no liquid is visible in the oral cavity. NOTE: Covering the nose helps ensure that the mouse will inhale the apoptotic cells into the lungs, as mice are obligate nose breathers.

3.6 Remove the mouse from the inoculation board and return to its cage, placing the mouse on its back to prevent bedding or debris from blocking the nares while the mouse is recovering from anesthesia.

3.7 Wait 90 min to allow alveolar macrophages to engulf influx of apoptotic cells after all the mice have awoken from anesthesia (Typically, this will take 1-2 minutes for the mice to awake following anesthesia, which should not affect the outcome/timing of the instillation).

3. Day 2: Bronchoalveolar Lavage (BAL) Fluid Collection and Processing

4.1 Euthanize each mouse per institutional guidelines 90 mins after dosing with apoptotic cells. Here, a lethal injection of ketamine/xylazine is used (90 mg/kg/10 mg/kg) followed by excising the diaphragm. **NOTE: This time point allows**

sufficient time for alveolar macrophages to sense and engulf apoptotic cells (Park et al., 2008).

4.2 Weigh all mice (in grams) on scale and record weight. Body weight is used to calculate BAL volume (26.25 mL/kg body weight).

4.3 Place mouse on their back and sterilize it by spraying fur with 70% ethanol over chest and neck area.

4.4 Make a 2 in longitudinal cut just below the sternum along the entire ventral side with surgical scissors and while holding the sternum with forceps, nick the diaphragm to allow the lungs to fall back into the chest cavity.

4.5 Cut laterally along the sides of the rib cage to allow lungs to have more room to expand when lavaging and fold chest cavity back with forceps.

4.6 Cut a 1 in vertical cut up along vascular up through the neck to expose the trachea.

4.7 , Use two forceps to pull muscle and tissue off trachea to expose it to avoid additional potential bleeding and cutting the trachea, since it is surrounded by vasculature, longitudinal muscles and connective tissue.

4.8 Use a needle to make a slit in the trachea (about ¼ of the way down from the head) and insert a cannula (18 G x 1 ¼ inches) with a syringe pre-loaded with 1x PBS (26.25 mL/kg body weight, approximately 0.7-1.0 ml in an 8-10-week-old female C57Bl/6J mouse) caudally into the trachea.

4.9 Push volume of PBS into the lungs slowly to allow the lungs to inflate then, pull the volume back out into the syringe. Repeat this process a total of 3 times. If PBS is

coming out of the nostrils, either the cannula has not been inserted far enough into the trachea or inflation is occurring too quickly. Alternatively, if the lungs are not inflating well, the cannula has been pushed in too far, so withdraw cannula slightly.

4.10 Collect pooled lavage fluid from each specific mouse in a 15 mL tube.

4.11 Centrifuge the bronchoalveolar lavage at 610 x g for 6 min at 4 °C and collect supernatant into a 1.5 mL tube and freeze at -80 °C. The pellet represents cells from the bronchoalveolar space.

4.12 Remove residual red blood cells in collected BAL fluid by adding 1 mL of ACK RBC Lysis buffer to the cell pellet, then vortex well, and lyse for 1 min on ice. Afterwards, add 4 mL of PBS to stop lysis reaction.

4.13 Pellet cells by centrifugation at 610 x g for 6 min at 4 °C and aspirate supernatant with vacuum aspirator.

4.14 Resuspend cells in 1 mL 1x PBS+10% FBS to each BAL sample tube.

Count cells on a hemocytometer for quantification of total airspace cells from each sample (No trypan blue). Each sample (120 µL) is centrifuged onto slides at 41 x g for 3 min, medium acceleration, using a cytocentrifuge. Slides are set aside to dry overnight.

4. Day 3: Calculation of Alveolar Macrophage Efferocytic Index

5.1 Stain slides with hematoxylin and eosin to allow for calculation of both efferocytic and differential cell counts, with at least 200 cells counted from each slide.

5.2 view slides on brightfield setting on a biological microscope (20 or 40 x objective will work best).

5.3 Calculate the efferocytic index based on the ratio of the number of alveolar macrophages that phagocytosed apoptotic Jurkat T cells to alveolar macrophages without apoptotic cell uptake out of a total 200 macrophages on a cell differential slide. The ratio is then converted to a percentage for data input. (Number of alveolar macrophages engulfed apoptotic cells/Number of alveolar macrophages that did not engulf cells *100). Examples of efferocytic macrophages are denoted by black arrows in figure 3.

2.4 RESULTS:

O_3 exposure is known to induce pulmonary inflammation and injury and efferocytosis is required to maintain tissue homeostasis. C57BL/6J female mice were exposed to filtered air (FA) or 1 ppm O_3 for 3 h and necropsied 24 h post exposure to examine pulmonary inflammation and injury. O_3 exposed mice displayed a significant increase in macrophages and neutrophils in their airspace compared to the FA control group (Figure 1A and B). Additionally, O_3 exposed mice had a significant increase in BAL protein, a marker of alveolar epithelial barrier dysfunction 24 h post exposure (Figure 1C). To determine if O_3-induced pulmonary inflammation was associated with defects in alveolar macrophage efferocytosis *in vivo*, C57BL/6J female mice were instilled with apoptotic Jurkat T cells via oropharyngeal aspiration 24 h post FA or O_3 exposure. Apoptosis in Jurkat T cells was confirmed by flow cytometry prior to dosing and there was a significant increase in early (Annexin V^+ PI^- and late (Annexin V^+ and PI^+) apoptotic cells (Figure 2A and B). The exposure level and incubation time resulted in repetitive results of ~75% apoptotic Jurkat T cells. A magnified image of what is identified as an efferocytic macrophage is shown in Figure 3A. Efferocytic macrophages were identified as macrophages that had engulfed a Jurkat T cell (indicated by black arrows), when compared to regular alveolar macrophage (indicated by white arrows) (Figure 3B). When alveolar macrophage efferocytosis was assessed utilizing the protocol described above, there was a statistically significant decrease in the efferocytic index in the O_3 exposed group when compared to FA controls (Figure 3B and C). These data indicate that O_3-induced pulmonary inflammation is associated with decreased clearance of apoptotic cells, which may prolong lung injury and inflammation.

A)

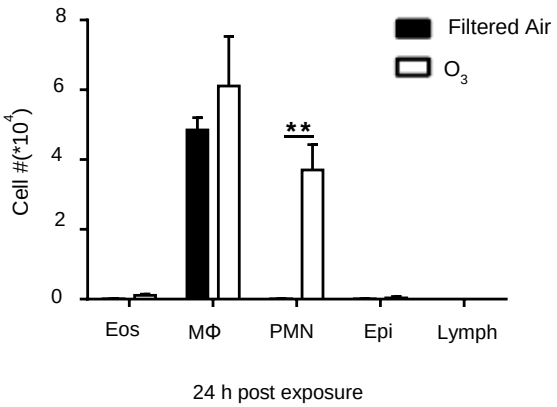

24 h post exposure

B)

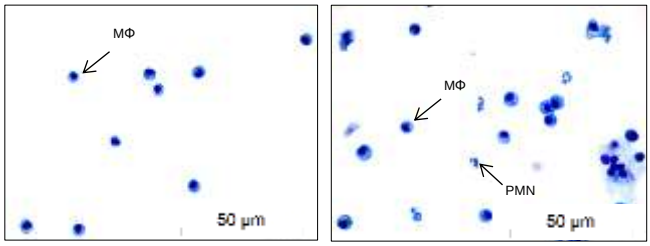

FA control

24 h post-O_3

C)

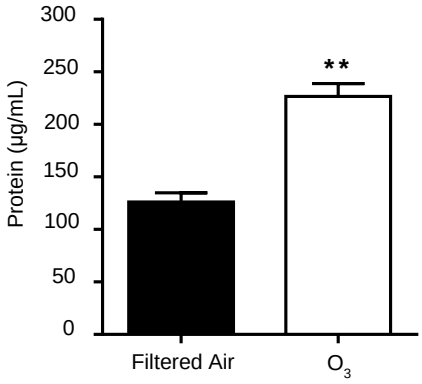

24 h post exposure

Figure 1: O_3 exposure induces pulmonary inflammation and injury. C57BL/6J female mice were exposed to filtered air (FA) or 1 ppm O_3 for 3 h. 24 h post exposure, mice were necropsied to analyze pulmonary inflammation and injury (n=6/group). A) Bronchoalveolar lavage (BAL) cell differentials were calculated and epithelial (epi), eosinophils (eos), lymphocytes (lymph), macrophages (Mϕ), and neutrophils (PMN) were identified with at least 200 cells counted from each slide. B) A representative image of cellular differentials. C) Total protein in the BAL fluid. Data are expressed as ±SEM **p<.01.

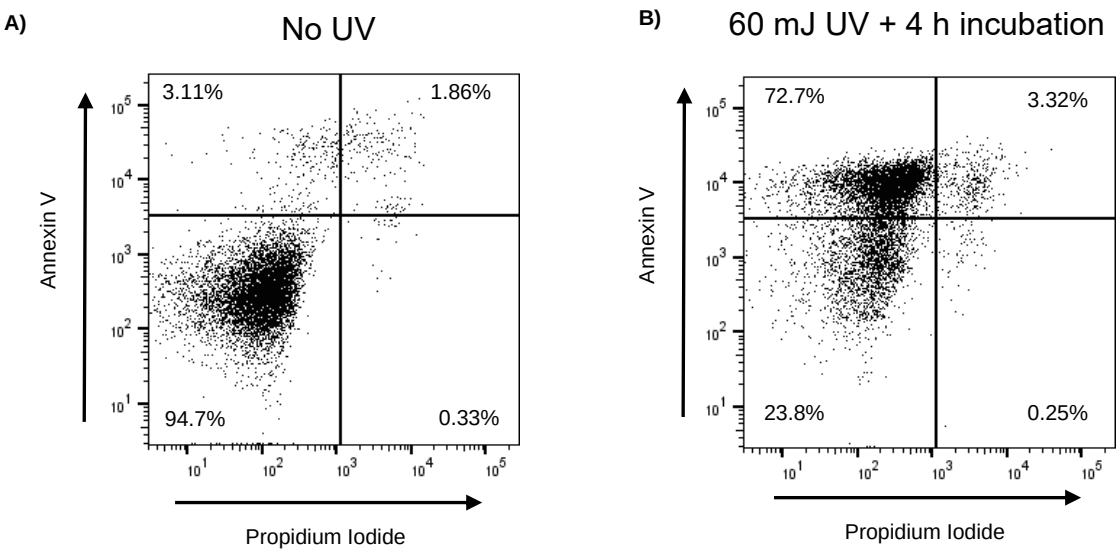
A)
No UV
3.11%
1.86%
94.7%
0.33%
Annexin V
Propidium Iodide
B)
60 mJ UV + 4 h incubation
72.7%
3.32%
23.8%
0.25%
Annexin V
Propidium Iodide

Figure 2: Confirmation of UV induced apoptosis in Jurkat T cells. Jurkat T cells were exposed to UV (60 mJ/cm^2) using a UV Crosslinker (Model 1800). Following UV exposure Jurkat T cells were incubated at 37 °C with 5% CO_2 for 4 h. Following incubation, Jurkat T cells were stained with Annexin V and Propidium Iodide (PI) and apoptosis was evaluated by flow cytometry. Early apoptotic, late apoptotic, and necrotic cells are identified as Annexin V^+/PI^- and Annexin V^+/PI^+, Annexin V^-/PI^+, respectively. Representative flow cytometry scatter plots, with 10,000 events recorded, of A) unexposed Jurkat T cells and B) UV exposed Jurkat T cells.

A)

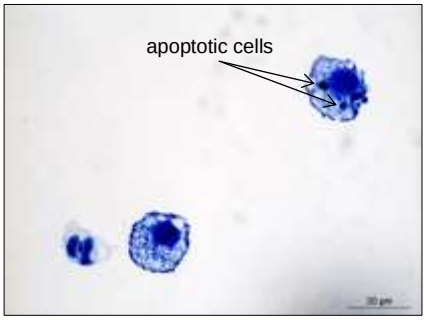
apoptotic cells

B)

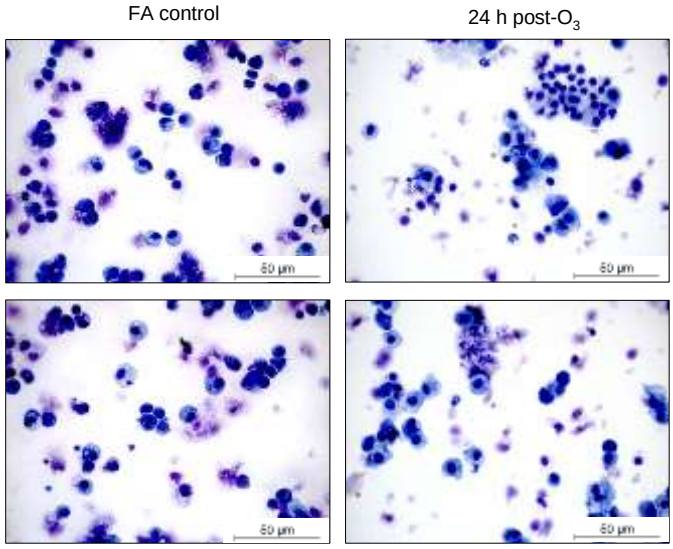
FA control
24 h post-O3
50 µm
50 µm
50 µm
50 µm

C)

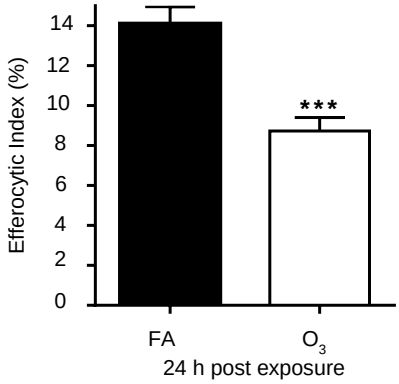
Efferocytic Index (%)
14
12
10
8
6
4
2
0
***
FA
O3
24 h post exposure

Figure 3: O_3 exposure decreases alveolar macrophage efferocytosis. C57BL/6J female mice were exposed to filtered air (FA) or 1 ppm O_3 for 3 h. 24 h post exposure mice were oropharyngeally instilled with approximately 5 x 10^6 apoptotic Jurkat T cells. 1.5 h after instillation, bronchoalveolar lavage (BAL) was performed and the efferocytic index was calculated in BAL macrophages by light microscopy after counting 200 macrophages (n=11/group). A) Representative image of an efferocytic macrophage. B) Identification of alveolar macrophages (white arrows) and efferocytic macrophage (black arrows) after FA or O_3 exposure. C) Calculation of the efferocytic index after FA or O_3 exposure. ***p<.0001.

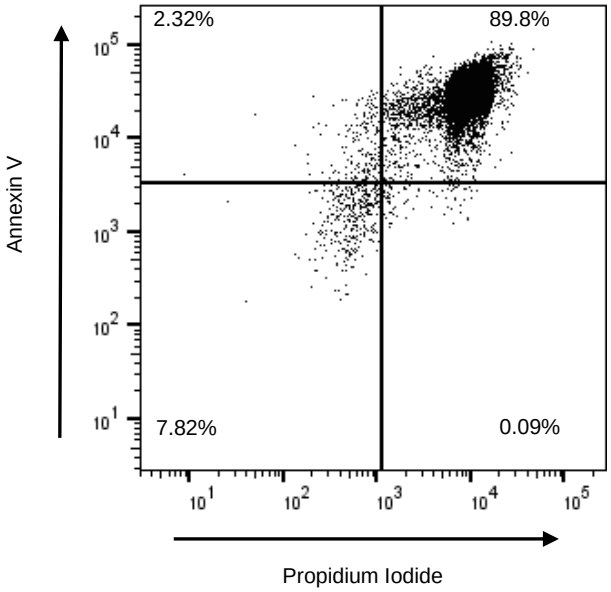
2.32%
89.8%
7.82%
0.09%
Annexin V
Propidium Iodide

Figure 4: Suboptimal Jurkat T cell apoptosis using 350 nm frosted bulbs. Jurkat T cells were irradiated using the UV Crosslinker Model 1800 for 10 min and incubated at 37 °C at 5% CO_2 for 1 h. Following UV exposure Jurkat T cells were incubated at 37 °C with 5% CO_2 for 4 h. Following incubation, Jurkat T cells were stained with Annexin V and Propidium Iodide (PI) and apoptosis was evaluated by flow cytometry. Early apoptotic, late apoptotic, and necrotic cells are identified as Annexin V^+/PI^- and Annexin V^+/PI^+, Annexin V^-/PI^+, respectively. Representative flow cytometry plots, with 10,000 events recorded, of UV exposed Jurkat T cells with 350 nm bulbs.

2.5 DISCUSSION:

Efferocytosis is an anti-inflammatory process whereby macrophages clear out apoptotic cells and debris as well as produce multiple anti-inflammatory mediators (Grabiec et al., 2017, Angsana et al., 2016, Brouckaert et al., 2004, O'Brien et al., 2002, Chen et al., 2001, Gao et al., 1998). Multiple models of efferocytosis have provided insight into how the macrophage is a critical cell in the resolution of inflammation (Donnelly et al., 2012 & Morimoto et al., 2012). Recently, the progression of chronic lung diseases has been associated with defects in efferocytosis (Hamon et al., 2018, Grabiec et al., 2017, Karaji et al., 2017, Angsana et al., 2016, Vandivier et al., 2009). However, it is currently unclear if exposure to air pollutants such as O_3, results in defects in efferocytosis. The protocol outlined here enables the evaluation of alveolar macrophage efferocytosis after O_3 exposure. This protocol quantifies efferocytosis *in vivo* using light microscopy and allots measurement of efferocytosis in the context of the lung microenvironment, without *ex vivo* manipulations or expensive fluorescent dyes. Although this protocol is performed in the context of O_3 exposure, multiple models of lung inflammation and injury can be used with this protocol to evaluate alveolar macrophage efferocytosis.

Advantages of this method over existing methods is the ability to analyze alveolar macrophages in the context of their physiological environment. *Ex vivo* analysis of alveolar macrophages includes plating and incubation with apoptotic cells. Plating alveolar macrophages can induce both physiological and genomic changes that may alter efferocytosis (Beattie et al., 2016, Van de Laar et al., 2016, Lavin et al., 2014). Additionally, in the lung, alveolar macrophages are in a microenvironment that contains surfactant and components of the lung lining fluid that are known to influences

macrophage function (Svedberg et al., 2019, Gomez Perdiguero et al., 2015, Silveyra et al., 2012, Crowther et al., 2004, Schagat et al., 2001). Our method allows efferocytosis measurements in the lung with no *ex vivo* manipulations, which is more physiologically relevant. Future applications of this protocol can lead to more in-depth studies about the how the lung microenvironment can alter alveolar macrophage efferocytosis.

A critical component of this protocol is the generation of apoptotic cells for evaluation of alveolar macrophage efferocytosis. This involves optimizing the correct UV exposure level to induce apoptosis not necrosis. Our protocol uses the UV crosslinker Model 1800 with 254 nm wavelength emission bulbs and an exposure level of 60 mJ/cm^2. The UV bulb choices is critical to producing apoptosis not necrosis. 350 nm UV bulbs are excellent for protein membrane cross-linking and sterilization but fail to induce apoptosis (Nebbioso et al., 2017, Gomez Perdiguero et al., 2015, Novak et al., 2004). An example dot plot of Jurkat T cells exposed to 60 mJ/cm^2 with 350 nm bulbs are shown in Figure 4 with a significant increase in late apoptotic and necrotic cells. Additionally, our protocol uses a 4 h incubation post UV exposure. To optimize this part of the protocol, we previously examined various incubation times. 1.5 and 2 h incubation post exposure only yielded approximately 40% apoptosis, with efferocytic index of less than 5% (data not shown). Based on current literature, ~70-80% total apoptotic cells are sufficient for measuring efferocytosis (Park et al., 2008).

We acknowledge a limitation to this protocol is that it examines the efferocytic response of all macrophages in the airspace after FA or O_3 exposure and does not distinguish tissue resident macrophages from recruited macrophages. The lung resident macrophage termed ‘alveolar macrophage’ originate from the fetal liver, whereas

recruited macrophages derive from a blood-borne embryonic origin. Upon injury, the lung can have a highly heterogeneous macrophage population with unique genetics and expression of cell surface markers (Svedberg et al., 2019, Beattie et al., 2016, Van de Laar et al., 2016, Gomez Perdiguero et al., 2015, Lavin et al., 2014, Silveyra et al., 2012, Crowther et al., 2004, Schagat et al., 2001). It is known that the immunological response and function of these macrophage populations are different, however recent studies have indicated that the tissue resident macrophage have a greater efferocytic response when compared to recruited macrophages (Svedberg et al., 2019, Beattie et al., 2016, Lavin et al., 2014). To determine the efferocytic response of tissue resident macrophages versus recruited macrophages can be assessed with the current protocol, however, the macrophage populations would need to be purified by FACS and then plated on slides for analysis. Additionally, this protocol only assesses alveolar macrophage efferocytic function in one strain of inbred, commercially available mice. It has previously been reported that different strains of mice have different response to O_3 exposure, including pulmonary inflammation (Wesselkamper et al., 2001 & Kleeberger et al., 2000). Therefore, there could be differences in alveolar macrophage efferocytosis based on strain examined. This is a variable that should be considered when performing this *in vivo* assay.

In conclusion, the protocol described above allows the evaluation of alveolar macrophage efferocytosis *in vivo*. This protocol is cost effective and simple, making it an assay that can be widely utilized. Moreover, this method can be applied to numerous models of lung injury and/or inflammation to increase our understanding of how various pulmonary insults can alter macrophage efferocytosis.

ACKNOWLEDGMENTS:

This study is funded by Health Effects Institute Walter A. Rosenblith Award and NIEHS R01ES028829 (to K.M.G). We would like to thank Dr. Dianne Walters (Department of Physiology, ECU) for her assistance with obtaining representative images of alveolar macrophages.

CHAPTER THREE: SCAVENGER RECEPTOR B-I MITIGATES OZONE-INDUCED PULMONARY INFLAMMATION THROUGH MAINTAINING ALVEOLAR MACROPHAGE EFFEROCYTOSIS

3.1 ABSTRACT:

Ozone (O_3), a criteria air pollutant, is the primary component of photochemical smog. Short and long-term exposure to O_3 has been associated with increased susceptibility and/or exacerbations of chronic pulmonary diseases through lung injury and inflammation. O_3 induces pulmonary inflammation in part through generating damage associated molecular patterns (DAMPs) including oxidized phospholipids (oxPLs). These DAMPs are then recognized by pattern recognition receptors (PRRs), such as toll-like receptors (TLRs) and scavenger receptors (SRs). Scavenger Receptor B-I (SR-BI), a class B SR, is known to recognize oxPLs and facilitate the clearance of apoptotic cells termed “efferocytosis.” The central hypothesis of this study was that SR-BI attenuates O_3-induced pulmonary inflammation by maintaining effective alveolar macrophage efferocytosis. Our findings demonstrated that O_3 increases the levels of SR-BI in the lung. Also, our model showed both acute O_3 exposure and oxidized 1-palmitoyl-2-arachidonyl-sn-glycero-3-phosphorylcholine (oxPAPC) induce pulmonary inflammation and injury. However, O_3 induced pulmonary injury was not dependent on the generation of oxPLs in either WT or SR-BI$^{-/-}$ mice. Additionally, SR-BI$^{-/-}$ mice exposed to O_3 had increased pulmonary neutrophilia that persisted up to 48 h post exposure and impaired alveolar macrophage (AM) efferocytosis 24 h post exposure. Furthermore, SR-BI$^{-/-}$ mice dosed with oxPAPC had augmented pulmonary inflammation and injury. Collectively, these

findings uncovered a protective role for SR-BI in the O_3 and O_3-induced DAMP pulmonary inflammatory response.

3.2 INTRODUCTION:

Despite increasing regulations, air pollution levels continue to rise and significantly contributing to global morbidity and mortality. Exposure to ozone (O_3), a criteria pollutant, exacerbates existing lung diseases, causes decrements in lung function, and increases susceptibility to respiratory infections (Zhang et al., 2019, Chen et al., 2015, Pino et al., 1992). These responses have profound health effects on at risk populations including individuals with underlying respiratory diseases (asthma, COPD), children, and the elderly. O_3 impairs respiratory responses by inducing pulmonary inflammation and injury which is characterized by epithelial cell damage, cytokine/chemokine release by macrophages, suppression of alveolar macrophage phagocytosis, and neutrophil (PMN) recruitment into the airspace (Al-Hegalan et al., 2011, Hollingsworth et al., 2007, Mikerov et al., 2008, Gilmour et al., 1991). If O_3-induced inflammation is not resolved, the lung does not return to homeostasis and chronic inflammation occurs; causing or exacerbating chronic pulmonary diseases.

When O_3 is inhaled, its primary target is the epithelial lung lining fluid. This results in the generation of secondary oxidation products termed danger associated molecular patterns (DAMPs). Known O_3-induced DAMPs include oxidized phospholipids (oxPLs), low molecular weight hyaluronan (HA), and oxysterols (Bromberg 2016). These DAMPs are recognized by pattern recognition receptors including toll-like receptors (TLRs) and scavenger receptors (SRs) and promote pulmonary inflammation and injury (Roh et al.,

2018, Komai et al., 2017, Bauer et al., 2011, Dahl et al., 2007, Williams et al., 2007). Adequate clearance of these DAMPs is critical for the restoration of the lung to homeostasis.

Scavenger Receptor B-I (SR-BI), a class B scavenger receptor, is a membrane bound receptor, mostly studied in vascular biology because of its role in cholesterol ester uptake from high density lipoprotein (HDL) (Linton et al., 2017, Zhang et al., 2005, Krieger et al., 1999). In addition to recognizing HDL, SR-BI has also been reported to bind a broad array of ligands, both endogenous (oxPLs, serum amyloid A, α-1 antitrypsin (A1AT) and exogenous (pathogens, lipopolysaccharide) (Shen et al., 2018, Cai et al. 2012, Cai et al., 2005). While there have been multiple studies investigating the role of class A SRs in lung diseases, the role of SR-BI in the lung is understudied. In the airspace, SR-BI is expressed on alveolar macrophages and alveolar epithelial cells where it mediates the uptake of Vitamin E (Santander et al., 2017, Valacchi et al., 2007, Kolleck et al., 2000). Recent studies from our lab indicate that SR-BI is critical in the pulmonary host defense response during bacterial pneumonia (Gowdy et al., 2015). However, the role of SR-BI in oxidant-induced lung diseases, such as pulmonary inflammation and injury noted after O_3 exposure, have not been defined. Therefore, we hypothesized that SR-BI is protective against O_3-induced pulmonary inflammation and injury through maintaining alveolar macrophage efferocytosis and clearance of DAMPs.

Herein, we report that SR-BI expression is increased in the lung after acute O_3 exposure, modeling levels seen during 'O_3 action days.' Additionally, SR-BI$^{-/-}$ mice have increased PMN recruitment to the airspace that is coupled with impaired alveolar

macrophage efferocytosis. Similar findings were noted when SR-BI$^{-/-}$ mice were dosed with an O_3-induced DAMP, oxPL and when SR-BI is pharmacologically inhibited in the airspace. Taken together, we report a new and essential role for SR-BI in the oxidant-induced pulmonary inflammatory response noted after O_3 exposure.

3.3 MATERIALS AND METHODS:

Animals

C57BL/6J (WT) and B6;129S2-Scarb1^{tm1Kri}/J (SR-BI$^{-/-}$) female mice, 8-13 weeks old and weighing 18-22g, were purchased from Jackson Laboratories (Bar Harbor, ME) and bred in house. SR-BI$^{-/-}$ mice were backcrossed >6 generations onto C57BL/6J before use. Previous experiments conducted using both littermate SR-BI$^{+/+}$ and commercial SR-BI$^{+/+}$ (C57BL/6J) controls confirmed very similar responses (Gowdy et al., 2014). All experiments were performed in accordance with the Animal Welfare Act and the U.S. Public Health Service Policy on Humane Care and Use of Laboratory Animals after review by the Animal Care and Use Committee of East Carolina University.

Murine in vivo exposures

WT and SR-BI$^{-/-}$ mice were placed in stainless steel wire exposure chambers inside a metal hinders chamber and exposed to filtered air (FA) or ozone (O_3) for 3 h at a dose of 1ppm. The 1 ppm O_3 exposure dose was designed to mimic a human exposure of 200 ppb and is based on prior data and published deposition fractions between rodents and humans (Hatch et al., 1994 & Wiester et al., 1988). O_3 is generated in the chamber by directing 100% oxygen through an ultraviolet light generator using a Teledyne T703 O_3

calibrator (Teledyne API, San Diego, CA) and then mixing with a filtered air supply. Temperature and humidity of chamber air are monitored continuously, as is the O_3 concentration with a Teledyne T400 ultraviolet light photometer (Teledyne API). For some experiments, mice were given Blocking Lipid Transport 2 (BLT-2) (ChemBridge, San Diego, CA; 250µg/kg) by oropharyngeal aspiration (o.p.) to block SR-BI in the airspace as previously described (Shannahan et al., 2015). To evaluate the role of O_3-induced oxidized phospholipids in pulmonary inflammation, 200µg/ml of oxidized 1-palmitoyl-2-arachidonyl-sn-glycero-3-phosphorylcholine (oxPAPC) (Hycult Biotech, Wayne, PA; 200µg/kg) was instilled o.p. The doses of BLT-2 and oxPAPC instilled in mice were used based on the previous publications (Aldossari et al., 2015 and Thimmulappa et al., 2012). Mice were euthanized with an intraperitoneal (i.p.) injection of ketamine/xylazine (90 mg/kg/10 mg/kg).

Bronchoalveolar lavage fluid (BALF) collection and analysis

BALF was collected immediately following sacrifice. The lung lobes were lavaged 3 times with 3 volumes of 0.9% saline solution (Braun Medical Inc., Irvine, CA). The lavage volume was based on bodyweight (26.25 ml/kg body weight) as previously described (Wang et al., 2011 & Draper et al., 2010). The resulting lavage was centrifuged (1800 RPM, 6 min, at 4°C). Total protein was measured in BALF supernatant using the bicinchoninic acid assay (BCA) Protein-Assay Kit (Thermo Scientific, Hercules, CA). Differential analyses of cells in BALF was performed as described previously (Kilburg-Basnyat et al., 2018 and Van Hoecke et al., 2017).

Isolation of alveolar and interstitial macrophages

To isolate alveolar macrophages, WT and SR-BI$^{-/-}$ mice were either naïve or exposed to 1ppm O_3 and necropsied 24 h and 48 h post exposure. Whole lung tissue was perfused with cold saline and digested with 10mg/ml of Collagenase A (Roche, Indianapolis, IN) and 20 mg/ml of DNase I (Roche) in Hanks' balanced salt solution with 5% fetal bovine serum and 10mM of 4-(2-hydroxyethyl)-1-piperazineethanesulfonic acid (HEPES). Lung tissues was digested at 37°C with continuous agitation for 30 minutes and washed with PBS until dissolved into single cell suspensions. Single cell suspension was then passed through at 70µm filter and counted on a hemocytometer. Cells were blocked and then stained with zombie aqua viability dye, (Biolegend, San Diego, CA) and additional markers to isolate alveolar macrophages. Alveolar macrophages were defined as CD45^{+}CD24^{-}Ly6G^{-}CD64^{+}CD11b^{low} by fluorescence activated cell sorting (FACS) using a BD FACSAria™ Fusion (BD Biosciences). Flow antibodies used were Anti-CD45 (APC-Cy7), Anti-CD64 (APC), Anti-CD11b (PE-Cy7), Anti-CD11c (PerCP Cy5.5), Anti-Ly6C (FITC), Anti-Ly6G (BV421), Anti-CD24 (BV421). clone #1A8), -CD11c (PerCP-Cy5.5, clone#N418), and -CD11b (Pacific Blue, clone#M1/70).

Oxidized phospholipid (oxPL) measurement in BALF

100 µl of sample was added to 1 ml of water and mixed with 1.8 ml methanol containing 3% acetic acid and 0.01% butylated hydroxytoluene (BHT). 5.3 µl of 0.5 µM [$^{2}H_4$]C16:0-platelet activating factor ([$^{2}H_4$] PAF) was added as an internal standard and the mixture

vortexed. 4 ml of heptane with 0.01% BHT was then added, the sample vortexed, and centrifuged at 1750 g for 10 min. The upper phase was then removed by aspiration and discarded and the lower phased washed two more times with heptane/BHT. To extract oxidized phosphatidylcholines (oxPC), a mixture of 4 ml of chloroform with 0.01% BHT (0.01%) and 1 ml of 0.7 M formic acid was added to the lower phase and vortexed well. After centrifugation, the resulting lower (chloroform) phase was collected and dried under nitrogen gas and the sample reconstituted in 100 µl of 85% methanol with 0.1% formic acid, sonicated, filtered through a 0.2 µm filter, and then transferred to autosample vials for injection on LC/MS.

LC/MS was carried out using Waters Acquity UPLC coupled to AB Sciex QTRAP6500 Solvent A was 0.1% formic acid in water, Solvent B was 0.1% formic acid in methanol, and the HPLC column was Waters BEH C18 1.7 µm 2.1x50 mm column. Initial conditions were a flow rate of 0.2 ml/min at 50% A for 3 min, followed by linear gradient ramp to 15% A for 2 min; then a gradient ramp to 0% A over 2 min along with ramp of flow rate to 0.4 ml/min; after a 2 min hold at these conditions, flow and solvent were returned to initial conditions and allowed to equilibrate for 1.5 min prior to starting the next injection . The mass spectrometer was operated in multiple reaction monitoring positive ion mode, with ion source spray voltage set at 5,500 V, temperature at 400^{o}C. Nitrogen was used for the ion source gas 1 and gas 2 at pressures of 30 and 50 arbitrary units, respectively. For each analyte, transition reactions to the m/z 184.1 product ion at -35 eV collision energy were monitored. Precursor ions for these transitions were as follows: PGPC m/z 610.3, SGPC m/z 638.3, POVPC m/z 594.3, SOVPC m/z 622.3, PONPC m/z 650.3, SONPC m/z 678.3, PAzPC m/z 666.3, SAzPC m/z 694.3, [$^{2}H_{4}$] PAF internal standard m/z 528.3.

Values in sample for each analyte were calculated using the ratio of peak areas for the analyte vs [$^{2}H_{4}$] PAF times the amount of internal standard added (2.7 pmol) divided by sample volume.

RNA isolation and quantitative polymerase chain reaction (qPCR)

RNA was isolated by RNEasy kit (Qiagen, Venlo, Netherlands). Complementary DNAs (cDNA) were generated from purified RNA using TaqMan reverse transcription reagents from Applied Biosystems (Foster City, CA). Real time PCR was performed in triplicate with Taqman PCR Mix (Applied Biosystems) in the HT7900 ABI sequence Detection System (Applied Biosystems). Predesigned primers were purchased from Applied Biosystems. Fold changes in expression for mRNA quantities were calculated using Ct values and the $2^{-\Delta\Delta Ct}$ method. Samples were normalized to 18S as previously described (Kilburg-Basnyat et al., 2018). See Table 1 for primer information.

Western Blot Analyses

Total proteins were extracted from lung tissue samples using a RIPA lysis buffer (Thermo Scientific, Rockford, IL) containing a protease inhibitor cocktail (Calbiochem, San Diego, CA), and NaF at 1M. Lysis buffer was added to each sample according to weight (50 µL/mg) and homogenized using a bead mill 4 homogenizer (Fisherbrand, Waltham, MA). Protein concentrations were quantified using a Pierce BCA Protein Assay Kit (Thermo Scientific, Rockford, IL). 30 µg of protein was mixed with an equal volume of 2x sample buffer, loaded on a 12% SDS-PAGE gel, electrophoresed and transferred to a polyvinylidene difluoride (PVDF) membrane by a transfer system (Bio-Rad Laboratories,

Inc. Des Plaines, IL). The membrane was blocked with 5% BSA in Tris-buffered saline with Tween 20 and incubated with a primary anti-rabbit polyclonal SR-B1 (82 kDa) antibody (1:1000) at 4°C overnight. A goat anti-rabbit lgG (H+L) secondary antibody (1:8000) was used to incubate the membrane at room temperature for 1 h followed by incubation for 1 minute with clarity western ECL substrate (Bio-Rad Laboratories, Inc. Des Plaines, IL). The blot was then imaged in molecular imager with β-actin (42 kDa) used as an internal control. The intensity of the blot band was quantified and analyzed by Image Lab.

In Vivo Efferocytosis Assay

Assay procedures were performed as previously described (Hodge et al., 2019). Jurkat T cells (ATCC® CRL-2899™), were grown based on manufacturer's instructions, plated, and UV irradiated (Stratalinker® UV Crosslinker model 1800) at 60mJ/cm^2 to induce apoptosis. Following irradiation, Jurkat T cells were incubated for 4 h at 37^{0}C with 5% CO_2. Apoptosis was confirmed via Annexin V and Propidium Iodide (PI) (Trevigen, Gaithersburg, MD) staining by flow cytometry (Analyzed on BD Biosciences LSRII). Cells were approximately 75% apoptotic. 1*10^6 cells were instilled o.p. and 1.5 h after dosing, mice were euthanized and BALF harvested for cytospins. The efferocytic index was calculated based on the number of alveolar macrophages that phagocytosed apoptotic Jurkat T cells compared to the number of alveolar macrophages without apoptotic cell uptake out of a total 200 macrophages.

In Vitro oxPAPC Stimulation and Efferocytosis Assay

To harvest peritoneal macrophages, WT and SR-BI$^{-/-}$ Mice were euthanized 96 h after i.p. injection of 2 ml 4% thioglycolate. Peritoneal cells were harvested by peritoneal lavage with sterile PBS and counted using an automated cell counter (Countess II Automated Cell Counter (Thermofisher, Waltham, MA). To determine differences in the inflammatory response between WT and SR-BI$^{-/-}$ mice, plated macrophages were incubated with RPMI + 0.1% FBS low-serum media or low-serum media plus 50µg/ml oxPAPC for 3 h. Cell lysates were used to isolate RNA for RT-PCR. To determine differences in the efferocytic response, peritoneal macrophages were incubated with Calcein AM (1mg/ml) (Thermofisher, Waltham, MA) fluorescent dye stained apoptotic Jurkat T cells for 20 min, with and without prior oxPAPC incubation, and the efferocytic index was calculated. Approximately 1000 macrophages were counted to calculate the efferocytic index.

Statistical Analysis

Data were pooled from 3 studies/experiments to compare O_3 and FA exposure. For the BLT-2 and oxPAPC studies, data were pooled from 2 exposure studies/experiments. Data are expressed as means ± SEM. Due to small sample sizes ($n<20$), data generated from experiments were analyzed using nonparametric one-way ANOVA (Kruskal-Wallis test) and two-way ANOVA followed by comparison using a Dunn's and Sidak's multiple comparisons test, respectively, in GraphPad Prism 7.00 (San Diego, CA). With comparisons of two groups an unpaired nonparametric t-test (Mann-Whitney tests) was utilized. A value of $p<0.05$ was significant.

3.4 RESULTS:

The expression of SR-BI is increased in the lung after O_3 exposure

Previous reports have noted that SRs (SR-A, MARCO, and CD36) can alter O_3-induced pulmonary inflammation. Additionally, recent studies have reported that SR-BI expression is increased in lung epithelial cells after O_3 exposure (Sticozzi et al., 2018). However, it is currently unknown if SR-BI expression is altered in the lung after O_3 exposure and if this SR has a role in O_3-induced pulmonary inflammation. We hypothesized that SR-BI is protective against O_3-induced pulmonary inflammation and injury through maintaining alveolar macrophage efferocytosis. To determine if O_3 exposure modulates the expression of SR-BI at the mRNA and/or protein level(s) in lung tissue, WT female mice were exposed to FA or 1ppm O_3. Mice were necropsied at 6, 24, or 48 h post exposure and lung tissue was harvested. When compared to the mRNA levels of SR-B1 from the lung of mice exposed to FA, O_3 significantly decreased SR-BI expression 24 h and 48 h following exposure. (Figure 1A). In contrast, when compared to FA, O_3 increased SR-BI protein levels increased 4 to 5-fold at both 6 h and 24 h post O_3 exposure, respectively, before decreasing 2-fold towards baseline 48 h post O_3 exposure (Figure 1B-C). Taken together, these results indicate that O_3 exposure alters SR-BI mRNA levels and protein production in whole lung tissue.

SR-BI protects against O_3-induced neutrophilic inflammation

Given that SR-BI expression was modulated by O_3 exposure, it was of interest to investigate the role of this SR in O_3-induced pulmonary inflammation and injury. WT and

SR-BI deficient (SR-BI$^{-/-}$) mice were exposed to FA or 1ppm of O_3 as described earlier and 24 h post exposure mice were necropsied to assess pulmonary inflammation and injury. When compared to WT controls, SR-BI$^{-/-}$ mice had a significant increase in the number of neutrophils in their airspace after O_3 exposure (Figure 2A). However, SR-BI$^{-/-}$ mice had no difference in BAL protein, an indicator of alveolar-epithelial barrier injury (Figure 2B). Subsequent pathological analysis of lung tissue sections from O_3-exposed WT and SR-BI$^{-/-}$ mice stained with hematoxylin and eosin also indicated minimal differences in pulmonary injury between the two strains (Figure 2C-D). To determine if these effects persisted past 24 h, markers of pulmonary inflammation and injury were assessed 48 h post O_3 exposure. Compared to WT control mice, SR-BI$^{-/-}$ mice again had an increase in the number of neutrophils in their airspace ($p=0.07$) and no difference in BAL protein 48 h post exposure (Figure 2E-F). Altogether, these findings indicated that SR-BI protects against inflammation and PMN infiltration into the airspace post O_3 exposure.

SR-BI deficiency increases alveolar macrophage expression of O_3-induced pro-inflammatory cytokines

Given the increased pulmonary neutrophilia in SR-BI$^{-/-}$ mice following O_3-exposure, we were interested in determining if this was associated with increased production of pro-inflammatory cyto/chemokines important in PMN recruitment. We have previously reported that SR-BI$^{-/-}$ mice do not have baseline increases in pulmonary inflammation and/or injury (Gowdy et al., 2015). However, following O_3-exposure the pulmonary expression of pro-inflammatory cytokines TNF-α, IL-6, IL-1β, PMN chemo-attractants

CXCL1 (also known as KC), CXCL2 (or Mφ inflammatory protein; MIP2), and CCL3 (or macrophage inflammatory protein 1-α (MIP-1-α)) were not different between strains (Figure 3A). Given that macrophages are a significant source of cytokine and chemokine production in the lung following O_3-exposure, we isolated alveolar macrophages ($CD45^+CD24^-Ly6G^-CD64^+CD11b^{low}$) to measure pro-inflammatory cyto/chemokine expression (Sunil et al., 2012 & Hollingsworth et al., 2007). TNF-α expression was unchanged between WT and SR-$BI^{-/-}$ alveolar macrophages regardless of exposure (Figure 3B). In contrast, when compared to WT controls, IL-6 and CXCL2 expression were upregulated in SR-$BI^{-/-}$ alveolar macrophages after FA or O_3 (Figure 3C). Overall, these results indicate that SR-BI deficiency in alveolar macrophages can lead to augmented pro-inflammatory cyto/chemokine expression.

SR-$BI^{-/-}$ mice do not have increased oxidized phospholipid levels in airspace after O_3 exposure

O_3 is thought to elicit pulmonary inflammation through the production of DAMPs including low molecular weight hyaluronan (HA) and oxidized phospholipids (oxPL) (Bromberg 2016). SR-BI has previously been reported to bind and recognize oxPLs (Lockett et al., 2015, Banerjee et al., 2011). To determine if excessive oxPLs in the airspace drives the increased pulmonary neutrophilia in SR-$BI^{-/-}$ mice, we used reverse phase HPLC tandem mass spectrometry to measure known oxPLs in BAL fluid. There were several oxPLs measurable in the BAL including 1-palmitoyl-2-glutaryl-sn-glycero-3-phosphocholine (PGPC), 1-stearoyl-2-glutaroyl-sn-glycero-3-phosphocholine (SGPC), 1-palmitoyl-2-(5'-oxo-valeroyl)-sn-glycero-3-phosphocholine (POVPC), 1-stearoyl-2-(5-oxovaleroyl)-sn-

glycero-3-phosphocholine (SOVPC), 1-Hexadecanoyl-2-(9-oxo-nonanoyl)-sn-glycero-3-phosphocholine (PONPC), 1-stearoyl-2-(9-oxo-nonanoyl)-sn-glycero-3-phosphocholine (SONPC), 1-Palmitoyl-2-azelaoyl-sn-glycero-3-phosphocholine (PAzPC), 1-stearoyl-sn-glycero-3-phosphocholine (SAzPC), and 1-O-octadecyl-2-acetyl-sn-glycero-3-phosphocholine (C18Kodia-PC). Despite SR-BI deficiency, we observed no significant differences in fold changes in airspace oxPL levels between WT or SR-BI$^{-/-}$ mice 6 h and 24 h following O_3 exposure (Figure 4A-B). These findings indicate that the amount of O_3-generated oxPLs in the airspace is independent of SR-BI expression/production.

oxPLs induce pulmonary neutrophilia and microvascular lung in SR-BI$^{-/-}$ mice

DAMPs, including oxPLs, are generated in the airspace after O_3 exposure and are known to induce pulmonary inflammation and injury (Dahl et al., 2007) but it is unclear if SR-BI mitigates the pulmonary inflammatory response to oxPLs. To determine whether SR-BI protects against oxPLs generated after O_3, we instilled a known oxPL, oxPAPC, oropharyngeally (o.p.) into WT and SR-BI$^{-/-}$ mice. 4 h after instillation, SR-BI$^{-/-}$ mice had an increase, although not statistically significant, in BAL macrophages and a significant increase in airspace neutrophils (Figure 5A). Likewise, when compared to WT mice, SR-BI$^{-/-}$ mice had increased protein in BAL fluid (Figure 5B). Given that SR-BI is expressed on multiple cells in the lung airspace, interstitial, and vascular spaces, we sought to determine if blocking SR-BI specifically in the airspace was sufficient to augment oxPAPC induced lung inflammation and injury. To block SR-BI in the airspace, we dosed WT mice o.p. with Blocking Lipid Transport 2 (BLT-2), an SR-BI inhibitor (Nieland et al., 2002), 1 h before oxPAPC dosing. BLT-2 treated mice had an increase, although not reaching

statistical significance, in BAL neutrophils (Figure 5C) and a significant increase in BAL protein (Figure 5D). Given the increased neutrophilic response and injury in SR-BI$^{-/-}$ mice after instillation of oxPAPC, we aimed to analyze how the immune response of SR-BI$^{-/-}$ macrophages contributes to the inflammatory response. To accomplish this, we harvested peritoneal macrophages from WT and SR-BI$^{-/-}$ mice using 4% thioglycolate. Plated peritoneal macrophages were then incubated with 50µg of oxPAPC or low-serum media for 3 h before harvesting cell lysates for RT-PCR. When compared to WT peritoneal macrophages incubated with oxPAPC, SR-BI$^{-/-}$ peritoneal macrophages had significantly higher expression of TNF-α, CXCL1, CXCL2, and CCL2 (Figure 5E). These results indicate SR-BI protects the lung against DAMPS known to drive O_3-induced inflammation.

SR-BI deficiency impairs alveolar macrophage efferocytosis and prolongs neutrophilia after O_3 exposure

After inflammation and injury, lung tissue returns to homeostasis in part through a resolution process termed ‘efferocytosis’ (Kim et al., 2018 & Janssen and Morimoto 2012). Efferocytosis is where phagocytic cells, including macrophages, detect and remove dead cells while subsequently producing anti-inflammatory factors including IL-10 and TGF-β (Gheibi Hayat et al., 2019, Angsana et al., 2016, Chen et al., 2001). Recently, SR-BI was reported to be critical in the recognition of phosphatidylserine on dead cells facilitating macrophage efferocytosis in atherosclerotic lesions (Tao et al., 2015). Given the prolonged pulmonary inflammation noted in O_3 exposed SR-BI$^{-/-}$ mice, we sought to determine if this was a result of impaired alveolar macrophage

efferocytosis. To first determine if SR-BI$^{-/-}$ mice have an increased accumulation of dead cells in the airspace after O_3 exposure, we utilized flow to determine the number of apoptotic (Annexin V$^+$ PI$^-$), late apoptotic (Annexin V$^+$PI$^+$) and necrotic (Annexin V$^-$PI$^+$) cells. SR-BI$^{-/-}$ mice had a ~4.5-fold increase in total apoptotic cells 24 h post O_3 exposure (Figure 6A). Next, to evaluate if the increase in dead cells is a result of impaired alveolar macrophage efferocytosis, WT and SR-BI$^{-/-}$ mice were exposed to FA or O_3 and 24 h post exposure, mice were o.p. instilled with apoptotic cells. 1.5 h after instillation, BAL cells were harvested and the efferocytic response of alveolar macrophages was evaluated as previously described (Hodge et al., 2019). Interestingly, regardless of genotype, O_3 exposure alone decreased alveolar macrophage efferocytosis. Additionally, SR-BI$^{-/-}$ alveolar macrophages had a significant decrease in efferocytosis at baseline that was further decreased after O_3 exposure (Figure 6B). Representative images of alveolar macrophages engulfing apoptotic cells from each treatment group are indicated by black arrows and alveolar macrophages that did not engulf apoptotic cells are designated by white arrows (Figure 6C). In total, these findings indicate that SR-BI deficiency and O_3 decrease in the efferocytic response in alveolar macrophages.

SR-BI deficiency increases efferocytic genes in alveolar macrophages

Given the decreases in macrophage efferocytosis seen after O_3 exposure and/or SR-BI deficiency, we sought to determine if this was a result of impaired activation of pathways known to be important in efferocytosis. c-Mer tyrosine kinase (MerTK), T-cell immunoglobulin and mucin domains containing protein 4 (Tim4), and CD36 promote efferocytosis through serving as receptors for phosphatidylserine (Nishi et al., 2019 & Kim

et al., 2018). Activation of these receptors on macrophages promotes the production of anti-inflammatory cytokines IL-10 and TGF-β (de Couto et al., 2019 & Nishi et al., 2019). To determine if O_3 exposure and/or SR-BI deficiency alters the pulmonary expression of these efferocytic pathways, MerTK, IL-10, TGF-β, and CD36 were measured in whole lung tissue 24 h post O_3 exposure. However, no significant changes in pulmonary expression of the genes associated with efferocytosis between WT and SR-BI-/- mice following exposure to O_3. (Figure 7A). Next, given that macrophages are the primary mediators of efferocytosis, we sorted alveolar macrophages from WT and SR-BI$^{-/-}$ mice exposed to FA or O_3 and analyzed efferocytic gene expression. At baseline, SR-BI$^{-/-}$ alveolar macrophages have dramatically increased MerTK that was unchanged with O_3 exposure (Figure 7B). In contrast, SR-BI deficiency and/or O_3 exposure did not change IL-10 expression in sorted alveolar macrophages; however, O_3 did significantly decreased IL-10 expression in WT alveolar macrophages (Figure 7C). However, O_3 exposure significantly decreased Tim4 expression in WT alveolar macrophages (Figure 7D). When compared to WT alveolar macrophages, SR-BI$^{-/-}$ alveolar macrophages had lower Tim4 expression after FA exposure, whereas after O_3 exposure, Tim4 expression was significantly increased compared to the WT O_3 exposed alveolar macrophages. Altogether, these results indicate that SR-BI deficiency and O_3 induce significant changes in genes important for mediating efferocytosis.

SR-BI deficiency impairs efferocytosis at baseline and is further decreased following incubation with oxPAPC *in vitro*

After observing that SR-BI deficiency and/or O_3 impairs alveolar macrophages efferocytosis, we sought to determine if this was a consequence of O_3-induced DAMPs. Therefore, WT and SR-BI$^{-/-}$ peritoneal macrophages were incubated with oxPAPC and then efferocytic capabilities were measured. Again, when compared to WT macrophages, SR-BI$^{-/-}$ macrophages had decreased efferocytosis. However, oxPAPC treatment decreased WT macrophage efferocytosis but did not alter the already reduced efferocytic response of SR-BI$^{-/-}$ macrophages (Figure 8A). Representative images of peritoneal macrophages engulfing apoptotic cells from each treatment group are indicated by black arrows and peritoneal macrophages that did not engulf apoptotic cells are designated by white arrows (Figure 8B). Taken together, these results support that SR-BI is important in mediating the macrophage efferocytosis but also indicate that O_3-induced DAMPs may be a mechanism by which exposure reduces macrophage efferocytosis.

Taqman Primers	
Primer	**Assay ID/Reference Number**
Euk 18S rRNA	4352655
TNF-α	Mm00443258_m1
IL-1β	Mm00434228_m1
IL-6	Mm00446190_m1
CXCL1	Mm04207460_m1
CXCL2	Mm00436450_m1
CCL2	Mm00441242_m1
CCL3	Mm00441259_g1
SR-BI	Mm00450234_m1
CD36	Mm00432403_m1
CD163	Mm00474091_m1
IL-10	Mm01288386_m1
TGF-β	Mm01178820_m1
MerTK	Mm00434920_m1
Tim4	Mm00724709_m1

Table 1: Primer sequences obtained from Taqman for quantitative PCR of chemokines and cytokine gene expression in whole lung homogenate.

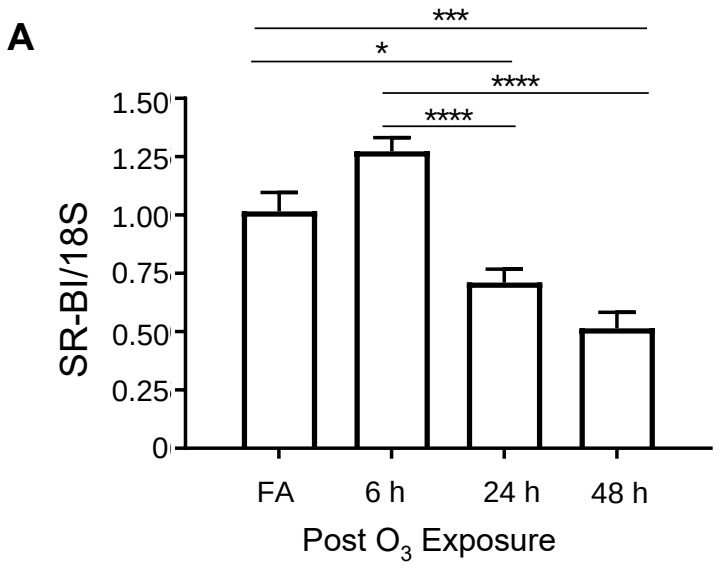
A
***
*
****
****
1.50
1.25
1.00
0.75
0.50
0.25
0
SR-BI/18S
FA
6 h
24 h
48 h
Post O3 Exposure

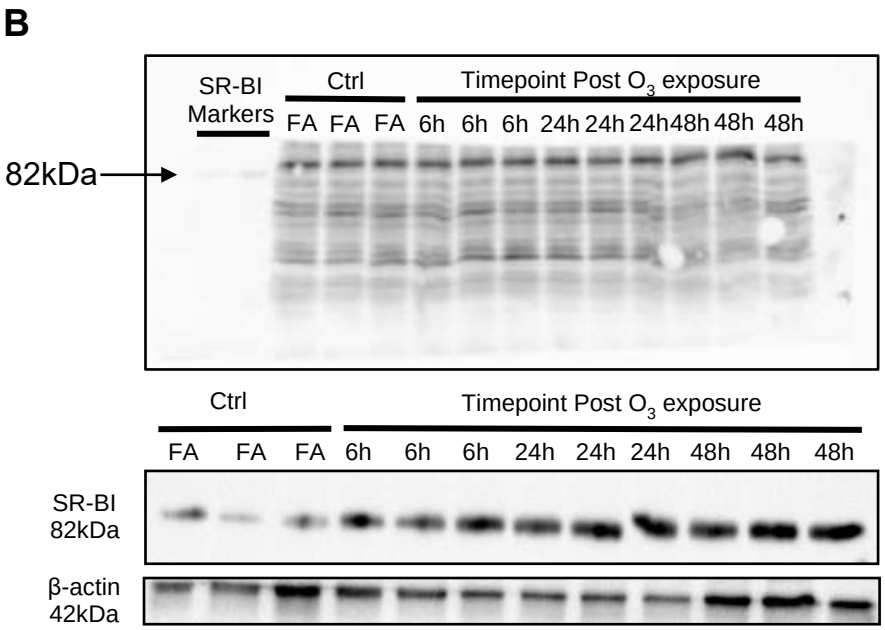
B
SR-BI Markers
Ctrl
Timepoint Post O3 exposure
FA FA FA 6h 6h 6h 24h 24h 24h 48h 48h 48h
82kDa
Ctrl
Timepoint Post O3 exposure
FA FA FA 6h 6h 6h 24h 24h 24h 48h 48h 48h
SR-BI 82kDa
β-actin 42kDa

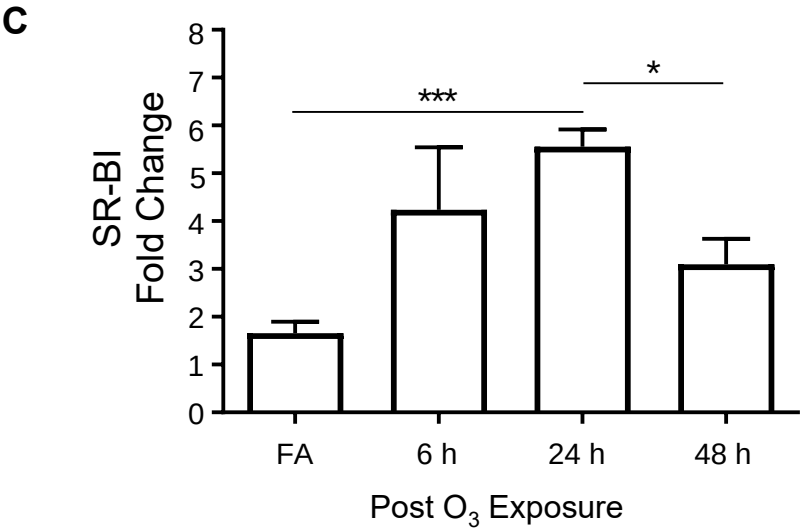
C
***
*
8
7
6
5
4
3
2
1
0
SR-BI Fold Change
FA
6 h
24 h
48 h
Post O3 Exposure

Figure 1: O_3 induces SR-BI expression in the lung and sorted pulmonary macrophages. C57Bl/6J (WT) mice were exposed to filtered air (FA) or 1ppm O_3 for 3 h and necropsied 6 h, 24 h, and 48 h following exposure. Lung tissue was harvested and analyzed for A) SR-BI mRNA expression, which was normalized to 18S, B) Whole western blot with protein ladder, samples, and beta actin controls and C) protein expression was normalized to beta actin and quantified using Image lab software. C). n=3-8 per group. *p<0.05, ***p<0.0001, ****p<0.0001.

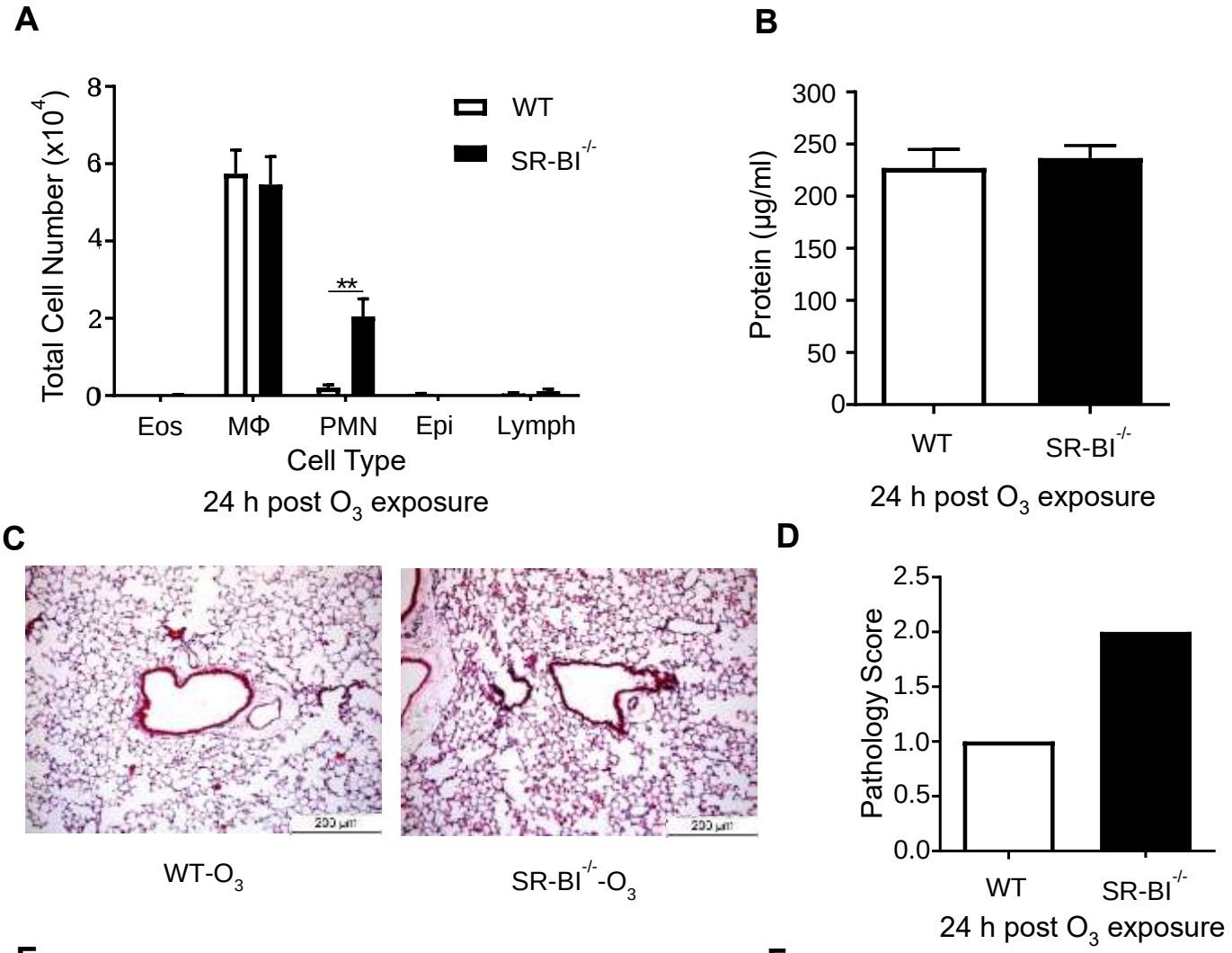
A
Total Cell Number (x10^4)
WT
SR-BI-/-
**
Eos
MΦ
PMN
Epi
Lymph
Cell Type
24 h post O3 exposure
B
Protein (µg/ml)
WT
SR-BI-/-
24 h post O3 exposure
C
WT-O3
SR-BI-/--O3
D
Pathology Score
WT
SR-BI-/-
24 h post O3 exposure
E
Total Cell Number (x10^4)
WT
SR-BI-/-
p=0.07
Eos
MΦ
PMN
Epi
Lymph
Cell Type
48 h post O3 exposure
F
Protein (µg/ml)
WT
SR-BI-/-
48 h post O3 exposure

Figure 2: SR-BI is protective against O_3 induced pulmonary inflammation. WT and SR-BI$^{-/-}$ mice were exposed to 1ppm O_3 (3 h) and necropsied 24 h and 48 h following exposure. Bronchoalveolar lavage (BAL) was analyzed for A) cell differentials and B) total protein 24 h post exposure. C) Lung tissue was sectioned and stained with hematoxylin and eosin to examine pulmonary damage and D) tissue histology scoring was measured on harvested lung tissue. Bronchoalveolar lavage (BAL) was analyzed for E) cell differentials and F) total protein 48 h post exposure. Pathology scoring system is described in supplementary methods. n=6-10 per group. *p<0.01.

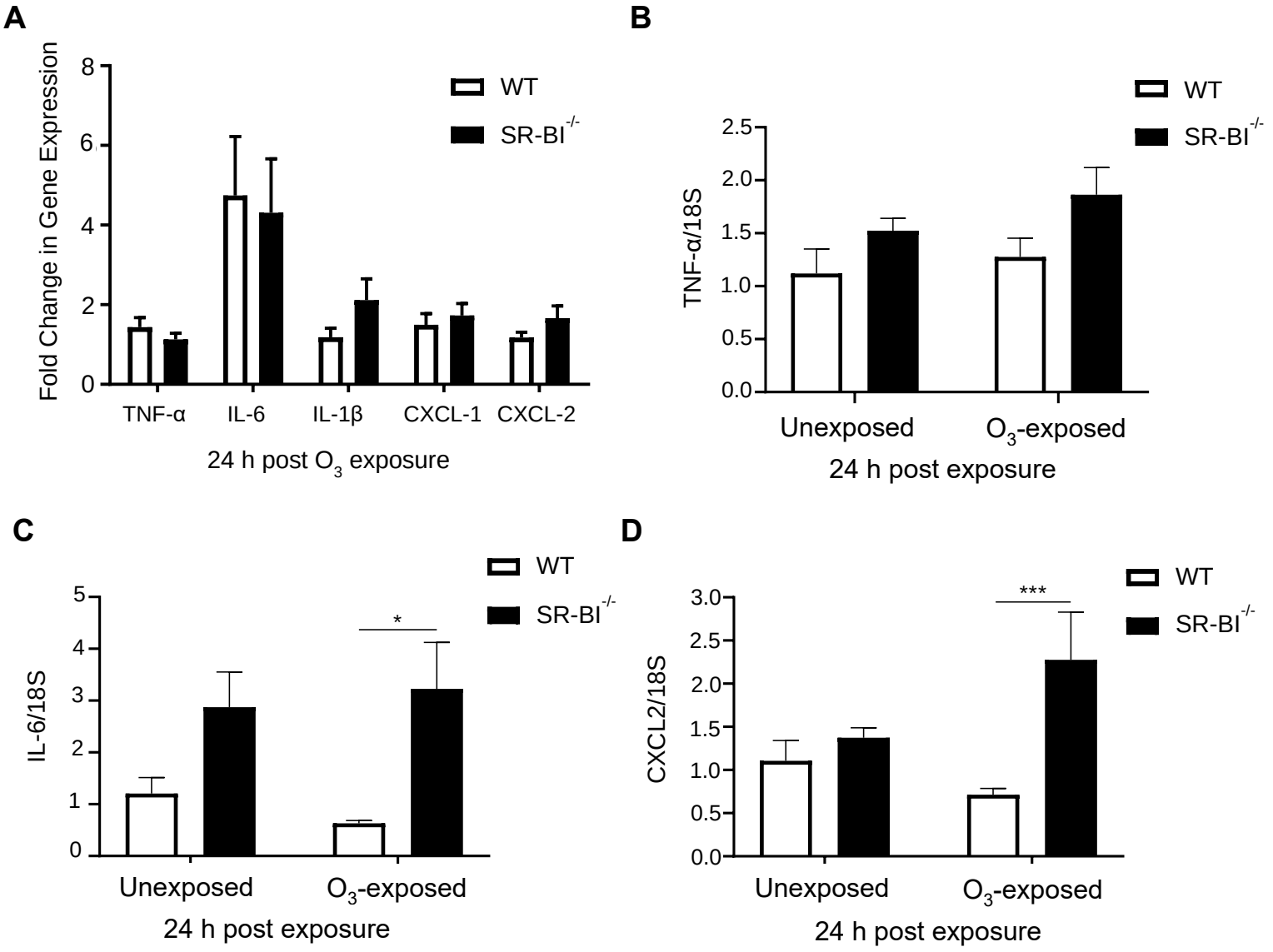
A
Fold Change in Gene Expression
8
6
4
2
0
WT
SR-BI-/-
TNF-α
IL-6
IL-1β
CXCL-1
CXCL-2
24 h post O3 exposure
B
TNF-α/18S
2.5
2.0
1.5
1.0
0.5
0.0
WT
SR-BI-/-
Unexposed
O3-exposed
24 h post exposure
C
IL-6/18S
5
4
3
2
1
0
WT
SR-BI-/-
*
Unexposed
O3-exposed
24 h post exposure
D
CXCL2/18S
3.0
2.5
2.0
1.5
1.0
0.5
0.0
WT
SR-BI-/-
***
Unexposed
O3-exposed
24 h post exposure

Figure 3: SR-BI deficiency augments expression of pro-inflammatory cytokines and chemokines in pulmonary macrophages, but not in whole lung after O_3. WT and SR-BI$^{-/-}$ mice were naïve or exposed to 1ppm O_3 (3 h) and necropsied 24 h following exposure. A) Whole lung homogenate was analyzed for gene expression of TNF-α, IL-1β, IL-6, CXCL1, and CXCL2. B) Lung tissue was digested for FACS isolation of alveolar macrophages (AM; CD45^{+}CD24^{-}Ly6G^{-}CD64^{+}CD11b^{low}) to determine TNF-α, C) IL-6, and D) CXCL2 expression in these purified populations. Gene expression was normalized to 18S. (n=6-8/treatment). *p<0.05; ***p<0.001.

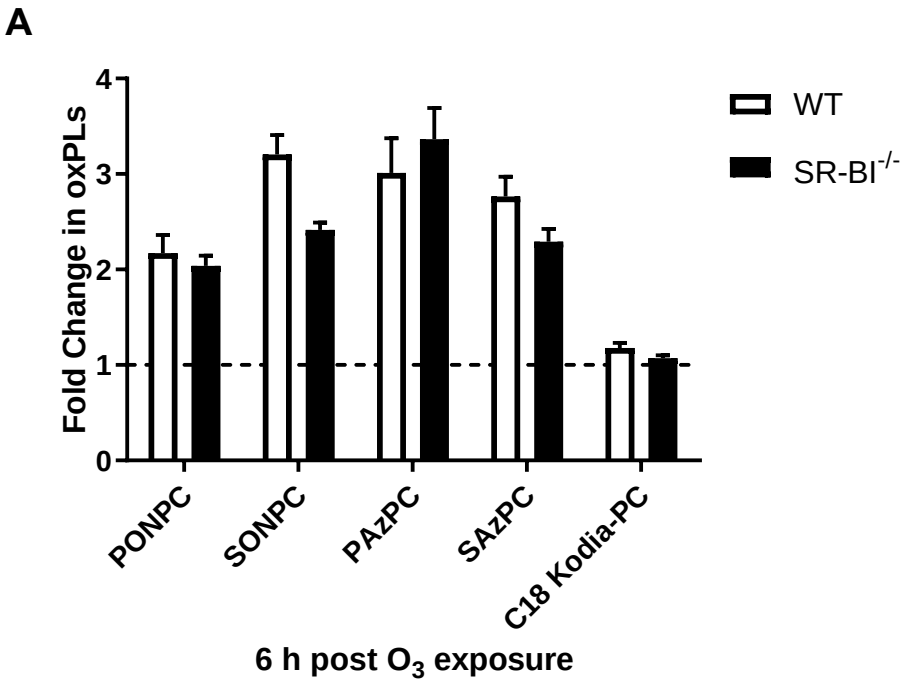
A
Fold Change in oxPLs
4
3
2
1
0
WT
SR-BI-/-
PONPC
SONPC
PAzPC
SAzPC
C18 Kodia-PC
6 h post O3 exposure

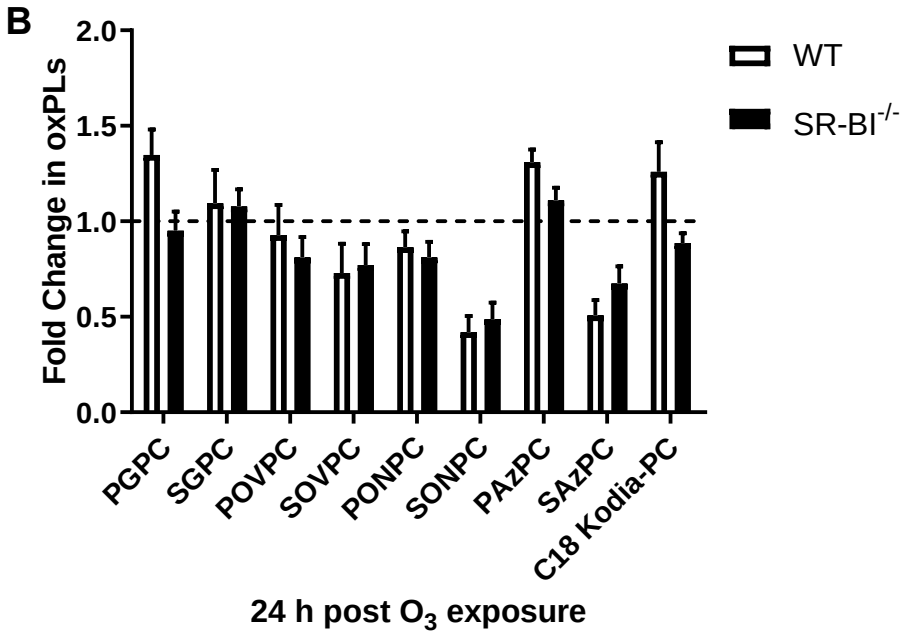
B
Fold Change in oxPLs
2.0
1.5
1.0
0.5
0.0
WT
SR-BI-/-
PGPC
SGPC
POVPC
SOVPC
PONPC
SONPC
PAzPC
SAzPC
C18 Kodia-PC
24 h post O3 exposure

Figure 4: SR-BI$^{-/-}$ mice have unaltered changes in the oxidized phospholipids present in their BAL fluid compared to WT mice after O_3 exposure. WT and SR-BI$^{-/-}$ mice were exposed to O_3 and necropsied A) 6 h and B) 24 h following exposure. Bronchoalveolar lavage (BAL) was analyzed for oxidized phospholipids (oxPLs) by LC-MS/MS and fold changes were normalized to WT FA levels in BAL. n=5/group. Dashed line represents WT FA group.

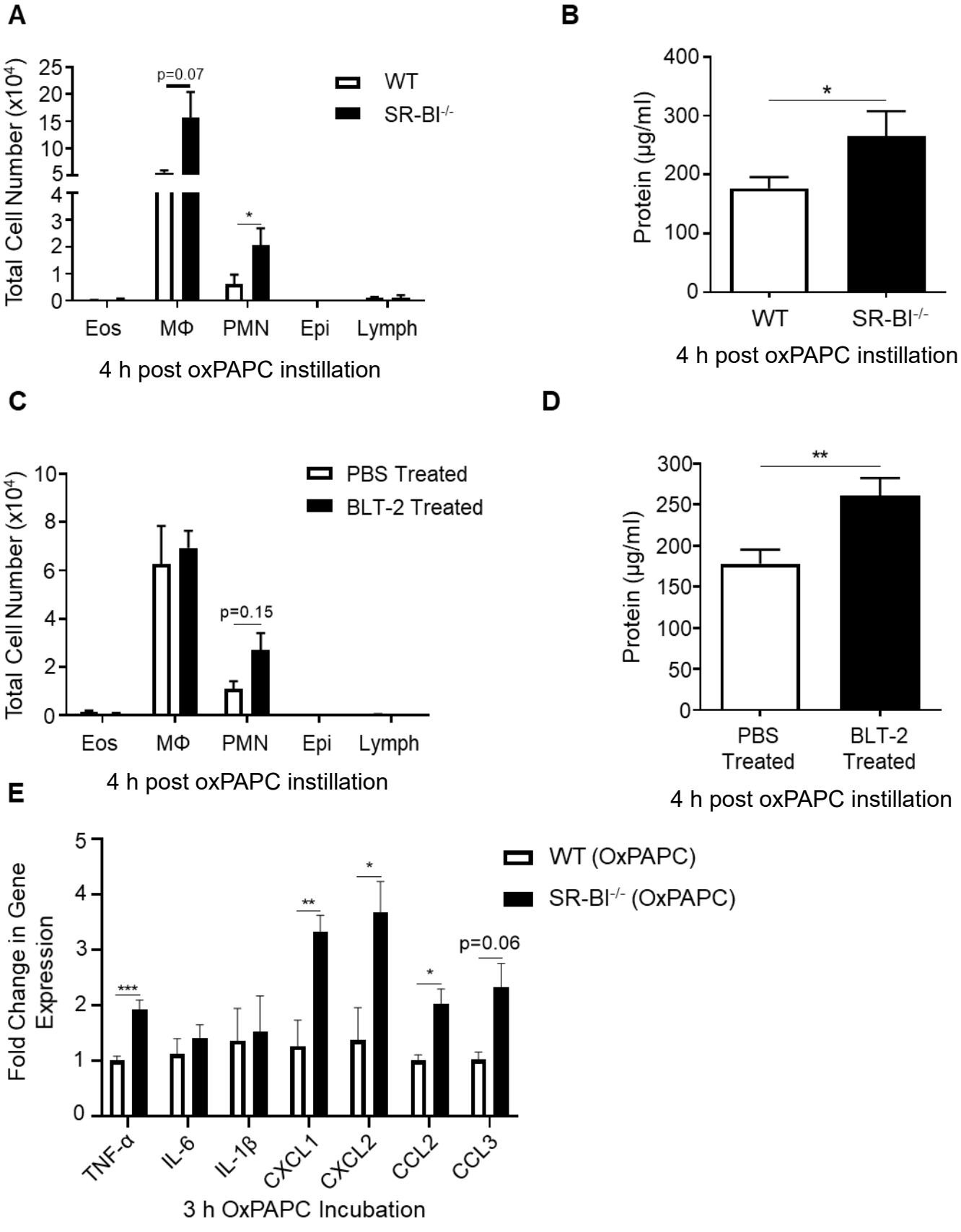
A
Total Cell Number (x10⁴)
p=0.07
*
WT
SR-BI-/-
Eos
MΦ
PMN
Epi
Lymph
4 h post oxPAPC instillation
B
Protein (µg/ml)
*
WT
SR-BI-/-
4 h post oxPAPC instillation
C
Total Cell Number (x10⁴)
PBS Treated
BLT-2 Treated
p=0.15
Eos
MΦ
PMN
Epi
Lymph
4 h post oxPAPC instillation
D
Protein (µg/ml)
**
PBS Treated
BLT-2 Treated
4 h post oxPAPC instillation
E
Fold Change in Gene Expression
WT (OxPAPC)
SR-BI-/- (OxPAPC)
***
**
*
*
p=0.06
TNF-α
IL-6
IL-1β
CXCL1
CXCL2
CCL2
CCL3
3 h OxPAPC Incubation

Figure 5: Pulmonary SR-BI protects against oxidized phospholipid (oxPL) induced pulmonary inflammation and injury. WT and SR-BI$^{-/-}$ mice were instilled oropharyngeally (o.p.) with 200μg/ml of oxPAPC. 4 h following exposure, bronchoalveolar lavage (BAL) was analyzed for A) cellular differentials and B) total protein. To determine if SR-BI in the lung was critical in protecting against oxPLs, WT mice were instilled o.p. with 1XPBS or BLT-2 (250μg/kg) 1h before oxPAPC exposure. Bronchoalveolar lavage (BAL) was analyzed for C) cellular differentials and D) total protein. Peritoneal macrophages were harvested from WT and SR-BI$^{-/-}$ mice and plated overnight. Macrophages were then incubated with either low-serum media or low-serum media plus 50μg/ml of oxPAPC for 3 h. E) Cell lysates were harvested for RT-PCR to measure pro-inflammatory gene expression. n=6-10/group. n=6 replicates/treatment. *$p<0.05$; **$p<0.01$; ***$p<0.001$.

A

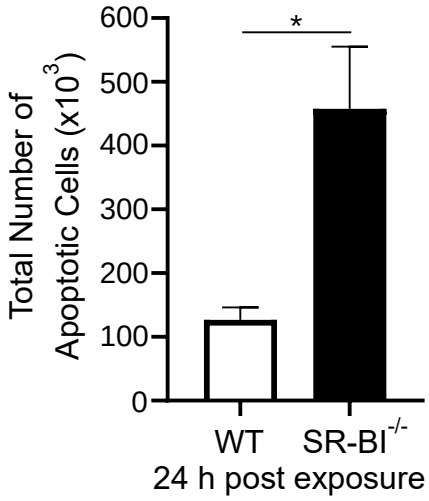
600
500
400
300
200
100
0
*
Total Number of Apoptotic Cells (x10^3)
WT
SR-BI-/-
24 h post exposure

B

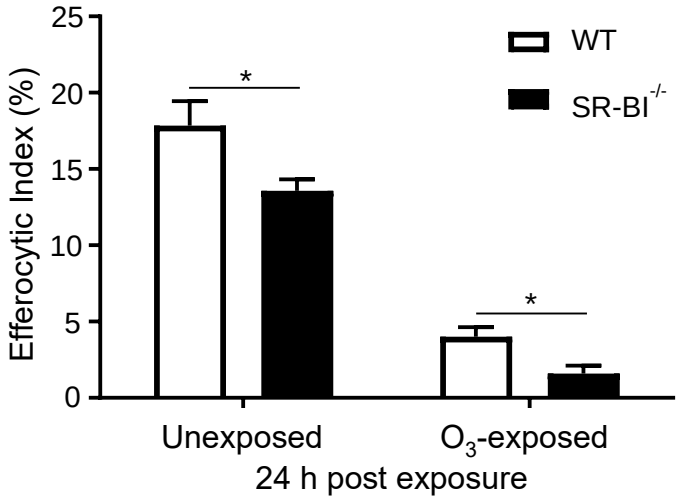
25
20
15
10
5
0
*
*
WT
SR-BI-/-
Efferocytic Index (%)
Unexposed
O3-exposed
24 h post exposure

C

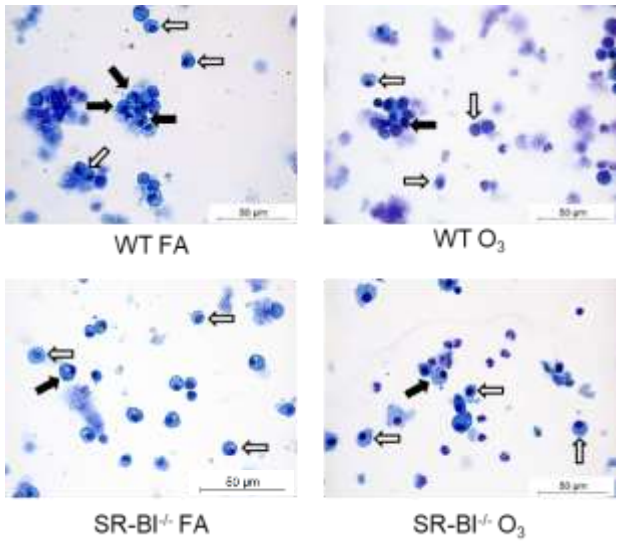
WT FA
WT O3
SR-BI-/- FA
SR-BI-/- O3

Figure 6: SR-BI deficiency impairs alveolar macrophage efferocytosis and resolution of O_3-induced pulmonary inflammation. WT and SR-BI$^{-/-}$ mice were exposed to filtered air (FA) or 1ppm O_3 (3 h). 24 h post exposure bronchoalveolar lavage (BAL) cells were analyzed via flow cytometry for markers of apoptosis and necrosis. Early apoptotic, late apoptotic, and necrotic cells are identified as Annexin V^+/PI^-, Annexin V^+/PI^+, and Annexin V^-/PI^+, respectively. A) Enumeration of the total number of Annexin V^+/PI^- and Annexin V^+/PI^+ cells after O_3 exposure based on total cell count were calculated. B) Efferocytic capabilities of alveolar macrophages after FA or O_3 exposure in WT and SR-BI$^{-/-}$ mice. C) Representative images of alveolar macrophages for calculation of efferocytic index. Black arrows represent alveolar macrophages that engulfed apoptotic cells and white arrows represent macrophages that did not. n=4-7/group. *$p<0.05$.

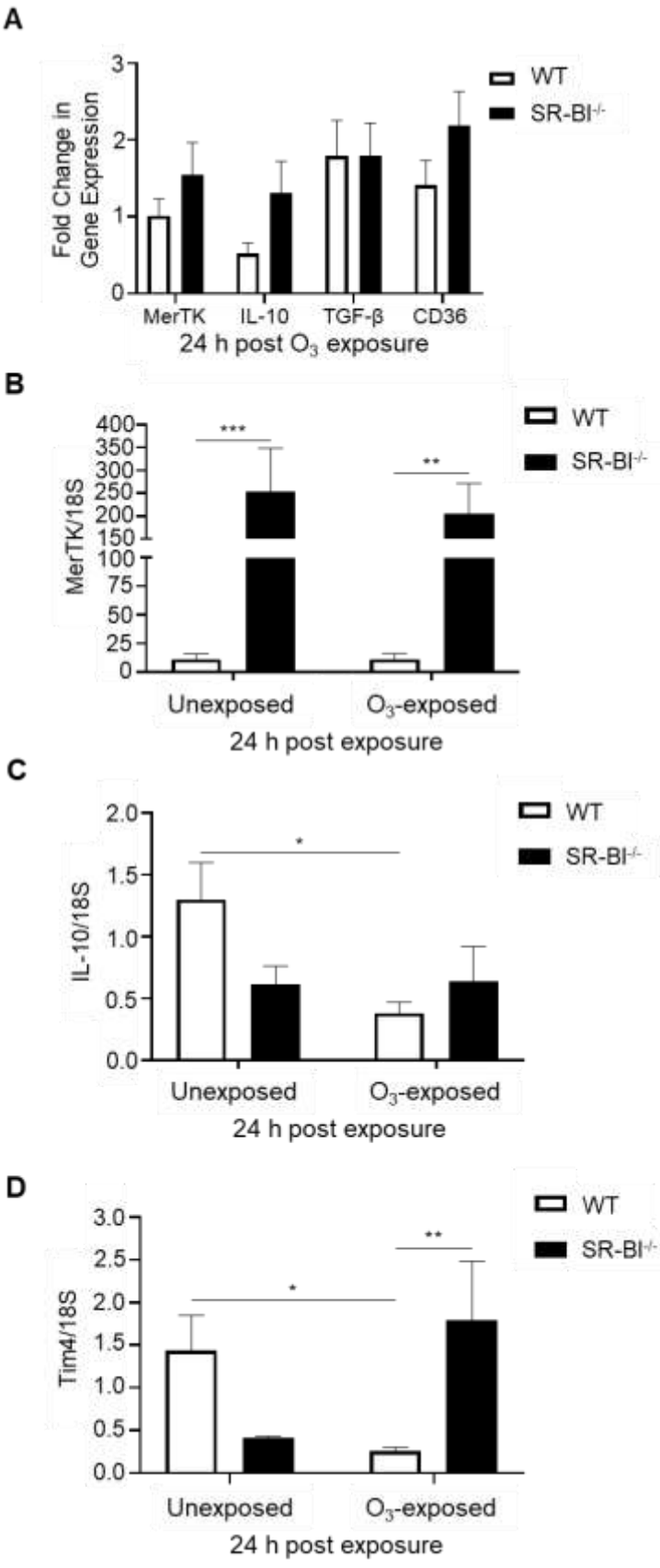
A
Fold Change in Gene Expression
3
2
1
0
WT
SR-BI-/-
MerTK
IL-10
TGF-β
CD36
24 h post O3 exposure
B
MerTK/18S
400
350
300
250
200
150
100
75
50
25
0
***
**
WT
SR-BI-/-
Unexposed
O3-exposed
24 h post exposure
C
IL-10/18S
2.0
1.5
1.0
0.5
0.0
*
WT
SR-BI-/-
Unexposed
O3-exposed
24 h post exposure
D
Tim4/18S
3.0
2.5
2.0
1.5
1.0
0.5
0.0
*
**
WT
SR-BI-/-
Unexposed
O3-exposed
24 h post exposure

Figure 7: SR-BI deficient alveolar macrophages have increased expression of efferocytosis markers. WT (and SR-BI$^{-/-}$) mice were exposed to 1ppm O_3 and necropsied 24 h following exposure. A) Whole lung tissue was analyzed for markers of efferocytosis by RT-PCR. The resulting RT-PCR analysis on sorted alveolar macrophages isolated from exposed WT mice. WT v SR-BI$^{-/-}$ RT-PCR analysis of genes associated with efferocytosis B) MerTK, C) IL-10, and D) Tim4 were measured in sorted alveolar macrophages. Gene expression was normalized to 18S. (n=3-8/treatment). *p<0.01, **p<0.01, ***p<0.001.

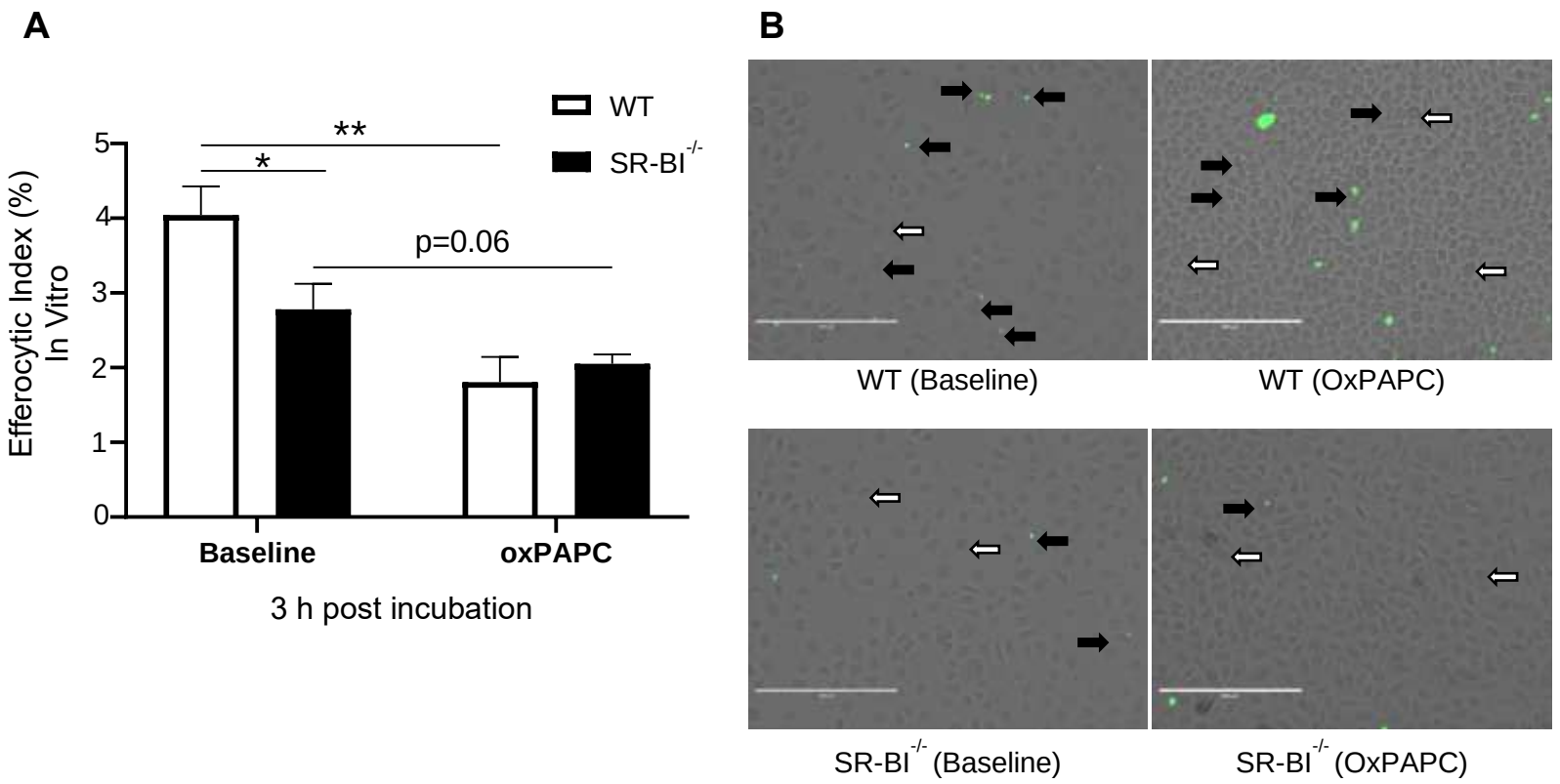
A
B
WT
SR-BI-/-
**
*
p=0.06
Efferocytic Index (%)
In Vitro
5
4
3
2
1
0
Baseline
oxPAPC
3 h post incubation
WT (Baseline)
WT (OxPAPC)
SR-BI-/- (Baseline)
SR-BI-/- (OxPAPC)

Figure 8: SR-BI deficiency augments inflammatory response to oxPAPC and impairs efferocytosis *in vitro.* Peritoneal macrophages were harvested from WT and SR-BI$^{-/-}$ mice and plated overnight. Macrophages were then incubated with either low-serum media or low-serum media plus 50μg/ml of oxPAPC for 3 h. A) The efferocytic index was calculated at baseline and after incubation with oxPAPC and apoptotic cells with harvested peritoneal macrophages from WT and SR-BI$^{-/-}$ mice. B) Representative images of plated WT and SR-BI$^{-/-}$ peritoneal macrophages and Calcein AM stained apoptotic cells for calculation of efferocytic index. (n=5 replicates/treatment). Additional representative images of plated WT and SR-BI$^{-/-}$ peritoneal macrophages and Calcein AM stained apoptotic cells after oxPAPC incubation for calculation of efferocytic index. (n=6 replicates/treatment). Black arrows represent peritoneal macrophages that engulfed apoptotic cells and white arrows represent macrophages that did not. *$p<0.05$; **$p<0.01$.

Supplemental Methods

Lung histopathological scoring

Lungs were fixed (10% neutral-buffered formalin for 24 h) 24 h post-O_3 exposure. The tissues were then processed, paraffin embedded, sectioned (5 μm), and stained with hematoxylin & eosin. Inflammation was semi-quantitatively scored on a 0-3 scale (shown below) by a pathologist blinded to genotype. After grading, the slides were scanned using an Aperio slide scanner (Leica Biosystems, IL) and images were captured using Aperio's ImageScope. Representative images of lung histology from C57BL/6J (WT) and SR-BI$^{-/-}$ mice 24 h post-O_3 exposure are shown in Figure 1D.

Table 2. Quantitation of Histopathologic Changes in the Lungs of Transplanted Mice

Score	Periluminal Infiltrates (around airways/vessels)	Pneumonitis (alveolar/interstitial)
0	No infiltrates*	No infiltrates*
1	1-3 cell diameters thick	Increased cells, only visible at high magnification (×400)
2	4-10 cell diameters thick	Easily seen cellular infiltrate or interstitial thickening
3	>10 cell diameters thick	Consolidation by inflammatory cells and interstitial thickening

The severity of histopathologic changes observed was scored using coded slides. The extent of injury was also quantitated according to the percentage of lung tissue involved (5% to 25% = 1; >25% to 50% = 2; >50% = 3). Values for total index were generated by summation of periluminal infiltrate and pneumonitis scores.

* Infiltrates are macrophages, neutrophils, lymphocytes, admixed fibrin, or edema fluid.

3.5 DISCUSSION:

Increases in ambient levels of O_3 have been associated with increased susceptibility to and exacerbations of chronic pulmonary diseases. These detrimental pulmonary consequences are thought to occur in part as a result of enhanced lung inflammation and injury (Environmental Protection Agency 2019 & Chen et al., 2015). In the current study, we used female mice because several studies have uncovered females are more susceptible to the negative effects of O_3 compared to their male counterparts (Fuentes et al., 2019). Additionally, we report that the PRR, SR-BI, is protective against O_3-induced pulmonary inflammation by dampening airspace neutrophilia and maintaining effective alveolar macrophage efferocytosis. Additionally, SR-BI deficient mice had augmented pulmonary inflammation and injury when dosed with the O_3-induced DAMP, oxPAPC, indicating that this PRR may protect the lung from DAMP-induced inflammation. Furthermore, *in vitro* culture of SR-BI deficient macrophages with oxPAPC, increased expression of pro-inflammatory cytokines/chemokines. Collectively, these data indicate a protective role for SR-BI in the O_3-induced pulmonary inflammatory and the resolution of this response.

In the current study, we observed that acute O_3 exposure modulates pulmonary SR-BI expression and production. Specifically, O_3 exposure increased SR-BI mRNA and protein expression. Our data adds to a growing body of literature indicating that O_3 can modulate SR-BI, yet the mechanisms are not completely understood (Sticozzi et al., 2018 & Valacchi et al., 2007). O_3-induced alterations in SR-BI expression/production could reflect differential regulation of transcription factors known to drive SR-BI expression

(Shen et al., 2018, Speen et al., 2016, Lopez et al., 1999, Cao et al., 1997). O_3 is known to inactivate LXR, a transcription factor known to regulate SR-BI expression (Shen et al., 2018 & Bromberg 2016). Furthermore, the increased pulmonary SR-BI production may be in response to O_3-induced DAMPs known to be SR-BI ligands including high mobility group box 1 protein (HMGB1) and oxPLs (Bromberg 2016, Lockett et al., 2015, Banerjee et al., 2011, Gillotte-Taylor et al., 2001, Cao et al., 1997). Lastly, O_3 exposure may increase the cholesterol demand of the lung, thus requiring increased cholesterol trafficking and SR-BI expression/production (Fessler et al., 2017 & Dai et al., 2012). These data highlight the increased pulmonary need for SR-BI in mitigating the O_3-induced pulmonary inflammatory response.

Our findings link SR-BI to enhanced airspace neutrophilia after O_3 exposure. These findings were independent of increased markers of lung injury (e.g. BAL protein or lung histology) and augmented pulmonary expression of CXCR2 ligands. The enhanced airspace neutrophilia in SR-BI$^{-/-}$ mice has previously been reported after bacterial pneumonia and/or pulmonary silicosis; however, these studies also reported increased lung injury (Gowdy et al., 2015 & Tsugita et al., 2017). The increased pulmonary neutrophilia noted in SR-BI$^{-/-}$ mice following O_3 exposure could be a result of insufficient glucocorticoid production leading to increased PMN chemotaxis (Ronchetti et al., 2018, Cavalcanti et al., 2006, Schleimer 2004). SR-BI$^{-/-}$ mice have been reported to be adrenally insufficient when challenged (Gowdy et al., 2015, Gilbert et al., 2014, Hoekstra et al., 2009). Additionally, O_3 is known to modulate the stress axis to induce corticosterone and corticosteroid production in rats and humans, respectively (Henriquez et al., 2017, Miller et al., 2016, Miller et al., 2015). Furthermore, the increased neutrophilia noted in the SR-

BI deficient mice could be a result of the impaired efferocytic response we observed. Neutrophils have a short half-life and become apoptotic once they have extravasated into inflamed tissues (Jones et al., 2016, Moret et al., 2011, Saffar et al., 2011). We did observe increased apoptotic cells in the airspace of SR-BI$^{-/-}$ mice following O_3 as well as impaired alveolar macrophage uptake of apoptotic cells. Therefore, it is possible that the augmented neutrophilia in noted in SR-BI deficient mice after could link this O_3 induced inflammatory response to glucocorticoid production and/or impaired uptake of apoptotic cells.

The increased airspace neutrophilia noted in SR-BI$^{-/-}$ mice led us to examine whether the efferocytic function of alveolar macrophages was dependent on SR-BI and if O_3 exposure mitigated this resolution process. SRs, including SR-BI, have previously been reported to mediate efferocytosis by recognizing phosphatidylserine on the cell surface of apoptotic cells promoting engulfment (Kim et al., 2018, Grabiec et al., 2016, Penberthy & Ravichandran et al., 2016, Parks et al., 2013, Zhang et al., 2019, Tao et al., 2015, Osada et al., 2009). However, whether SR-BI expression on alveolar macrophages is critical to resolve O_3 induced lung inflammation is unknown. Our data, both *in vitro* and *in vivo,* confirm that SR-BI is critical for macrophage efferocytosis. Surprisingly, we found that O_3 exposure decreased alveolar macrophage efferocytosis. It has previously been reported that O_3 exposure impairs alveolar macrophage phagocytosis of extracellular pathogens but to our knowledge these are the first data to report reduced efferocytic function (Jakab et al., 1995 & Gilmour et al., 1991). O_3 induced impairments in alveolar macrophage efferocytosis could be a result of suppressed production of specialized pro-resolving lipid mediators (SPMs) known to promote macrophage efferocytosis and the

resolution of inflammation (Dalli and Serhan 2017 & Serhan et al., 2009). Previous studies from our laboratory have demonstrated that acute O_3 exposure decreases pulmonary SPM levels (Rymut et al., 2020 & Kilburg-Basnyat et al., 2018). Additionally, O_3 exposure generates DAMPs, such as oxPLs and high mobility group box 1 (HMGB1), which are known to disrupt macrophage efferocytosis by competing with apoptotic cells for engulfment (Linton et al., 2016, Banerjee et al., 2011, Kadl et al., 2004). We did observe decreased efferocytosis in peritoneal macrophages following incubation with oxPAPC. Taken together, these data reveal a novel pathway by which O_3 alters the pulmonary inflammation by potentially delaying processes known to promote tissue resolution.

O_3 produces DAMPs known to induce pulmonary inflammation and injury (Bromberg 2016 Bauer et al., 2012 & Bauer et al., 2011). In our study, SR-BI deficiency did not alter the amount of oxPLs in the airspace after O_3 exposure. In contrast, SR-BI$^{-/-}$ mice and BLT-2 instilled WT mice had significantly increased lung injury and airspace neutrophilia after dosing with oxPAPC, supporting our hypothesis that SR-BI is essential in regulating the pulmonary immune response to oxPLs. It is known that oxPLs are ligands for SR-BI, TLR2, and TLR4 and produce a pulmonary inflammatory response via NF-κB signaling (Kadl et al., 2011 & Imai et al., 2008). However, we speculate that the increased injury and inflammation in SR-BI$^{-/-}$ mice may be the result of several factors. First being diminished cellular uptake pathways, which tempers subsequent TLR signaling. Other studies have proven that SR-BI cooperates with TLR signaling through observing potentiated TNF-α secretion in mice with isolated hematopoietic cell SR-BI deficiency following exposure to LPS, PAM3, and other TLR ligands, which supports our *in vitro* oxPL data (Gowdy et al., 2015). Although not characterized with SR-BI, class A

scavenger receptors are known to facilitate clearance of oxidized lipids and cholesterol (Dahl et al., 2007). Second, our results may be the result of decreased suppressive effects of HDL in the lung. SR-BI$^{-/-}$ mice are known to have altered lipid profiles and their HDL does not nearly produce as many antioxidants as WT mice do, resulting in increased oxidative stress in these animals (Van Eck et al., 2007 & Rigotti et al., 1997). It would be of interest to confirm these whether these factors are involved in the protective role of SR-BI in DAMP induced pulmonary inflammation and injury.

Despite our novel findings, we acknowledge that our study has limitations. First being that we only used female mice. There are known sex differences in the pulmonary responses to O_3 and development of chronic lung diseases (Buja et al., 2020 & Cho et al., 2019). Including both sexes would strengthen the significance of this study. This study mainly focuses on the pulmonary inflammatory and injury at two timepoints, 24 h and 48 h, following O_3 exposure whereas the efferocytic response was only examined 24 h following O_3. Measuring the efferocytic response at further timepoints would uncover if this impairment persists or if efferocytic responses were restored. Additionally, we acknowledge that we only measured one class of phospholipids, phosphatidylcholines, following O_3 exposure. Phosphatidylcholines are the most abundant class of phospholipids in the airspace (Karnati et al., 2018 & Agassandian and Mallampalli 2013) however, there are other classes of phospholipids that also stimulate innate immune responses including phosphatidylinositols and phosphatidylglycerols (Voelker and Numata 2019). Lastly, we chemically inhibited SR-BI in the lung through BLT-2 to observe if SR-BI expression in the lung is responsible for mitigating O_3-induced inflammation. Unfortunately, this does not allow us to evaluate cell-specific SR-BI

expression. Future studies will utilize cell specific SR-BI deficient mice in order to better decipher the role of SR-BI in protecting the lung from O_3 exposure.

In conclusion, these data provide evidence that SR-BI mitigates the pro-inflammatory effects of O_3 through decreasing airspace neutrophilia, mediating alveolar macrophage efferocytosis. Given that genetic and pharmacological alterations in SR-BI have been identified in the human population, this could contribute to the pulmonary pathogenesis after O_3 exposure (Helgadottir et al., 2018 & Vickers and Rodriguez 2015). Further studies will be needed to identify cell specific contributions and the signaling mechanism of how SR-BI mediates efferocytosis and mitigates airspace neutrophilia. Overall these data indicate that augmenting SR-BI and identification of individuals with known loss-of-function mutations may be a potential strategy to decrease the negative health effects of O_3 (Zanoni et al., 2016 & Vergeer et al., 2011).

ACKNOWLEDGEMENTS:

This research was supported by the Health Effects Institute Walter A. Rosenblith Award (to K.M.G.). Additionally, we would like to thank Ms. Christine Psaltis and Ms. Elizabeth Browder for technical assistance with experiments. Purchase of the Aria fusion sorter was funded by NIH SIG 1S10OD021615-01.

DISCLOSURE:

The authors declare no conflict of interest.

CHAPTER FOUR: GENERAL DISCUSSION AND SUMMARY

The present study was designed to investigate the molecular mechanisms of how the criteria air pollutant, O_3, increases the susceptibility to chronic lung diseases and if SR-BI is protective against the O_3-induced pulmonary inflammation known to drive lung disease. In aim 1, we determined whether acute O_3 exposure impairs alveolar macrophage efferocytosis, a reparative process known to be critical in restoring damaged tissue to homeostasis and preventing chronic inflammation, secondary necrosis, and autoimmunity (Elliot et al., 2017 & Angsana et al., 2016). Whereas the premise of aim 2 is to investigate the role of SR-BI, an innate immune receptor known to promote macrophage efferocytosis, during O_3-induced pulmonary inflammation and injury. These data generated in this report provide insight into understanding how O_3 alters the pulmonary innate immune response and how SRs protective the lung from unresolved inflammations can mitigate these changes.

Aim 1 of this project focuses on the resolution of O_3-induced pulmonary inflammation and injury. O_3 in known to cause and exacerbate chronic lung diseases in mice and humans (Sun et al., 2017 & Hansel et al., 2016). In the present study, we found that acute O_3 exposure impairs the efferocytic response of alveolar macrophages (Hodge et al., 2019). However, the underlying molecular mechanisms that induce this impairment are still unknown. Unresolved pulmonary inflammation and injury specifically through impaired efferocytosis is a key characteristic of several chronic lung diseases, such as asthma, pulmonary fibrosis, and chronic obstructive pulmonary disorder (COPD) (Berenson et al., 2013). Perhaps, the O_3 induced perturbations in macrophage

efferocytosis is one of the reasons why individuals living in areas of increased ambient levels of O_3 have a higher incidence of chronic lung disease and/or more frequent exacerbations.

There are several hypotheses that could explain the molecular mechanisms by which O_3 impairs alveolar macrophage efferocytosis. First, it is known that O_3 induces oxidative stress in the lung and systemically (Castaneda et al., 2017, Rivas-Arancibia et al., 2010, Kirkham 2007). Increased oxidative stress has previously been shown to impair efferocytosis by inducing apoptosis in healthy phagocytes, oxidizing externalized phosphatidylserine on apoptotic cells, and inducing necrosis, thus preventing the resolution of inflammation (Lee and Surh 2013 & Anderson et al., 2002). Secondly, in apoptotic cells undergo secondary necrosis are known to produce autoantigens, which can stimulate other immune cells to produce inflammatory cytokines and reactive oxygen species, leading to decreased efferocytosis (Kawano and Nagata 2018, McCubbrey and Curtis 2013, Hanayama et al., 2004). Third, in chronic pulmonary diseases where oxidative stress is enhanced, RhoA protein levels in phagocytes are significantly increased, which inhibits Rac, a G-protein responsible for mediating cytoskeletal rearrangement to engulf apoptotic cells (McCubbrey and Curtis 2013 & Richens et al., 2009). Lastly, decreases in the efferocytic response following O_3 exposure may reflect the increased presence of O_3-generated DAMPs, such as high mobility group box 1 protein (HMGB1) and oxPLs, both which suppress efferocytosis signaling pathways in macrophages (Yurdagul et al., 2018 & Michaudel et al., 2016). Our data report that there are increased apoptotic cells in the airspace following acute O_3 exposure, however how this relates to oxidative stress, cell death, autoantigens, DAMPs, or RhoA activation was

not evaluated. Collectively, these data may reveal the causation of how O_3 can increase one's susceptibility to and exacerbations of chronic lung disease as impaired efferocytosis in part is responsible for the progression of chronic pulmonary diseases. However, more work needs to be done to determine the exact molecular mechanisms by which O_3 impairs the resolution of pulmonary inflammation and/or injury.

Aim 2 of this study focuses on defining the role of SR-BI in regulating the O_3-induced pulmonary inflammation and the resolution of this response. In our study, we found that mice lacking SR-BI have increased pulmonary neutrophilia, impaired alveolar macrophage efferocytosis, and potentiated oxPL-induced pulmonary injury and macrophage production of proinflammatory cytokine expression despite no change in oxPL levels in the BAL following O_3 exposure. However, the underlying mechanisms of how SR-BI regulates efferocytosis and inflammatory gene expression in macrophages are unknown. Although our data supports previous studies highlighting the ability of SR-BI to mediate efferocytosis, to our knowledge, we are the first lab to uncover that mice lacking SR-BI have an impaired alveolar macrophage efferocytic responses that is further decreased following acute O_3 exposure (Tao et al., 2015, Osada et al., 2009). The baseline impaired efferocytosis observed in SR-BI$^{-/-}$ mice, that is exacerbated by O_3, may be the result of decreased recognition of phosphatidylserine (PS), which would delay engulfment as phagocytes deficient in other PS receptors, such as MerTK and MFG-E8 produce similar responses (de Couto et al., 2019, Wang et al., 2017, Elliot et al., 2017). Another consideration for decreased efferocytosis in SR-BI$^{-/-}$ macrophages is that in addition to delayed recognition of PS, they cannot secure an apoptotic cell for engulfment as SR-BI has been shown to be able to tether and mediate internalization of silica dust

and cholesterol (Tsugita et al., 2017 & de la Llera-Moya et al., 1999). Additionally, the potentiated inflammatory and injury response in SR-BI$^{-/-}$ mice and peritoneal macrophages we observed after exposure to oxPLs reveal another role of SR-BI in regulating the innate immune response to DAMPs. A consideration for this phenomenon would be that SR-BI mitigates inflammatory signaling induced by oxPLs through cooperating with TLR4, which has been implicated in multiple studies (Gowdy et al., 2015, Cai et al., 2012). Although SR-BI can bind to apoptotic cells, oxPLs are a known ligand for SR-BI as well (Kadl et al., 2011 & Imai et al., 2008). The increased pulmonary injury and neutrophilia we observed in SR-BI$^{-/-}$ mice may reflect decreased cellular uptake pathways and decreased levels of HDL-derived antioxidants, which quiesces inflammatory signaling pathways such as TLR4/NF-κB. Collectively, these data indicate provide evidence for a novel protective role for SR-BI in the lung following O_3 exposure.

Altogether, these two distinct aims of this dissertation project uncovered the negative effects of O_3 on resolution of inflammation and injury as well as providing data that shows how SR-BI regulates the pulmonary immune response. First, we determined that acute O_3 exposure impairs alveolar macrophage efferocytosis. Second, we defined the role of SR-BI during O_3-induced pulmonary inflammation and injury as being a mediator of efferocytosis and suppressing neutrophilic inflammation. These data could reveal susceptibilities to developing chronic pulmonary diseases in individuals with single nucleotide polymorphism (SNPs) loss-of-function mutations in SR-BI (Zanoni et al., 2016 & Vergeer et al., 2011). Long-term O_3 exposure studies have correlated O_3 and reduced lung function; however, studies have not analyzed pulmonary function in people with SR-BI SNPs (Paulin et al., 2019). Future clinical studies/observations on these individuals

may prove our findings in SR-BI$^{-/-}$ mice congruent with a specific susceptible population. Additionally, several therapeutic drugs and nutraceuticals such as statins, aspirin, nifedipine, and Vitamin E have increase SR-BI expression and production (Higuchi et al., 2013, Zhang et al., 2013, Lu et al., 2010, Kimura et al., 2008). Aspirin, nifedipine, and Vitamin E all increase the SR-BI binding activity and have all been used to attenuate pulmonary inflammation, injury and hypertension in various lung disease models but have yet to be described in the pulmonary effects of O_3 exposure (Hamid et al., 2017 , Cook-Mills et al., 2013, Moon et al., 2010). Future studies may include the use these pharmaceuticals in conjunction with O_3 exposure to evaluate pulmonary inflammation and/or efferocytosis at doses known to increase SR-BI production.

4.1: CONCLUSIONS

In conclusion, our data indicate that O_3 alters pulmonary macrophage efferocytosis and SR-BI is protective in the lung through dampening neutrophil recruitment to the lung and maintaining efferocytosis. These are the first data, to our knowledge, that analyzed the efferocytic response of macrophages in the lung following acute O_3 exposure. Additionally, our data describe a novel role of the pattern recognition receptor, SR-BI, in the lung following O_3 exposure. Although more studies are needed to fully understand the signaling mechanisms of how O_3 can induce these effects, these data indicate a pathway of how O_3 can increase exacerbation/susceptibility of chronic lung diseases and a possible therapeutic target for susceptible individuals. Future studies will also help us to understand whether individuals with known loss-of-function mutations in SR-BI are more vulnerable to developing chronic lung diseases after exposure to air pollutants. These

data add to a growing body of evidence that further our understanding how O_3 modulates pulmonary inflammation and injury.

4.2: LIMITATIONS

Although our findings are novel, we understand that this study has limitations. We were able to isolate and analyze differences in expression of inflammatory cytokines and efferocytosis genes in sorted alveolar macrophages between WT and SR-BI$^{-/-}$ mice. However, the lung has multiple subset populations that contribute to pulmonary innate immunity (Kapellos et al., 2018 & Morales-Nebreda et al., 2015). Sorting other understudied pulmonary macrophage populations, such as interstitial macrophages, residual, and inflammatory monocytes to analyze cytokine expression and function would allow us to determine the effects of O_3 and SR-BI on other immune cells and how these cells function during chronic lung diseases. Unfortunately, the contribution of these various monocyte/macrophage populations to regulating pulmonary immunity is not completely understood. Additionally, we found that SR-BI deficiency causes increased pulmonary injury and neutrophilia. It would be interesting if we had overexpressed SR-BI in our model to analyze whether injury, neutrophilia, and efferocytosis improve even beyond what we see in our WT mice. Lastly, we showed that there is impaired efferocytosis following O_3 exposure in WT and SR-BI$^{-/-}$ mice. However, efferocytosis is a multi-step process going from recognition to engulfment of apoptotic cells. Determining whether O_3 inhibits recognition of apoptotic cells in alveolar macrophage or inhibits the ability to rearrange its cytoskeleton to make a phagocytic cup for engulfment would allow us to further understand what we observed in our efferocytosis assay experiments. Using immunofluorescence and imaging techniques, we could measure and quantify the

different stages of the phagocytosis of apoptotic cells (Yeo et al., 2013 & Morioka et al., 2018). Although our study has limitations, future studies can uncover the underlying mechanisms regarding O_3 impairing efferocytosis and increasing one's susceptibility to and exacerbations of chronic lung disease.

4.3: FUTURE DIRECTIONS

Future research projects will build on these results of this to bridge knowledge gaps in two important areas. First, studies on determining the underlying molecular mechanisms in pulmonary macrophages that cause an impaired efferocytic response following acute O_3 exposure. Additional experiments analyzing the how O_3 modulates efferocytosis and cytokine secretion in pulmonary macrophage populations would help us further understand the negative effects of O_3 on innate immunity. Second, to examine the signaling mechanism of SR-BI mediated efferocytosis following O_3 exposure. Future experiments with Cre driver mice would prove fruitful in further understanding the effects of SR-BI deficiency in specific cell types. Recent evidence has discovered gene variants of SR-BI in humans, including gain of function and some loss of function SNP mutations (Manichaikul et al., 2018, Zanoni et al., 2016, Wu et al., 2012, Vergeer et al., 2011). Future clinical studies on these individuals will help us to understand whether they are more susceptible to the negative effects of air pollutants like O_3, such as increased susceptibilities/exacerbations of chronic lung diseases. With O_3 levels increasing despite stricter regulations and millions suffering from chronic lung diseases, these novel findings will advance our understanding of the negative effects of criteria air pollutants on the immune system and the implications of using scavenger receptors to mitigate those effects.

REFERENCES

Agassandian, M., & Mallampalli, R. K. (2013). Surfactant phospholipid metabolism. *Biochim Biophys Acta, 1831*(3), 612-625. doi:10.1016/j.bbalip.2012.09.010

Aldossari, A. A., Shannahan, J. H., Podila, R., & Brown, J. M. (2015). Influence of physicochemical properties of silver nanoparticles on mast cell activation and degranulation. *Toxicol In Vitro, 29*(1), 195-203. doi:10.1016/j.tiv.2014.10.008

Al-Hegelan, M., Tighe, R. M., Castillo, C., & Hollingsworth, J. W. (2011). Ambient ozone and pulmonary innate immunity. *Immunol Res, 49*(1-3), 173-191. doi:10.1007/s12026-010-8180-z

Anderson, H. A., Englert, R., Gursel, I., & Shacter, E. (2002). Oxidative stress inhibits the phagocytosis of apoptotic cells that have externalized phosphatidylserine. *Cell Death Differ, 9*(6), 616-625. doi:10.1038/sj.cdd.4401013

Angsana, J., Chen, J., Liu, L., Haller, C. A., & Chaikof, E. L. (2016). Efferocytosis as a regulator of macrophage chemokine receptor expression and polarization. *Eur J Immunol, 46*(7), 1592-1599. doi:10.1002/eji.201546262

Banerjee, S., de Freitas, A., Friggeri, A., Zmijewski, J. W., Liu, G., & Abraham, E. (2011). Intracellular HMGB1 negatively regulates efferocytosis. *J Immunol, 187*(9), 4686-4694. doi:10.4049/jimmunol.1101500

Baranova, I. N., Vishnyakova, T. G., Bocharov, A. V., Leelahavanichkul, A., Kurlander, R., Chen, Z., . . . Eggerman, T. L. (2012). Class B scavenger receptor types I and II and CD36 mediate bacterial recognition and proinflammatory signaling induced by Escherichia coli, lipopolysaccharide, and cytosolic chaperonin 60. *J Immunol, 188*(3), 1371-1380. doi:10.4049/jimmunol.110035

Bauer, A. K., Rondini, E. A., Hummel, K. A., Degraff, L. M., Walker, C., Jedlicka, A. E., & Kleeberger, S. R. (2011). Identification of candidate genes downstream of TLR4 signaling after ozone exposure in mice: a role for heat-shock protein 70. *Environ Health Perspect, 119*(8), 1091-1097. doi:10.1289/ehp.1003326

Bauer, R. N., Diaz-Sanchez, D., & Jaspers, I. (2012). Effects of air pollutants on innate immunity: the role of Toll-like receptors and nucleotide-binding oligomerization domain-like receptors. *J Allergy Clin Immunol, 129*(1), 14-24; quiz 25-16. doi:10.1016/j.jaci.2011.11.004

Behnia, F., Sheller, S., & Menon, R. (2016). Mechanistic Differences Leading to Infectious and Sterile Inflammation. *Am J Reprod Immunol, 75*(5), 505-518. doi:10.1111/aji.12496

Berenson, C. S., Kruzel, R. L., Eberhardt, E., & Sethi, S. (2013). Phagocytic dysfunction of human alveolar macrophages and severity of chronic obstructive pulmonary disease. *J Infect Dis, 208*(12), 2036-2045. doi:10.1093/infdis/jit400

Bromberg, P. A. (2016). Mechanisms of the acute effects of inhaled ozone in humans. *Biochim Biophys Acta, 1860*(12), 2771-2781. doi:10.1016/j.bbagen.2016.07.015

Brouckaert, G., Kalai, M., Krysko, D. V., Saelens, X., Vercammen, D., Ndlovu, M. N., . . . Vandenabeele, P. (2004). Phagocytosis of necrotic cells by macrophages is phosphatidylserine dependent and does not induce inflammatory cytokine production. *Mol Biol Cell, 15*(3), 1089-1100. doi:10.1091/mbc.e03-09-0668

Buja, A., De Polo, A., De Battisti, E., Sperotto, M., Baldovin, T., Cocchio, S., . . . Ebell, M. (2020). The importance of sex as a risk factor for hospital readmissions due to

pulmonary diseases. BMC Public Health, 20(1), 53. doi:10.1186/s12889-019-8138-6

Cai, L., de Beer, M. C., de Beer, F. C., & van der Westhuyzen, D. R. (2005). Serum amyloid A is a ligand for scavenger receptor class B type I and inhibits high density lipoprotein binding and selective lipid uptake. *J Biol Chem, 280*(4), 2954-2961. doi:10.1074/jbc.M411555200

Cai, L., Wang, Z., Meyer, J. M., Ji, A., & van der Westhuyzen, D. R. (2012). Macrophage SR-BI regulates LPS-induced pro-inflammatory signaling in mice and isolated macrophages. *J Lipid Res, 53*(8), 1472-1481. doi:10.1194/jlr.M023234

Cao, G., Garcia, C. K., Wyne, K. L., Schultz, R. A., Parker, K. L., & Hobbs, H. H. (1997). Structure and localization of the human gene encoding SR-BI/CLA-1. Evidence for transcriptional control by steroidogenic factor 1. *J Biol Chem, 272*(52), 33068-33076. doi:10.1074/jbc.272.52.33068

Castaneda, O. A., Lee, S. C., Ho, C. T., & Huang, T. C. (2017). Macrophages in oxidative stress and models to evaluate the antioxidant function of dietary natural compounds. *J Food Drug Anal, 25*(1), 111-118. doi:10.1016/j.jfda.2016.11.006

Cavalcanti, D. M., Lotufo, C. M., Borelli, P., Tavassi, A. M., Pereira, A. L., Markus, R. P., & Farsky, S. H. (2006). Adrenal deficiency alters mechanisms of neutrophil mobilization. *Mol Cell Endocrinol, 249*(1-2), 32-39. doi:10.1016/j.mce.2006.01.007

Chen, C. H., Chan, C. C., Chen, B. Y., Cheng, T. J., & Leon Guo, Y. (2015). Effects of particulate air pollution and ozone on lung function in non-asthmatic children. *Environ Res, 137*, 40-48. doi:10.1016/j.envres.2014.11.021

Chen, W., Frank, M. E., Jin, W., & Wahl, S. M. (2001). TGF-beta released by apoptotic T

cells contributes to an immunosuppressive milieu. *Immunity, 14*(6), 715-725.

Cho, Y., Abu-Ali, G., Tashiro, H., Brown, T. A., Osgood, R. S., Kasahara, D. I., . . . Shore, S. A. (2019). Sex Differences in Pulmonary Responses to Ozone in Mice. Role of the Microbiome. Am J Respir Cell Mol Biol, 60(2), 198-208. doi:10.1165/rcmb.2018-0099OC

Cook-Mills, J. M., Abdala-Valencia, H., & Hartert, T. (2013). Two faces of vitamin E in the lung. *Am J Respir Crit Care Med, 188*(3), 279-284. doi:10.1164/rccm.201303-0503ED

Crowther, J. E., Kutala, V. K., Kuppusamy, P., Ferguson, J. S., Beharka, A. A., Zweier, J. L., . . . Schlesinger, L. S. (2004). Pulmonary surfactant protein a inhibits macrophage reactive oxygen intermediate production in response to stimuli by reducing NADPH oxidase activity. *J Immunol, 172*(11), 6866-6874.

Dahl, M., Bauer, A. K., Arredouani, M., Soininen, R., Tryggvason, K., Kleeberger, S. R., & Kobzik, L. (2007). Protection against inhaled oxidants through scavenging of oxidized lipids by macrophage receptors MARCO and SR-AI/II. *J Clin Invest, 117*(3), 757-764. doi:10.1172/JCI29968

Dai, C., Yao, X., Keeran, K. J., Zywicke, G. J., Qu, X., Yu, Z. X., . . . Levine, S. J. (2012). Apolipoprotein A-I attenuates ovalbumin-induced neutrophilic airway inflammation via a granulocyte colony-stimulating factor-dependent mechanism. *Am J Respir Cell Mol Biol, 47*(2), 186-195. doi:10.1165/rcmb.2011-0322OC

Dalli, J., & Serhan, C. N. (2017). Pro-Resolving Mediators in Regulating and Conferring Macrophage Function. *Front Immunol, 8*, 1400. doi:10.3389/fimmu.2017.01400

Darrow, L. A., Klein, M., Flanders, W. D., Mulholland, J. A., Tolbert, P. E., & Strickland,

M. J. (2014). Air pollution and acute respiratory infections among children 0-4 years of age: an 18-year time-series study. *Am J Epidemiol, 180*(10), 968-977. doi:10.1093/aje/kwu234

Davies, S. S., & Guo, L. (2014). Lipid peroxidation generates biologically active phospholipids including oxidatively N-modified phospholipids. *Chem Phys Lipids, 181*, 1-33. doi:10.1016/j.chemphyslip.2014.03.002

de Couto, G., Jaghatspanyan, E., DeBerge, M., Liu, W., Luther, K., Wang, Y., . . . Marban, E. (2019). Mechanism of Enhanced MerTK-Dependent Macrophage Efferocytosis by Extracellular Vesicles. *Arterioscler Thromb Vasc Biol, 39*(10), 2082-2096. doi:10.1161/ATVBAHA.119.313115

de la Llera-Moya, M., Rothblat, G. H., Connelly, M. A., Kellner-Weibel, G., Sakr, S. W., Phillips, M. C., & Williams, D. L. (1999). Scavenger receptor BI (SR-BI) mediates free cholesterol flux independently of HDL tethering to the cell surface. *J Lipid Res, 40*(3), 575-580.

Donnelly, L. E., & Barnes, P. J. (2012). Defective phagocytosis in airways disease. *Chest, 141*(4), 1055-1062. doi:10.1378/chest.11-2348

Draper, D. W., Madenspacher, J. H., Dixon, D., King, D. H., Remaley, A. T., & Fessler, M. B. (2010). ATP-binding cassette transporter G1 deficiency dysregulates host defense in the lung. *Am J Respir Crit Care Med, 182*(3), 404-412. doi:10.1164/rccm.200910-1580OC

Elliott, M. R., Koster, K. M., & Murphy, P. S. (2017). Efferocytosis Signaling in the Regulation of Macrophage Inflammatory Responses. *J Immunol, 198*(4), 1387-1394. doi:10.4049/jimmunol.1601520

Endemann, G., Stanton, L. W., Madden, K. S., Bryant, C. M., White, R. T., & Protter, A. A. (1993). CD36 is a receptor for oxidized low density lipoprotein. *J Biol Chem, 268*(16), 11811-11816.

Fan, E. K. Y., & Fan, J. (2018). Regulation of alveolar macrophage death in acute lung inflammation. *Respir Res, 19*(1), 50. doi:10.1186/s12931-018-0756-5

Fessler, M. B. (2017). A New Frontier in Immunometabolism. Cholesterol in Lung Health and Disease. *Ann Am Thorac Soc, 14*(Supplement_5), S399-S405. doi:10.1513/AnnalsATS.201702-136AW

Fuentes, N., Cabello, N., Nicoleau, M., Chroneos, Z. C., & Silveyra, P. (2019). Modulation of the lung inflammatory response to ozone by the estrous cycle. Physiol Rep, 7(5), e14026. doi:10.14814/phy2.14026

Gao, D., Ashraf, M. Z., Kar, N. S., Lin, D., Sayre, L. M., & Podrez, E. A. (2010). Structural basis for the recognition of oxidized phospholipids in oxidized low density lipoproteins by class B scavenger receptors CD36 and SR-BI. *J Biol Chem, 285*(7), 4447-4454. doi:10.1074/jbc.M109.082800

Gheibi Hayat, S. M., Bianconi, V., Pirro, M., & Sahebkar, A. (2019). Efferocytosis: molecular mechanisms and pathophysiological perspectives. *Immunol Cell Biol, 97*(2), 124-133. doi:10.1111/imcb.12206

Gilibert, S., Galle-Treger, L., Moreau, M., Saint-Charles, F., Costa, S., Ballaire, R., . . . Huby, T. (2014). Adrenocortical scavenger receptor class B type I deficiency exacerbates endotoxic shock and precipitates sepsis-induced mortality in mice. *J Immunol, 193*(2), 817-826. doi:10.4049/jimmunol.1303164

Gillotte-Taylor, K., Boullier, A., Witztum, J. L., Steinberg, D., & Quehenberger, O. (2001).

Scavenger receptor class B type I as a receptor for oxidized low density lipoprotein. *J Lipid Res, 42*(9), 1474-1482.

Gilmour, M. I., Hmieleski, R. R., Stafford, E. A., & Jakab, G. J. (1991). Suppression and recovery of the alveolar macrophage phagocytic system during continuous exposure to 0.5 ppm ozone. *Exp Lung Res, 17*(3), 547-558.

Gonzalez-Guevara, E., Martinez-Lazcano, J. C., Custodio, V., Hernandez-Ceron, M., Rubio, C., & Paz, C. (2014). Exposure to ozone induces a systemic inflammatory response: possible source of the neurological alterations induced by this gas. *Inhal Toxicol, 26*(8), 485-491. doi:10.3109/08958378.2014.922648

Gowdy, K. M., Madenspacher, J. H., Azzam, K. M., Gabor, K. A., Janardhan, K. S., Aloor, J. J., & Fessler, M. B. (2015). Key role for scavenger receptor B-I in the integrative physiology of host defense during bacterial pneumonia. *Mucosal Immunol, 8*(3), 559-571. doi:10.1038/mi.2014.88

Grabiec, A. M., Denny, N., Doherty, J. A., Happonen, K. E., Hankinson, J., Connolly, E., . . . Hussell, T. (2017). Diminished airway macrophage expression of the Axl receptor tyrosine kinase is associated with defective efferocytosis in asthma. *J Allergy Clin Immunol, 140*(4), 1144-1146 e1144. doi:10.1016/j.jaci.2017.03.024

Grabiec, A. M., & Hussell, T. (2016). The role of airway macrophages in apoptotic cell clearance following acute and chronic lung inflammation. *Semin Immunopathol, 38*(4), 409-423. doi:10.1007/s00281-016-0555-3

Gregoire, M., Uhel, F., Lesouhaitier, M., Gacouin, A., Guirriec, M., Mourcin, F., . . . Tadie, J. M. (2018). Impaired efferocytosis and neutrophil extracellular trap clearance by macrophages in ARDS. *Eur Respir J, 52*(2). doi:10.1183/13993003.02590-2017

Guth, A. M., Janssen, W. J., Bosio, C. M., Crouch, E. C., Henson, P. M., & Dow, S. W. (2009). Lung environment determines unique phenotype of alveolar macrophages. *Am J Physiol Lung Cell Mol Physiol, 296*(6), L936-946. doi:10.1152/ajplung.90625.2008

Hamid, U., Krasnodembskaya, A., Fitzgerald, M., Shyamsundar, M., Kissenpfennig, A., Scott, C., . . . O'Kane, C. M. (2017). Aspirin reduces lipopolysaccharide-induced pulmonary inflammation in human models of ARDS. *Thorax, 72*(11), 971-980. doi:10.1136/thoraxjnl-2016-208571

Hamon, R., Tran, H. B., Roscioli, E., Ween, M., Jersmann, H., & Hodge, S. (2018). Bushfire smoke is pro-inflammatory and suppresses macrophage phagocytic function. *Sci Rep, 8*(1), 13424. doi:10.1038/s41598-018-31459-6

Hanayama, R., Tanaka, M., Miyasaka, K., Aozasa, K., Koike, M., Uchiyama, Y., & Nagata, S. (2004). Autoimmune disease and impaired uptake of apoptotic cells in MFG-E8-deficient mice. *Science, 304*(5674), 1147-1150. doi:10.1126/science.1094359

Hansel, N. N., McCormack, M. C., & Kim, V. (2016). The Effects of Air Pollution and Temperature on COPD. *COPD, 13*(3), 372-379. doi:10.3109/15412555.2015.1089846

Hatch, G. E., Slade, R., Harris, L. P., McDonnell, W. F., Devlin, R. B., Koren, H. S., . . . McKee, J. (1994). Ozone dose and effect in humans and rats. A comparison using oxygen-18 labeling and bronchoalveolar lavage. *Am J Respir Crit Care Med, 150*(3), 676-683. doi:10.1164/ajrccm.150.3.8087337

Helgadottir, A., Sulem, P., Thorgeirsson, G., Gretarsdottir, S., Thorleifsson, G., Jensson, B. O., . . . Stefansson, K. (2018). Rare SCARB1 mutations associate with high-

density lipoprotein cholesterol but not with coronary artery disease. *Eur Heart J, 39*(23), 2172-2178. doi:10.1093/eurheartj/ehy169

Henriquez, A., House, J., Miller, D. B., Snow, S. J., Fisher, A., Ren, H., . . . Kodavanti, U. P. (2017). Adrenal-derived stress hormones modulate ozone-induced lung injury and inflammation. *Toxicol Appl Pharmacol, 329*, 249-258. doi:10.1016/j.taap.2017.06.009

Higuchi, H., Ito, E., Iwano, H., Oikawa, S., & Nagahata, H. (2013). Effects of vitamin E supplementation on cellular alpha-tocopherol concentrations of neutrophils in Holstein calves. *Can J Vet Res, 77*(2), 120-125.

Hodge, M. X., Reece, S. W., Madenspacher, J. H., & Gowdy, K. M. (2019). In Vivo Assessment of Alveolar Macrophage Efferocytosis Following Ozone Exposure. *J Vis Exp*(152). doi:10.3791/60109

Hoekstra, M., van der Sluis, R. J., Van Eck, M., & Van Berkel, T. J. (2013). Adrenal-specific scavenger receptor BI deficiency induces glucocorticoid insufficiency and lowers plasma very-low-density and low-density lipoprotein levels in mice. *Arterioscler Thromb Vasc Biol, 33*(2), e39-46. doi:10.1161/ATVBAHA.112.300784

Hollingsworth, J. W., Maruoka, S., Li, Z., Potts, E. N., Brass, D. M., Garantziotis, S., . . . Schwartz, D. A. (2007). Ambient ozone primes pulmonary innate immunity in mice. *J Immunol, 179*(7), 4367-4375. doi:10.4049/jimmunol.179.7.4367

Hu, Z., Hu, J., Zhang, Z., Shen, W. J., Yun, C. C., Berlot, C. H., . . . Azhar, S. (2013). Regulation of expression and function of scavenger receptor class B, type I (SR-BI) by Na+/H+ exchanger regulatory factors (NHERFs). *J Biol Chem, 288*(16), 11416-11435. doi:10.1074/jbc.M112.437368

Hussell, T., & Bell, T. J. (2014). Alveolar macrophages: plasticity in a tissue-specific context. *Nat Rev Immunol, 14*(2), 81-93. doi:10.1038/nri3600

Imai, Y., Kuba, K., Neely, G. G., Yaghubian-Malhami, R., Perkmann, T., van Loo, G., . . . Penninger, J. M. (2008). Identification of oxidative stress and Toll-like receptor 4 signaling as a key pathway of acute lung injury. *Cell, 133*(2), 235-249. doi:10.1016/j.cell.2008.02.043

Jakab, G. J., Spannhake, E. W., Canning, B. J., Kleeberger, S. R., & Gilmour, M. I. (1995). The effects of ozone on immune function. *Environ Health Perspect, 103 Suppl 2*, 77-89. doi:10.1289/ehp.95103s277

Janssen, W. J., & Morimoto, K. (2012). Apoptotic cell clearance and fibrotic lung disease. *Eur Respir J, 40*(2), 289-290. doi:10.1183/09031936.00020612

Jones, H. R., Robb, C. T., Perretti, M., & Rossi, A. G. (2016). The role of neutrophils in inflammation resolution. *Semin Immunol, 28*(2), 137-145. doi:10.1016/j.smim.2016.03.007

Kadl, A., Bochkov, V. N., Huber, J., & Leitinger, N. (2004). Apoptotic cells as sources for biologically active oxidized phospholipids. *Antioxid Redox Signal, 6*(2), 311-320. doi:10.1089/152308604322899378

Kadl, A., Sharma, P. R., Chen, W., Agrawal, R., Meher, A. K., Rudraiah, S., . . . Leitinger, N. (2011). Oxidized phospholipid-induced inflammation is mediated by Toll-like receptor 2. *Free Radic Biol Med, 51*(10), 1903-1909. doi:10.1016/j.freeradbiomed.2011.08.026

Kapellos, T. S., Bassler, K., Aschenbrenner, A. C., Fujii, W., & Schultze, J. L. (2018). Dysregulated Functions of Lung Macrophage Populations in COPD. *J Immunol*

Res, 2018, 2349045. doi:10.1155/2018/2349045

Karaji, N., & Sattentau, Q. J. (2017). Efferocytosis of Pathogen-Infected Cells. *Front Immunol, 8*, 1863. doi:10.3389/fimmu.2017.01863

Karnati, S., Garikapati, V., Liebisch, G., Van Veldhoven, P. P., Spengler, B., Schmitz, G., & Baumgart-Vogt, E. (2018). Quantitative lipidomic analysis of mouse lung during postnatal development by electrospray ionization tandem mass spectrometry. *PLoS One, 13*(9), e0203464. doi:10.1371/journal.pone.0203464

Kawano, M., & Nagata, S. (2018). Lupus-like autoimmune disease caused by a lack of Xkr8, a caspase-dependent phospholipid scramblase. *Proc Natl Acad Sci U S A, 115*(9), 2132-2137. doi:10.1073/pnas.1720732115

Kierstein, S., Poulain, F. R., Cao, Y., Grous, M., Mathias, R., Kierstein, G., . . . Haczku, A. (2006). Susceptibility to ozone-induced airway inflammation is associated with decreased levels of surfactant protein D. *Respir Res, 7*, 85. doi:10.1186/1465-9921-7-85

Kilburg-Basnyat, B., Reece, S. W., Crouch, M. J., Luo, B., Boone, A. D., Yaeger, M., . . . Gowdy, K. M. (2018). Specialized Pro-Resolving Lipid Mediators Regulate Ozone-Induced Pulmonary and Systemic Inflammation. *Toxicol Sci, 163*(2), 466-477. doi:10.1093/toxsci/kfy040

Kim, K. K., Dotson, M. R., Agarwal, M., Yang, J., Bradley, P. B., Subbotina, N., . . . Sisson, T. H. (2018). Efferocytosis of apoptotic alveolar epithelial cells is sufficient to initiate lung fibrosis. *Cell Death Dis, 9*(11), 1056. doi:10.1038/s41419-018-1074-z

Kimura, T., Mogi, C., Tomura, H., Kuwabara, A., Im, D. S., Sato, K., . . . Okajima, F. (2008). Induction of scavenger receptor class B type I is critical for simvastatin

enhancement of high-density lipoprotein-induced anti-inflammatory actions in endothelial cells. *J Immunol, 181*(10), 7332-7340. doi:10.4049/jimmunol.181.10.7332

Kirkham, P. (2007). Oxidative stress and macrophage function: a failure to resolve the inflammatory response. *Biochem Soc Trans, 35*(Pt 2), 284-287. doi:10.1042/BST0350284

Kleeberger, S. R., Reddy, S., Zhang, L. Y., & Jedlicka, A. E. (2000). Genetic susceptibility to ozone-induced lung hyperpermeability: role of toll-like receptor 4. *Am J Respir Cell Mol Biol, 22*(5), 620-627. doi:10.1165/ajrcmb.22.5.3912

Kolleck, I., Witt, W., Wissel, H., Sinha, P., & Rustow, B. (2000). HDL and vitamin E in plasma and the expression of SR-BI on lung cells during rat perinatal development. *Lung, 178*(4), 191-200. doi:10.1007/s004080000023

Komai, K., Shichita, T., Ito, M., Kanamori, M., Chikuma, S., & Yoshimura, A. (2017). Role of scavenger receptors as damage-associated molecular pattern receptors in Toll-like receptor activation. *Int Immunol, 29*(2), 59-70. doi:10.1093/intimm/dxx010

Kosmider, B., Loader, J. E., Murphy, R. C., & Mason, R. J. (2010). Apoptosis induced by ozone and oxysterols in human alveolar epithelial cells. *Free Radic Biol Med, 48*(11), 1513-1524. doi:10.1016/j.freeradbiomed.2010.02.032

Krieger, M., & Kozarsky, K. (1999). Influence of the HDL receptor SR-BI on atherosclerosis. *Curr Opin Lipidol, 10*(6), 491-497. doi:10.1097/00041433-199912000-00003

Lavin, Y., Winter, D., Blecher-Gonen, R., David, E., Keren-Shaul, H., Merad, M., . . . Amit, I. (2014). Tissue-resident macrophage enhancer landscapes are shaped by the

local microenvironment. *Cell, 159*(6), 1312-1326. doi:10.1016/j.cell.2014.11.018

Lee, H. N., Kundu, J. K., Cha, Y. N., & Surh, Y. J. (2013). Resolvin D1 stimulates efferocytosis through p50/p50-mediated suppression of tumor necrosis factor-alpha expression. *J Cell Sci, 126*(Pt 17), 4037-4047. doi:10.1242/jcs.131003

Lee, H. N., & Surh, Y. J. (2013). Resolvin D1-mediated NOX2 inactivation rescues macrophages undertaking efferocytosis from oxidative stress-induced apoptosis. *Biochem Pharmacol, 86*(6), 759-769. doi:10.1016/j.bcp.2013.07.002

Linton, M. F., Babaev, V. R., Huang, J., Linton, E. F., Tao, H., & Yancey, P. G. (2016). Macrophage Apoptosis and Efferocytosis in the Pathogenesis of Atherosclerosis. *Circ J, 80*(11), 2259-2268. doi:10.1253/circj.CJ-16-0924

Linton, M. F., Tao, H., Linton, E. F., & Yancey, P. G. (2017). SR-BI: A Multifunctional Receptor in Cholesterol Homeostasis and Atherosclerosis. *Trends Endocrinol Metab, 28*(6), 461-472. doi:10.1016/j.tem.2017.02.001

Lockett, A. D., Petrusca, D. N., Justice, M. J., Poirier, C., Serban, K. A., Rush, N. I., . . . Petrache, I. (2015). Scavenger receptor class B, type I-mediated uptake of A1AT by pulmonary endothelial cells. *Am J Physiol Lung Cell Mol Physiol, 309*(4), L425-434. doi:10.1152/ajplung.00376.2014

Lopez, D., Sandhoff, T. W., & McLean, M. P. (1999). Steroidogenic factor-1 mediates cyclic 3',5'-adenosine monophosphate regulation of the high density lipoprotein receptor. *Endocrinology, 140*(7), 3034-3044. doi:10.1210/endo.140.7.6846

Lu, L., Liu, H., Peng, J., Gan, L., Shen, L., Zhang, Q., . . . Jiang, Y. (2010). Regulations of the key mediators in inflammation and atherosclerosis by aspirin in human macrophages. *Lipids Health Dis, 9*, 16. doi:10.1186/1476-511X-9-16

Martin-Fuentes, P., Civeira, F., Recalde, D., Garcia-Otin, A. L., Jarauta, E., Marzo, I., & Cenarro, A. (2007). Individual variation of scavenger receptor expression in human macrophages with oxidized low-density lipoprotein is associated with a differential inflammatory response. *J Immunol, 179*(5), 3242-3248. doi:10.4049/jimmunol.179.5.3242

McCubbrey, A. L., & Curtis, J. L. (2013). Efferocytosis and lung disease. *Chest, 143*(6), 1750-1757. doi:10.1378/chest.12-2413

Mikerov, A. N., Umstead, T. M., Gan, X., Huang, W., Guo, X., Wang, G., . . . Floros, J. (2008). Impact of ozone exposure on the phagocytic activity of human surfactant protein A (SP-A) and SP-A variants. *Am J Physiol Lung Cell Mol Physiol, 294*(1), L121-130. doi:10.1152/ajplung.00288.2007

Miller, D. B., Ghio, A. J., Karoly, E. D., Bell, L. N., Snow, S. J., Madden, M. C., . . . Kodavanti, U. P. (2016). Ozone Exposure Increases Circulating Stress Hormones and Lipid Metabolites in Humans. *Am J Respir Crit Care Med, 193*(12), 1382-1391. doi:10.1164/rccm.201508-1599OC

Miller, D. B., Karoly, E. D., Jones, J. C., Ward, W. O., Vallanat, B. D., Andrews, D. L., . . . Kodavanti, U. P. (2015). Inhaled ozone (O3)-induces changes in serum metabolomic and liver transcriptomic profiles in rats. *Toxicol Appl Pharmacol, 286*(2), 65-79. doi:10.1016/j.taap.2015.03.025

Moon, H. G., Kim, Y. S., Choi, J. P., Choi, D. S., Yoon, C. M., Jeon, S. G., . . . Kim, Y. K. (2010). Aspirin attenuates the anti-inflammatory effects of theophylline via inhibition of cAMP production in mice with non-eosinophilic asthma. *Exp Mol Med, 42*(1), 47-60. doi:10.3858/emm.2010.42.1.005

Morales-Nebreda, L., Misharin, A. V., Perlman, H., & Budinger, G. R. (2015). The heterogeneity of lung macrophages in the susceptibility to disease. *Eur Respir Rev, 24*(137), 505-509. doi:10.1183/16000617.0031-2015

Moret, I., Lorenzo, M. J., Sarria, B., Cases, E., Morcillo, E., Perpina, M., . . . Menendez, R. (2011). Increased lung neutrophil apoptosis and inflammation resolution in nonresponding pneumonia. *Eur Respir J, 38*(5), 1158-1164. doi:10.1183/09031936.00190410

Morimoto, K., Janssen, W. J., & Terada, M. (2012). Defective efferocytosis by alveolar macrophages in IPF patients. *Respir Med, 106*(12), 1800-1803. doi:10.1016/j.rmed.2012.08.020

Morioka, S., Perry, J. S. A., Raymond, M. H., Medina, C. B., Zhu, Y., Zhao, L., . . . Ravichandran, K. S. (2018). Efferocytosis induces a novel SLC program to promote glucose uptake and lactate release. *Nature, 563*(7733), 714-718. doi:10.1038/s41586-018-0735-5

Nayak, D. K., Mendez, O., Bowen, S., & Mohanakumar, T. (2018). Isolation and In Vitro Culture of Murine and Human Alveolar Macrophages. *J Vis Exp*(134). doi:10.3791/57287

Nebbioso, A., Benedetti, R., Conte, M., Carafa, V., De Bellis, F., Shaik, J., . . . Altucci, L. (2017). Time-resolved analysis of DNA-protein interactions in living cells by UV laser pulses. *Sci Rep, 7*(1), 11725. doi:10.1038/s41598-017-12010-5

Nieland, T. J., Penman, M., Dori, L., Krieger, M., & Kirchhausen, T. (2002). Discovery of chemical inhibitors of the selective transfer of lipids mediated by the HDL receptor SR-BI. *Proc Natl Acad Sci U S A, 99*(24), 15422-15427.

doi:10.1073/pnas.222421399

Nishi, C., Yanagihashi, Y., Segawa, K., & Nagata, S. (2019). MERTK tyrosine kinase receptor together with TIM4 phosphatidylserine receptor mediates distinct signal transduction pathways for efferocytosis and cell proliferation. *J Biol Chem, 294*(18), 7221-7230. doi:10.1074/jbc.RA118.006628

Nishi, C., Yanagihashi, Y., Segawa, K., & Nagata, S. (2019). MERTK tyrosine kinase receptor together with TIM4 phosphatidylserine receptor mediates distinct signal transduction pathways for efferocytosis and cell proliferation. *J Biol Chem, 294*(18), 7221-7230. doi:10.1074/jbc.RA118.006628

Novak, M. L., & Thorp, E. B. (2013). Shedding light on impaired efferocytosis and nonresolving inflammation. *Circ Res, 113*(1), 9-12. doi:10.1161/CIRCRESAHA.113.301583

Osada, Y., Sunatani, T., Kim, I. S., Nakanishi, Y., & Shiratsuchi, A. (2009). Signalling pathway involving GULP, MAPK and Rac1 for SR-BI-induced phagocytosis of apoptotic cells. *J Biochem, 145*(3), 387-394. doi:10.1093/jb/mvn176

Park, Y. J., Liu, G., Lorne, E. F., Zhao, X., Wang, J., Tsuruta, Y., . . . Abraham, E. (2008). PAI-1 inhibits neutrophil efferocytosis. *Proc Natl Acad Sci U S A, 105*(33), 11784-11789. doi:10.1073/pnas.0801394105

Parks, B. W., Black, L. L., Zimmerman, K. A., Metz, A. E., Steele, C., Murphy-Ullrich, J. E., & Kabarowski, J. H. (2013). CD36, but not G2A, modulates efferocytosis, inflammation, and fibrosis following bleomycin-induced lung injury. *J Lipid Res, 54*(4), 1114-1123. doi:10.1194/jlr.M035352

Paulin, L. M., Gassett, A. J., Alexis, N. E., Kirwa, K., Kanner, R. E., Peters, S., . . . for, S.

i. (2019). Association of Long-term Ambient Ozone Exposure With Respiratory Morbidity in Smokers. *JAMA Intern Med*. doi:10.1001/jamainternmed.2019.5498

Peiser, L., Mukhopadhyay, S., & Gordon, S. (2002). Scavenger receptors in innate immunity. *Curr Opin Immunol, 14*(1), 123-128. doi:10.1016/s0952-7915(01)00307-7

Penberthy, K. K., & Ravichandran, K. S. (2016). Apoptotic cell recognition receptors and scavenger receptors. *Immunol Rev, 269*(1), 44-59. doi:10.1111/imr.12376

Pfeiler, S., Khandagale, A. B., Magenau, A., Nichols, M., Heijnen, H. F., Rinninger, F., . . . Engelmann, B. (2016). Distinct surveillance pathway for immunopathology during acute infection via autophagy and SR-BI. *Sci Rep, 6*, 34440. doi:10.1038/srep34440

Pino, M. V., McDonald, R. J., Berry, J. D., Joad, J. P., Tarkington, B. K., & Hyde, D. M. (1992). Functional and morphologic changes caused by acute ozone exposure in the isolated and perfused rat lung. *Am Rev Respir Dis, 145*(4 Pt 1), 882-889. doi:10.1164/ajrccm/145.4_Pt_1.882

Puttur, F., Gregory, L. G., & Lloyd, C. M. (2019). Airway macrophages as the guardians of tissue repair in the lung. *Immunol Cell Biol*. doi:10.1111/imcb.12235

Richens, T. R., Linderman, D. J., Horstmann, S. A., Lambert, C., Xiao, Y. Q., Keith, R. L., . . . Vandivier, R. W. (2009). Cigarette smoke impairs clearance of apoptotic cells through oxidant-dependent activation of RhoA. *Am J Respir Crit Care Med, 179*(11), 1011-1021. doi:10.1164/rccm.200807-1148OC

Rigotti, A., Trigatti, B. L., Penman, M., Rayburn, H., Herz, J., & Krieger, M. (1997). A targeted mutation in the murine gene encoding the high density lipoprotein (HDL)

receptor scavenger receptor class B type I reveals its key role in HDL metabolism. *Proc Natl Acad Sci U S A, 94*(23), 12610-12615. doi:10.1073/pnas.94.23.12610

Rivas-Arancibia, S., Guevara-Guzman, R., Lopez-Vidal, Y., Rodriguez-Martinez, E., Zanardo-Gomes, M., Angoa-Perez, M., & Raisman-Vozari, R. (2010). Oxidative stress caused by ozone exposure induces loss of brain repair in the hippocampus of adult rats. *Toxicol Sci, 113*(1), 187-197. doi:10.1093/toxsci/kfp252

Robb, C. T., Regan, K. H., Dorward, D. A., & Rossi, A. G. (2016). Key mechanisms governing resolution of lung inflammation. *Semin Immunopathol, 38*(4), 425-448. doi:10.1007/s00281-016-0560-6

Robertson, S., Colombo, E. S., Lucas, S. N., Hall, P. R., Febbraio, M., Paffett, M. L., & Campen, M. J. (2013). CD36 mediates endothelial dysfunction downstream of circulating factors induced by O3 exposure. *Toxicol Sci, 134*(2), 304-311. doi:10.1093/toxsci/kft107

Rock, K. L., Latz, E., Ontiveros, F., & Kono, H. (2010). The sterile inflammatory response. *Annu Rev Immunol, 28*, 321-342. doi:10.1146/annurev-immunol-030409-101311

Roh, J. S., & Sohn, D. H. (2018). Damage-Associated Molecular Patterns in Inflammatory Diseases. *Immune Netw, 18*(4), e27. doi:10.4110/in.2018.18.e27

Ronchetti, S., Ricci, E., Migliorati, G., Gentili, M., & Riccardi, C. (2018). How Glucocorticoids Affect the Neutrophil Life. *Int J Mol Sci, 19*(12). doi:10.3390/ijms19124090

Rymut, N., Heinz, J., Sadhu, S., Hosseini, Z., Riley, C. O., Marinello, M., . . . Fredman, G. (2020). Resolvin D1 promotes efferocytosis in aging by limiting senescent cell-induced MerTK cleavage. *FASEB J, 34*(1), 597-609. doi:10.1096/fj.201902126R

Saffar, A. S., Ashdown, H., & Gounni, A. S. (2011). The molecular mechanisms of glucocorticoids-mediated neutrophil survival. *Curr Drug Targets, 12*(4), 556-562. doi:10.2174/138945011794751555

Santander, N., Lizama, C., Parga, M. J., Quiroz, A., Perez, D., Echeverria, G., . . . Busso, D. (2017). Deficient Vitamin E Uptake During Development Impairs Neural Tube Closure in Mice Lacking Lipoprotein Receptor SR-BI. *Sci Rep, 7*(1), 5182. doi:10.1038/s41598-017-05422-w

Schleimer, R. P. (2004). Glucocorticoids suppress inflammation but spare innate immune responses in airway epithelium. *Proc Am Thorac Soc, 1*(3), 222-230. doi:10.1513/pats.200402-018MS

Serhan, C. N., Yang, R., Martinod, K., Kasuga, K., Pillai, P. S., Porter, T. F., . . . Spite, M. (2009). Maresins: novel macrophage mediators with potent antiinflammatory and proresolving actions. *J Exp Med, 206*(1), 15-23. doi:10.1084/jem.20081880

Shannahan, J. H., Bai, W., & Brown, J. M. (2015). Implications of scavenger receptors in the safe development of nanotherapeutics. *Receptors Clin Investig, 2*(3), e811. doi:10.14800/rci.811

Shen, W. J., Asthana, S., Kraemer, F. B., & Azhar, S. (2018). Scavenger receptor B type 1: expression, molecular regulation, and cholesterol transport function. *J Lipid Res, 59*(7), 1114-1131. doi:10.1194/jlr.R083121

Shen, Z. X., Chen, X. Q., Sun, X. N., Sun, J. Y., Zhang, W. C., Zheng, X. J., . . . Duan, S. Z. (2017). Mineralocorticoid Receptor Deficiency in Macrophages Inhibits Atherosclerosis by Affecting Foam Cell Formation and Efferocytosis. *J Biol Chem, 292*(3), 925-935. doi:10.1074/jbc.M116.739243

Silverstein, R. L., & Febbraio, M. (2009). CD36, a scavenger receptor involved in immunity, metabolism, angiogenesis, and behavior. *Sci Signal, 2*(72), re3. doi:10.1126/scisignal.272re3

Silveyra, P., & Floros, J. (2012). Genetic variant associations of human SP-A and SP-D with acute and chronic lung injury. *Front Biosci (Landmark Ed), 17*, 407-429.

Speen, A. M., Kim, H. H., Bauer, R. N., Meyer, M., Gowdy, K. M., Fessler, M. B., . . . Jaspers, I. (2016). Ozone-derived Oxysterols Affect Liver X Receptor (LXR) Signaling: A POTENTIAL ROLE FOR LIPID-PROTEIN ADDUCTS. *J Biol Chem, 291*(48), 25192-25206. doi:10.1074/jbc.M116.732362

Sticozzi, C., Pecorelli, A., Romani, A., Belmonte, G., Cervellati, F., Maioli, E., . . . Valacchi, G. (2018). Tropospheric ozone affects SRB1 levels via oxidative post-translational modifications in lung cells. *Free Radic Biol Med, 126*, 287-295. doi:10.1016/j.freeradbiomed.2018.07.007

Sun, Z., Li, F., Zhou, X., & Wang, W. (2017). Generation of a Chronic Obstructive Pulmonary Disease Model in Mice by Repeated Ozone Exposure. *J Vis Exp*(126). doi:10.3791/56095

Sunil, V. R., Patel-Vayas, K., Shen, J., Laskin, J. D., & Laskin, D. L. (2012). Classical and alternative macrophage activation in the lung following ozone-induced oxidative stress. *Toxicol Appl Pharmacol, 263*(2), 195-202. doi:10.1016/j.taap.2012.06.009

Tancevski, I., Wehinger, A., Schgoer, W., Eller, P., Cuzzocrea, S., Foeger, B., . . . Ritsch, A. (2006). Aspirin regulates expression and function of scavenger receptor-BI in macrophages: studies in primary human macrophages and in mice. *FASEB J, 20*(9), 1328-1335. doi:10.1096/fj.05-5368com

Tao, H., Yancey, P. G., Babaev, V. R., Blakemore, J. L., Zhang, Y., Ding, L., . . . Linton, M. F. (2015). Macrophage SR-BI mediates efferocytosis via Src/PI3K/Rac1 signaling and reduces atherosclerotic lesion necrosis. *J Lipid Res, 56*(8), 1449-1460. doi:10.1194/jlr.M056689

Thimmulappa, R. K., Gang, X., Kim, J. H., Sussan, T. E., Witztum, J. L., & Biswal, S. (2012). Oxidized phospholipids impair pulmonary antibacterial defenses: evidence in mice exposed to cigarette smoke. *Biochem Biophys Res Commun, 426*(2), 253-259. doi:10.1016/j.bbrc.2012.08.076

Todt, J. C., Hu, B., & Curtis, J. L. (2008). The scavenger receptor SR-A I/II (CD204) signals via the receptor tyrosine kinase Mertk during apoptotic cell uptake by murine macrophages. *J Leukoc Biol, 84*(2), 510-518. doi:10.1189/jlb.0307135

Tsugita, M., Morimoto, N., Tashiro, M., Kinoshita, K., & Nakayama, M. (2017). SR-B1 Is a Silica Receptor that Mediates Canonical Inflammasome Activation. *Cell Rep, 18*(5), 1298-1311. doi:10.1016/j.celrep.2017.01.004

Valacchi, G., Vasu, V. T., Yokohama, W., Corbacho, A. M., Phung, A., Lim, Y., . . . Davis, P. A. (2007). Lung vitamin E transport processes are affected by both age and environmental oxidants in mice. *Toxicol Appl Pharmacol, 222*(2), 227-234. doi:10.1016/j.taap.2007.04.010

van de Laar, L., Saelens, W., De Prijck, S., Martens, L., Scott, C. L., Van Isterdael, G., . . . Guilliams, M. (2016). Yolk Sac Macrophages, Fetal Liver, and Adult Monocytes Can Colonize an Empty Niche and Develop into Functional Tissue-Resident Macrophages. *Immunity, 44*(4), 755-768. doi:10.1016/j.immuni.2016.02.017

Van Eck, M., Hoekstra, M., Hildebrand, R. B., Yaong, Y., Stengel, D., Kruijt, J. K., . . .

Pratico, D. (2007). Increased oxidative stress in scavenger receptor BI knockout mice with dysfunctional HDL. *Arterioscler Thromb Vasc Biol, 27*(11), 2413-2419. doi:10.1161/ATVBAHA.107.145474

Van Hoecke, L., Job, E. R., Saelens, X., & Roose, K. (2017). Bronchoalveolar Lavage of Murine Lungs to Analyze Inflammatory Cell Infiltration. *J Vis Exp*(123). doi:10.3791/55398

Vandivier, R. W., Richens, T. R., Horstmann, S. A., deCathelineau, A. M., Ghosh, M., Reynolds, S. D., . . . Henson, P. M. (2009). Dysfunctional cystic fibrosis transmembrane conductance regulator inhibits phagocytosis of apoptotic cells with proinflammatory consequences. *Am J Physiol Lung Cell Mol Physiol, 297*(4), L677-686. doi:10.1152/ajplung.00030.2009

Vergeer, M., Korporaal, S. J., Franssen, R., Meurs, I., Out, R., Hovingh, G. K., . . . Kuivenhoven, J. A. (2011). Genetic variant of the scavenger receptor BI in humans. *N Engl J Med, 364*(2), 136-145. doi:10.1056/NEJMoa0907687

Vickers, K. C., & Rodriguez, A. (2014). Human scavenger receptor class B type I variants, lipid traits, and cardiovascular disease. *Circ Cardiovasc Genet, 7*(6), 735-737. doi:10.1161/CIRCGENETICS.114.000929

Voelker, D. R., & Numata, M. (2019). Phospholipid regulation of innate immunity and respiratory viral infection. *J Biol Chem, 294*(12), 4282-4289. doi:10.1074/jbc.AW118.003229

Wang, M., Sampson, P. D., Sheppard, L. E., Stein, J. H., Vedal, S., & Kaufman, J. D. (2019). Long-Term Exposure to Ambient Ozone and Progression of Subclinical Arterial Disease: The Multi-Ethnic Study of Atherosclerosis and Air Pollution.

Environ Health Perspect, 127(5), 57001. doi:10.1289/EHP3325

Wang, X., Katwa, P., Podila, R., Chen, P., Ke, P. C., Rao, A. M., . . . Brown, J. M. (2011). Multi-walled carbon nanotube instillation impairs pulmonary function in C57BL/6 mice. *Part Fibre Toxicol, 8*, 24. doi:10.1186/1743-8977-8-24

Wiester, M. J., Tepper, J. S., King, M. E., Menache, M. G., & Costa, D. L. (1988). Comparative study of ozone (O3) uptake in three strains of rats and in the guinea pig. *Toxicol Appl Pharmacol, 96*(1), 140-146. doi:10.1016/0041-008x(88)90256-6

Williams, A. S., Leung, S. Y., Nath, P., Khorasani, N. M., Bhavsar, P., Issa, R., . . . Chung, K. F. (2007). Role of TLR2, TLR4, and MyD88 in murine ozone-induced airway hyperresponsiveness and neutrophilia. *J Appl Physiol (1985), 103*(4), 1189-1195. doi:10.1152/japplphysiol.00172.2007

Yeo, J. C., Wall, A. A., Stow, J. L., & Hamilton, N. A. (2013). High-throughput quantification of early stages of phagocytosis. *Biotechniques, 55*(3), 115-124. doi:10.2144/000114075

Yurdagul, A., Jr., Doran, A. C., Cai, B., Fredman, G., & Tabas, I. A. (2017). Mechanisms and Consequences of Defective Efferocytosis in Atherosclerosis. *Front Cardiovasc Med, 4*, 86. doi:10.3389/fcvm.2017.00086

Zanoni, P., Khetarpal, S. A., Larach, D. B., Hancock-Cerutti, W. F., Millar, J. S., Cuchel, M., . . . Global Lipids Genetics, C. (2016). Rare variant in scavenger receptor BI raises HDL cholesterol and increases risk of coronary heart disease. *Science, 351*(6278), 1166-1171. doi:10.1126/science.aad3517

Zhang, J. J., Wei, Y., & Fang, Z. (2019). Ozone Pollution: A Major Health Hazard Worldwide. *Front Immunol, 10*, 2518. doi:10.3389/fimmu.2019.02518

Zhang, Q., Ma, A. Z., Song, Z. Y., Wang, C., & Fu, X. D. (2013). Nifedipine enhances cholesterol efflux in RAW264.7 macrophages. *Cardiovasc Drugs Ther, 27*(5), 425-431. doi:10.1007/s10557-013-6472-y

Zhang, X., Goncalves, R., & Mosser, D. M. (2008). The isolation and characterization of murine macrophages. *Curr Protoc Immunol, Chapter 14*, Unit 14 11. doi:10.1002/0471142735.im1401s83

Zhang, Y., Da Silva, J. R., Reilly, M., Billheimer, J. T., Rothblat, G. H., & Rader, D. J. (2005). Hepatic expression of scavenger receptor class B type I (SR-BI) is a positive regulator of macrophage reverse cholesterol transport in vivo. *J Clin Invest, 115*(10), 2870-2874. doi:10.1172/JCI25327

APPENDIX A- INSTITUTIONAL ANIMAL CARE AND USE COMMITTEE FORM

East Carolina University

Animal Care and Use Commitee
212 Ed Warren Life Sciences Building
East Carolina University
Greenville, NC 27834

252-744-2436 office
252-744-2355 fax

August 24, 2015

Kymberly Gowdy, Ph.D.
Department of Pharmacology
Brody 6S-10
ECU Brody School of Medicine

Dear Dr. Gowdy:

Your Animal Use Protocol entitled, "The Role of Scavenger Receptor B1 (SR-B1) in Environmental Lung Diseases in Mice" (AUP #W244) was reviewed by this institution's Animal Care and Use Committee on August 24, 2015. The following action was taken by the Committee:

"Approved as submitted"

Please contact Dale Aycock at 744-2997 prior to hazard use

A copy is enclosed for your laboratory files. Please be reminded that all animal procedures must be conducted as described in the approved Animal Use Protocol. Modifications of these procedures cannot be performed without prior approval of the ACUC. The Animal Welfare Act and Public Health Service Guidelines require the ACUC to suspend activities not in accordance with approved procedures and report such activities to the responsible University Official (Vice Chancellor for Health Sciences or Vice Chancellor for Academic Affairs) and appropriate federal Agencies. **Please ensure that all personnel associated with this protocol have access to this approved copy of the AUP and are familiar with its contents.**

Sincerely yours,

SB McRae

Susan McRae, Ph.D.

APPENDIX B- SUPPLEMENTARY DATA

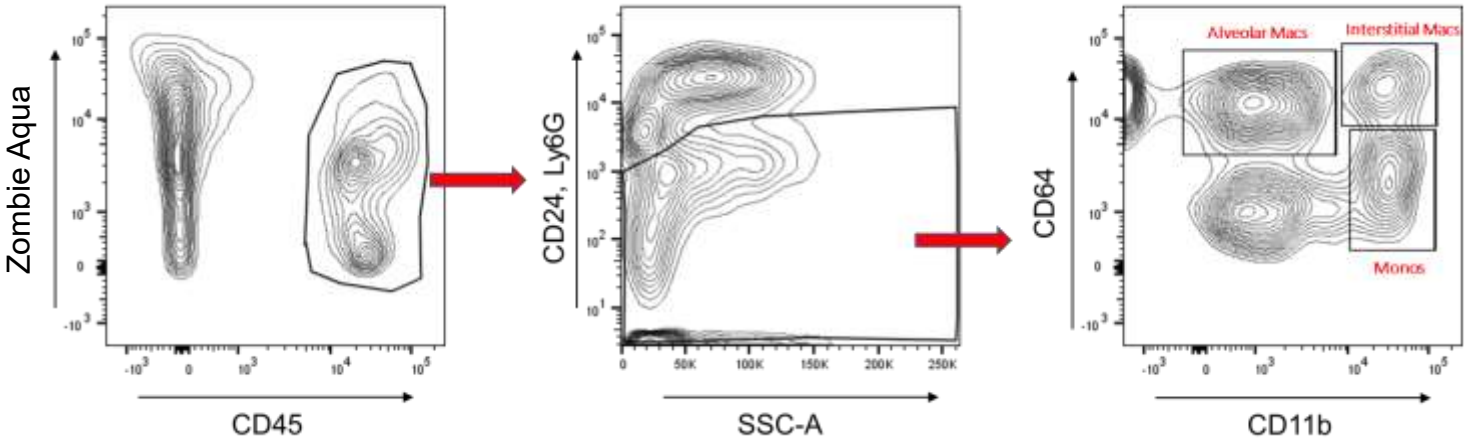

Supplementary Figure 1: Flow cytometry panel for sorting pulmonary macrophage populations from whole lung tissue. Alveolar macrophages (AMs) were defined as $CD45^{+}CD24^{-}Ly6G^{-}CD64^{+}CD11b^{low}$ and interstitial macrophages (IMs) were defined as $CD45^{+}CD24^{-}Ly6G^{-}CD64^{+}CD11b^{high}$ by fluorescence activated cell sorting (FACS) using a BD FACSAria™ Fusion (BD Biosciences). Zombie aqua was used as a viability dye so the machine will sort only live macrophages.

A

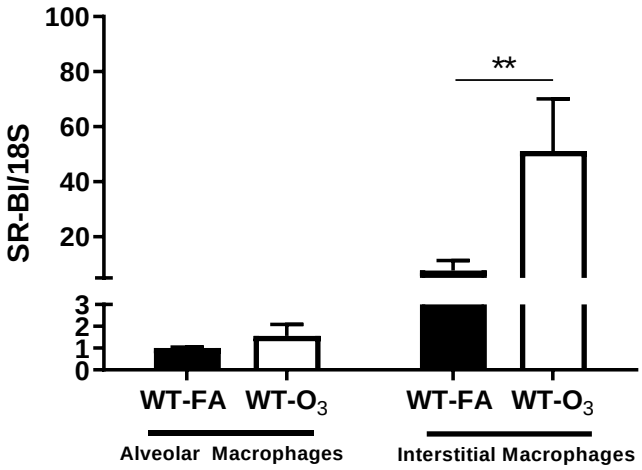

24 h post exposure

B

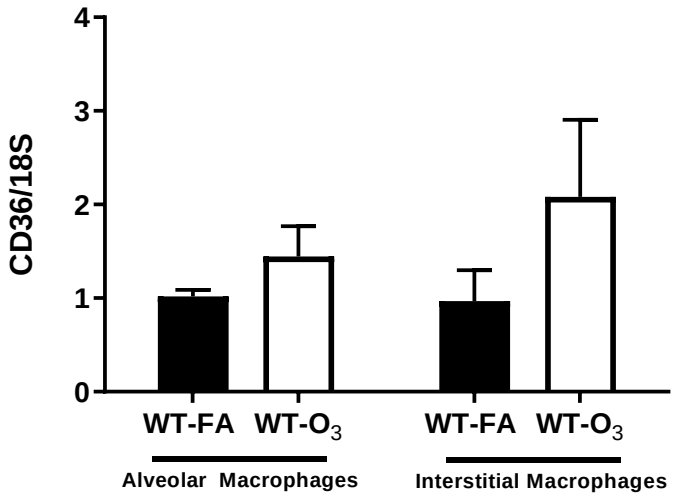

24 h post exposure

C

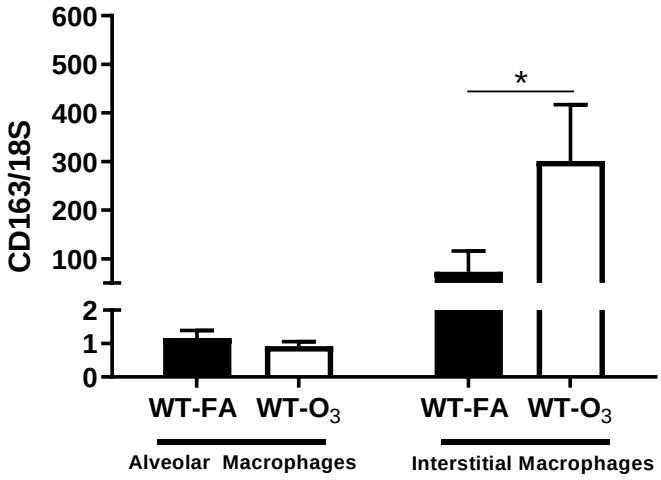

24 h post exposure

Supplementary Figure 2: O_3 induces SR-BI expression in the lung and sorted pulmonary macrophages. WT (and SR-BI$^{-/-}$) mice were exposed to filtered air (FA) or 1ppm O_3 (3 h) and necropsied 24 h following exposure. Lung tissue was digested for FACS isolation of alveolar macrophages (AM; CD45^{+}CD24^{-}Ly6G^{-}CD64^{+}CD11b^{low}) and interstitial macrophages (IM; CD45^{+}CD24^{-}Ly6G^{-}CD64^{+}CD11b^{high}) to determine A) SR-BI B) CD-36, and C) CD163 scavenger receptor expression in these pulmonary macrophage populations. Gene expression was normalized to 18S. (n=4-7/treatment). *p<0.05.

A

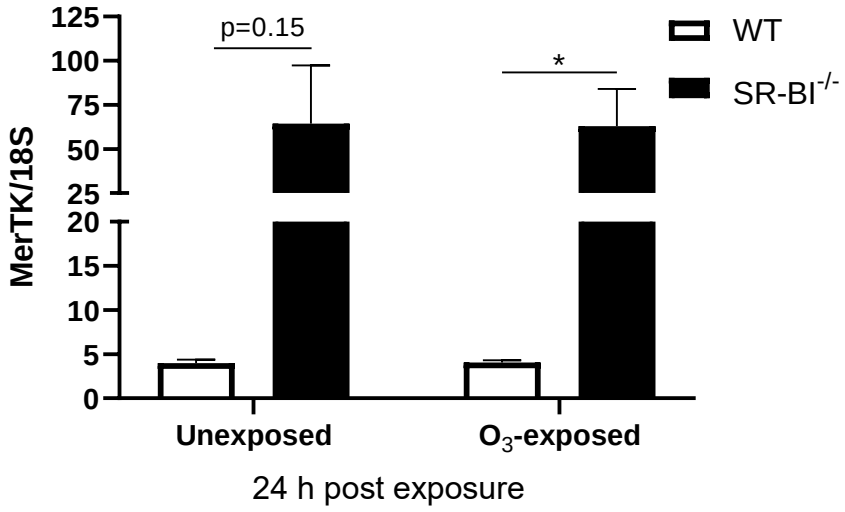
p=0.15
*
WT
SR-BI-/-
MerTK/18S
125
100
75
50
25
20
15
10
5
0
Unexposed
O3-exposed
24 h post exposure

B

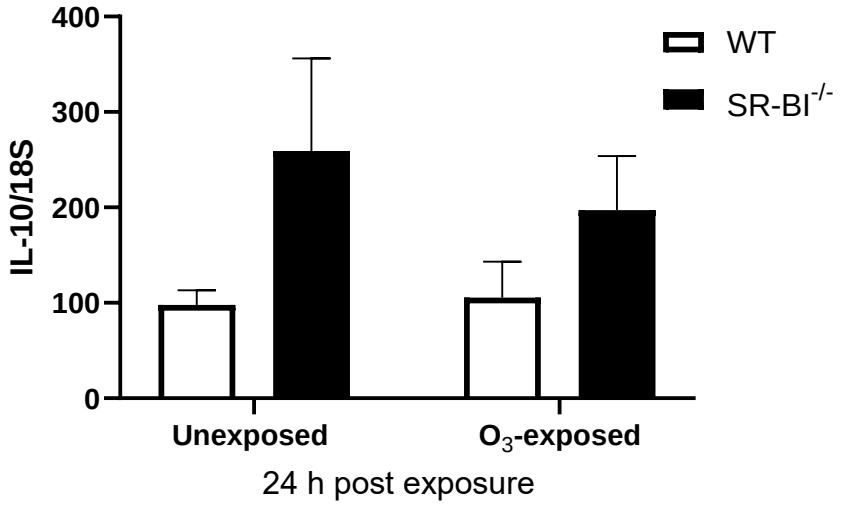
WT
SR-BI-/-
IL-10/18S
400
300
200
100
0
Unexposed
O3-exposed
24 h post exposure

C

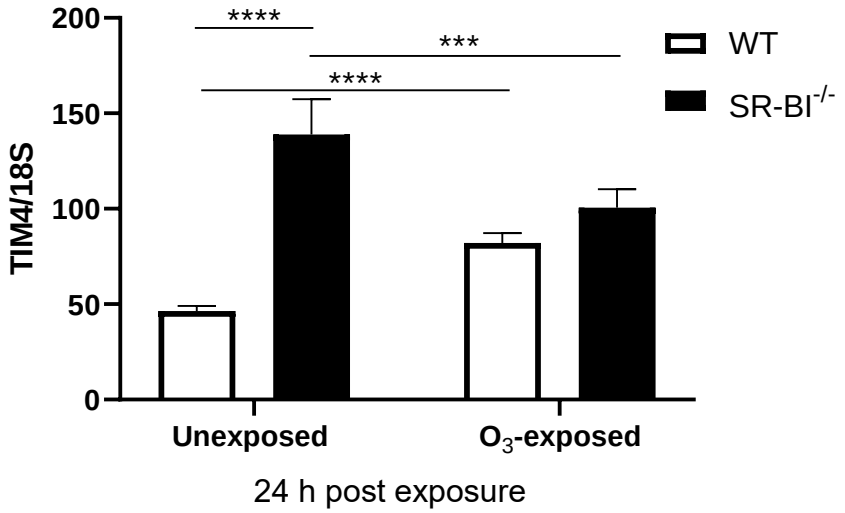
****
***
****
WT
SR-BI-/-
TIM4/18S
200
150
100
50
0
Unexposed
O3-exposed
24 h post exposure

Supplementary Figure 3: SR-BI deficient interstitial macrophages have increased expression of efferocytosis markers. WT (and SR-BI$^{-/-}$) mice were exposed to filtered air (FA) or 1ppm O_3 and necropsied 24 h following exposure. Lung tissue was digested for FACS isolation of interstitial macrophages (IM; CD45^{+}CD24^{-}Ly6G^{-}CD64^{+}CD11b^{high}) to determine A) MerTK, B) IL-10, and C) Tim4 expression in this pulmonary macrophage population. Gene expression was normalized to 18S. (n=4-8/treatment). *p<0.05, **p<0.01, ***p<0.001, ****p<0.0001.

A

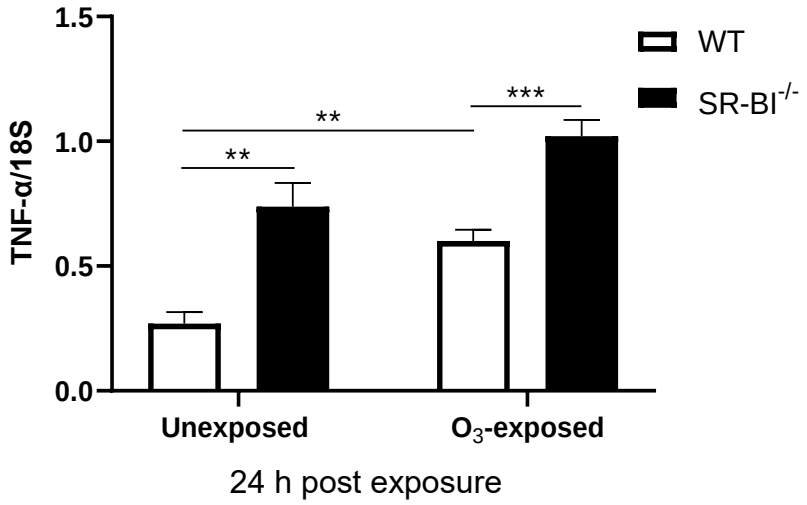
1.5
1.0
0.5
0.0
TNF-α/18S
WT
SR-BI-/-
**
**
***
Unexposed
O3-exposed
24 h post exposure

B

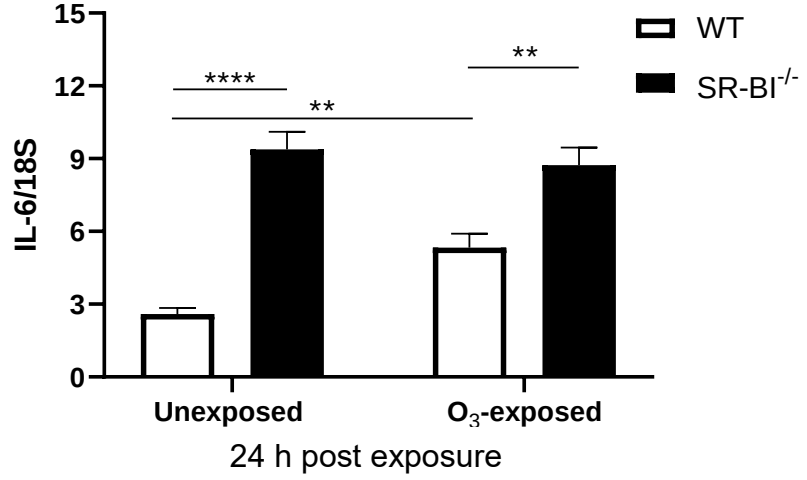
15
12
9
6
3
0
IL-6/18S
WT
SR-BI-/-
****
**
**
Unexposed
O3-exposed
24 h post exposure

C

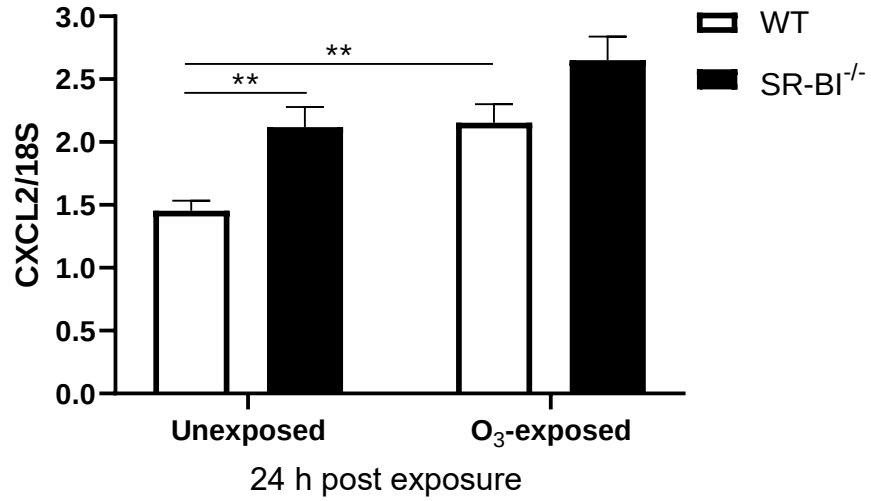
3.0
2.5
2.0
1.5
1.0
0.5
0.0
CXCL2/18S
WT
SR-BI-/-
**
**
Unexposed
O3-exposed
24 h post exposure

Supplementary Figure 4: SR-BI deficiency augments expression of pro-inflammatory cytokines and chemokines in pulmonary macrophages, but not in whole lung after O_3. WT (and SR-BI$^{-/-}$) mice were exposed to filtered air (FA) or 1ppm O_3 (3 h) and necropsied 24 h following exposure. Lung tissue was digested for FACS isolation of interstitial macrophages (IM; CD45^{+}CD24^{-}Ly6G^{-}CD64^{+}CD11b^{high}) to determine A) TNF-α, B) IL-6, and C) CXCL2 expression in this pulmonary macrophage population. Gene expression was normalized to 18S. (n=7-8/treatment). **p<0.01, ***p<0.001.

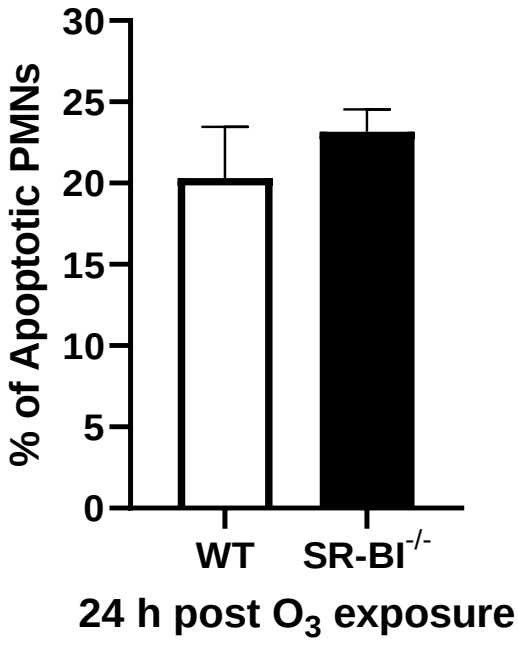
30
25
20
15
10
5
0
% of Apoptotic PMNs
WT
SR-BI-/-
24 h post O3 exposure

Supplementary Figure 5: SR-BI deficiency impairs alveolar macrophage efferocytosis and resolution of O_3-induced pulmonary inflammation. WT and SR-BI$^{-/-}$ mice were exposed to filtered air (FA) or 1ppm O_3 (3 h). 24 h post exposure neutrophils (PMNs) in the bronchoalveolar lavage (defined as Ly6G$^+$) (BAL) were analyzed via flow cytometry for markers of apoptosis and necrosis. The percentage of early apoptotic, late apoptotic, and necrotic PMNs were indicated by Annexin V$^+$/PI$^-$/Ly6G$^+$, Annexin V$^+$/PI$^+$/Ly6G$^+$, and Annexin V$^-$/PI$^+$/Ly6G$^+$ staining, respectively.